Supporting information

Table of contents

1. Investigation of excimer formation by compounds **5** and **6** 2
2. Protonation studies of compounds **5**, **6** and **10** 3
   2.1. Spectrophotometric studies 3
   2.2. Fluorescence studies 9
   2.3. NMR studies of the compound **6** 15
3. Metal binding studies of compounds **5**, **6** and **10** 17
   3.1. Compound **10** 17
   3.2. Compound **5** 19
   3.3. Compound **6** 23
   3.4. Visual detection using paper stripes 31
4. Investigation of the structure of complexes 32
   4.1. NMR-studies of $[Zn(\mathbf{6})]^{2+}$ complex 32
   4.2. DFT-studies of $[Zn(\mathbf{6})]^{2+}$ complex 42
   4.3. IR-studies 46
   4.4. ESI-spectra of $[Hg(\mathbf{6})]^{2+}$ complex 47
   4.5. NMR-studies of $[Hg(\mathbf{6})]^{2+}$ complex 48
5. Detection of sulfide anions 51
6. Characterization of compounds **5**, **6**, **9a-f**, **10** 52

1. Investigation of excimer formation by compounds 5 and 6

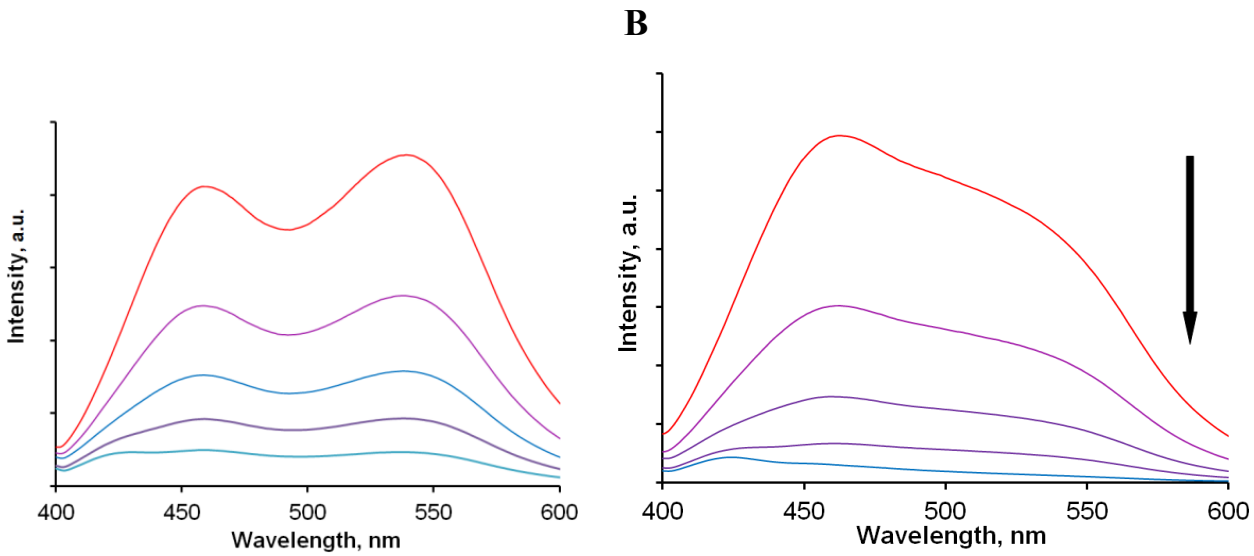

Figure S1. Dependence of emission spectra on dilution of the aqueous solutions of : A – ligand **5** (in the 1.7 µM–26µM concentration range; 0.03M HEPES, pH = 7.4; λ_{ex} =356 nm); B – ligand **6** (in the 40 nM–4.3µM concentration range; 0.03M HEPES, pH = 7.4; λ_{ex} =365 nm).

2. Protonation studies of compounds 5, 6 and 10

2.1. Spectrophotometric studies

Spectrophotometric studies of protonation of compound **5**

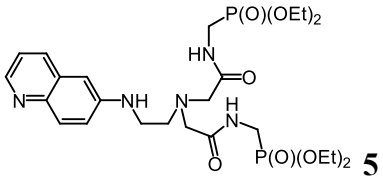

5

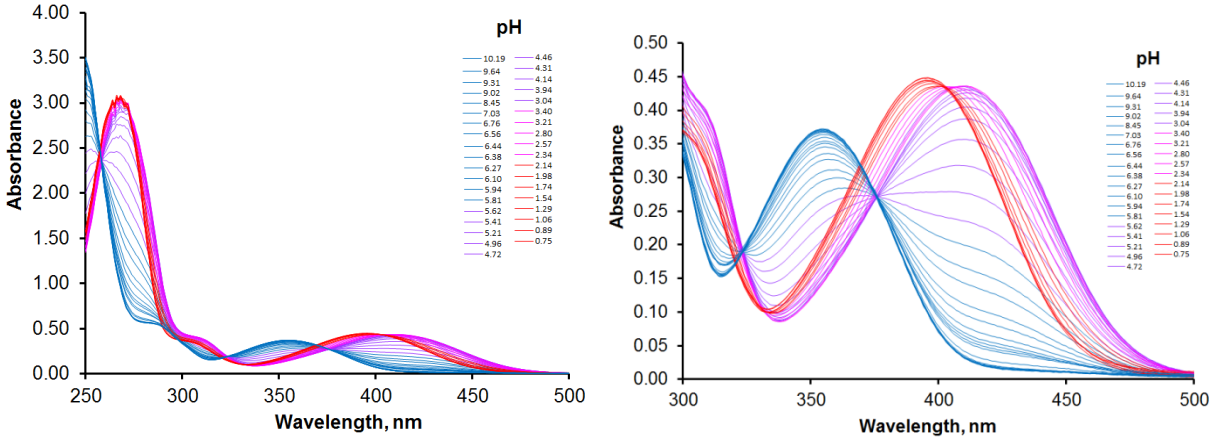

Figure S2. Spectrophotometric titration of **5** as a function of pH. [**5**] = 133 μM, I = 0.1 M KCl, pH = 0.75–10.19.

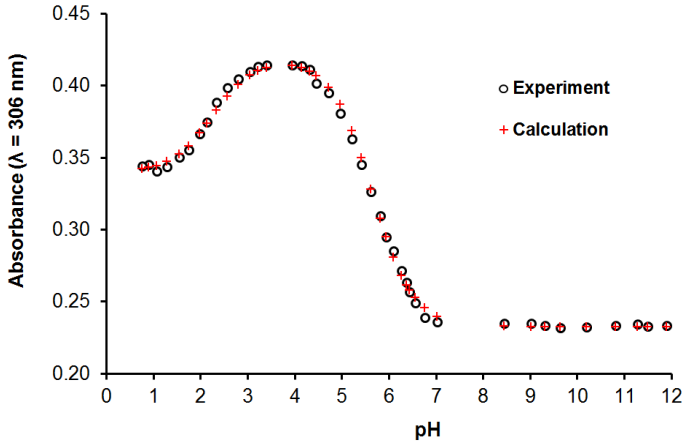

Figure S3. Evolution of absorbance with pH at 306 nm.

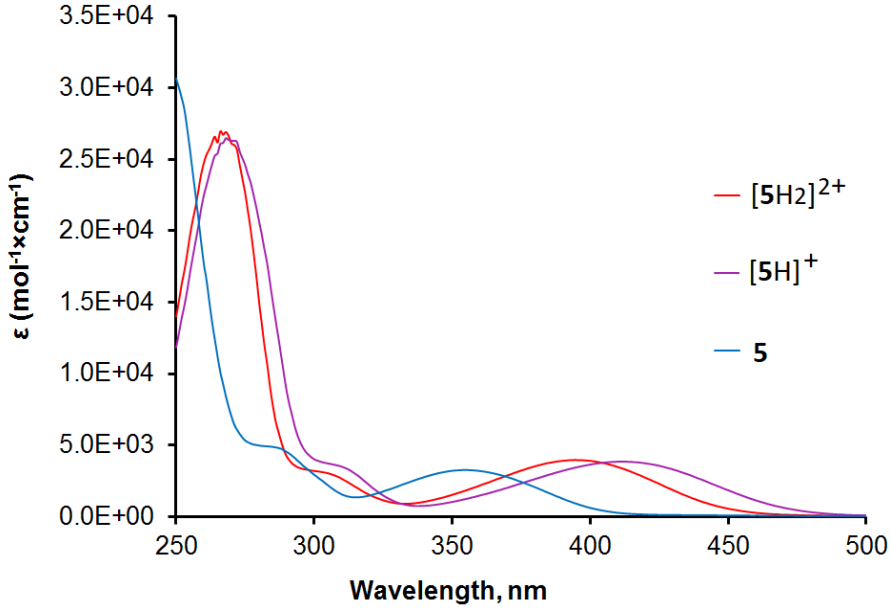

Figure S4. Calculated with the Specfit/32 program UV–vis spectra of **5**, $[\mathbf{5}H]^{+}$ and $[\mathbf{5}H_2]^{2+}$ in water.

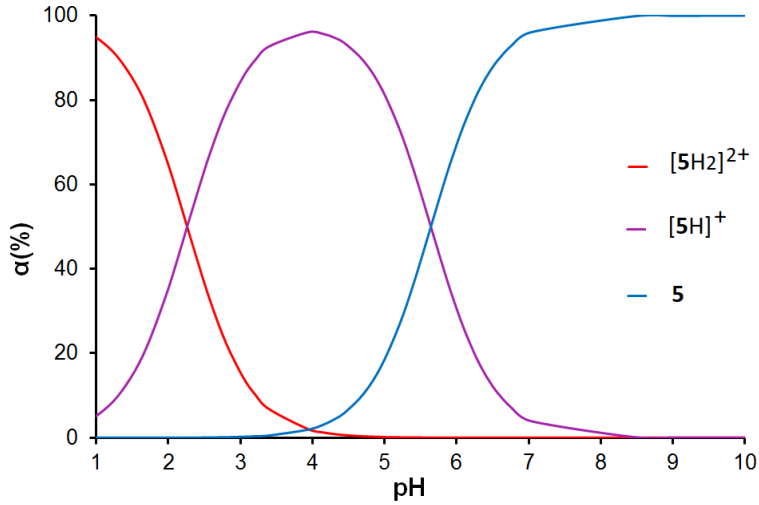

Figure S5. Distribution diagram of the protonated species of **5** calculated with the Specfit/32 program.

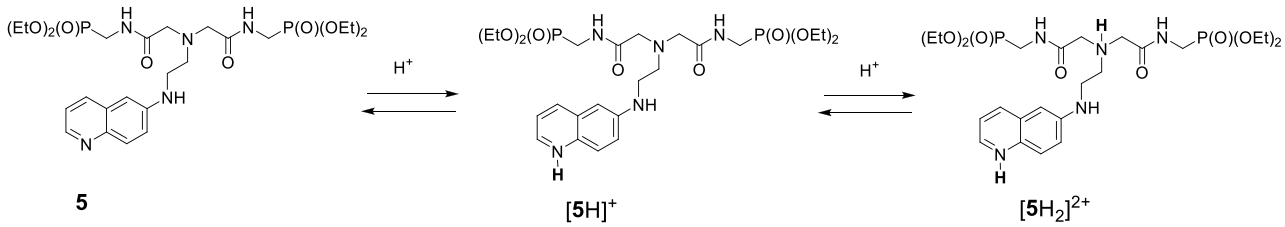

Scheme S1. Protonation sequence for ligand **5**.

Spectrophotometric studies of protonation of compound **6**

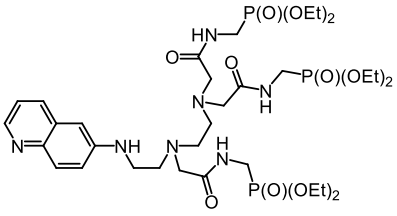

6

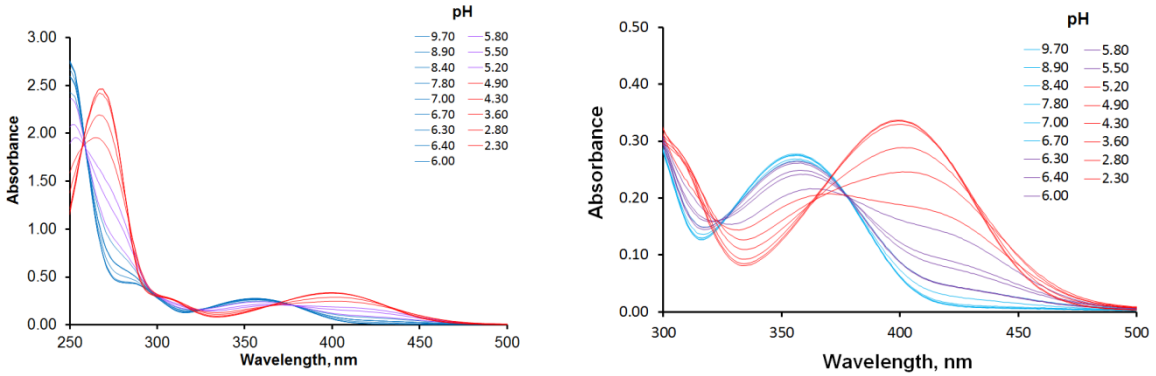

Figure S6. Spectrophotometric titration of **6** as a function of pH. [**6**] = 133 μM, I = 0.1 M KCl, pH = 2.30–9.70.

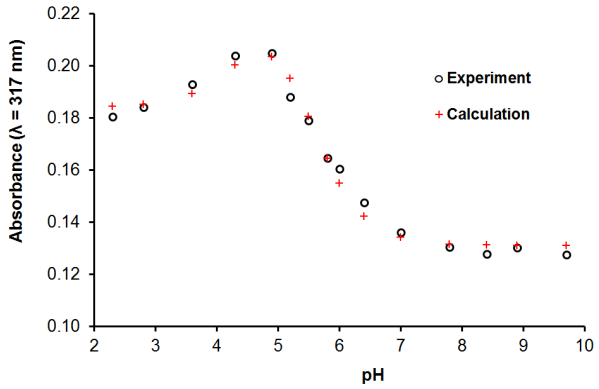

Figure S7. Evolution of absorbance with pH at 317 nm.

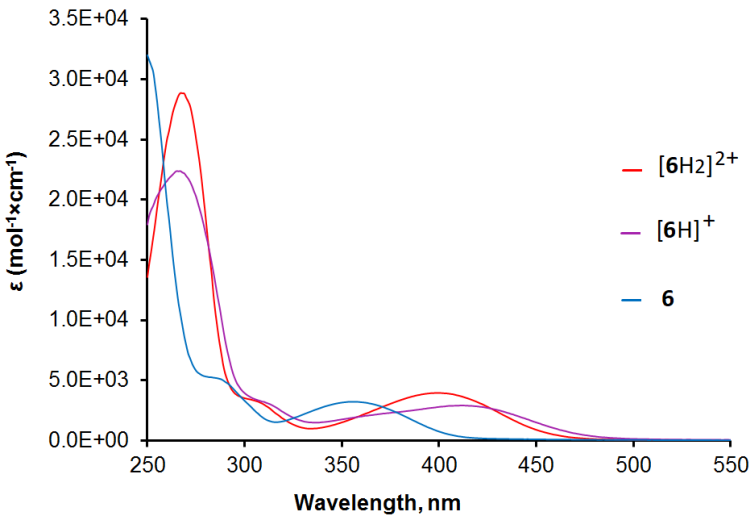

Figure S8. Calculated with the Specfit/32 program UV–vis spectra of **6**, $[\mathbf{6}H]^{+}$ and $[\mathbf{6}H_2]^{2+}$ in water.

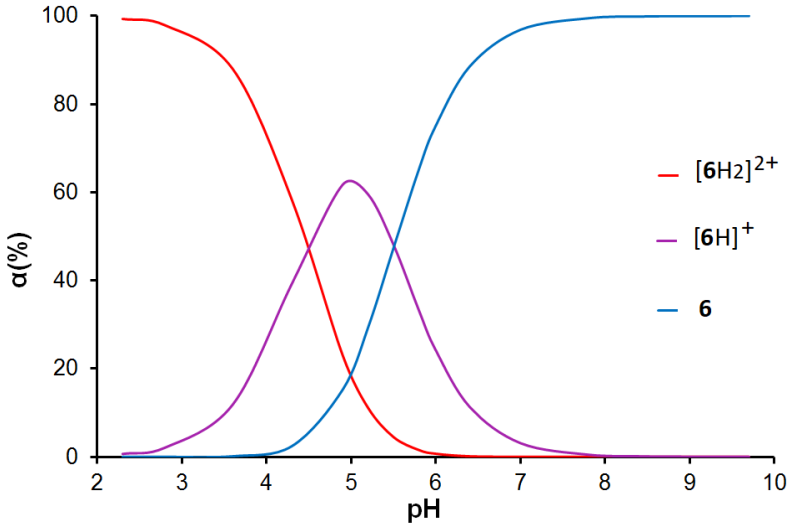

Figure S9. Distribution diagram of the protonated species of **6** calculated with the Specfit/32 program.

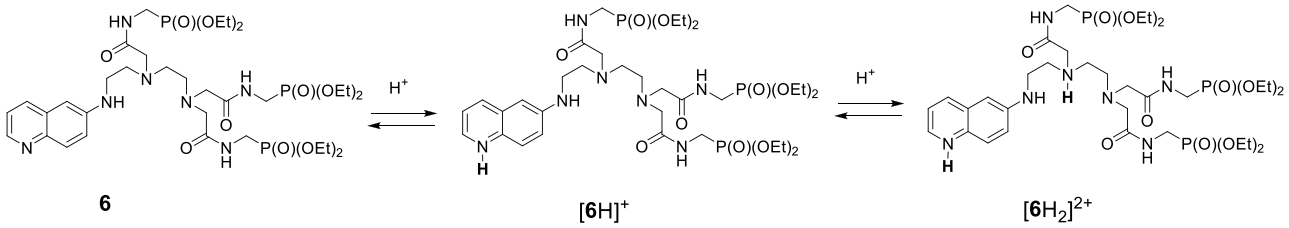

Scheme S2. Protonation sequence for ligand **6**.

Spectrophotometric studies of protonation of compound **10**

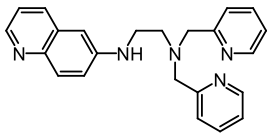

10

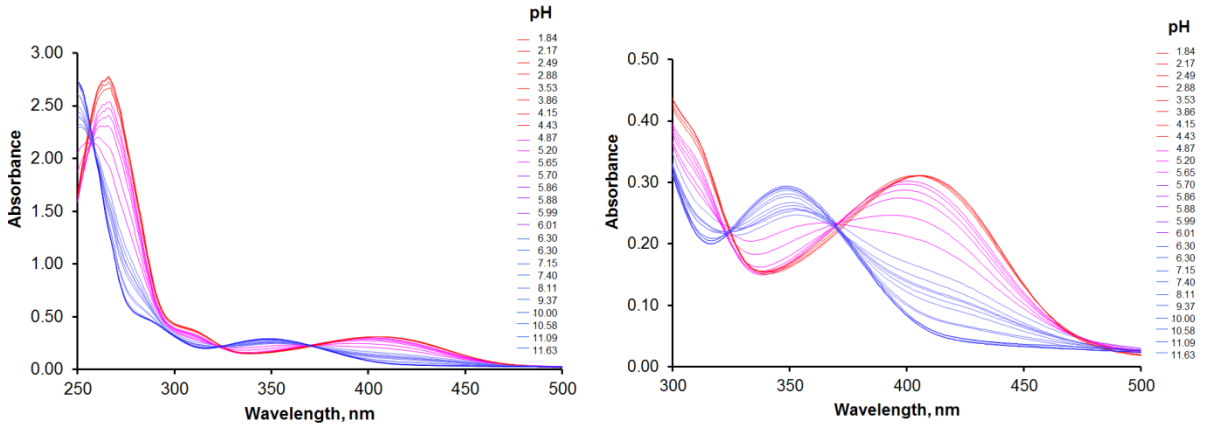

Figure S10. Spectrophotometric titration of **10** as a function of pH. [**10**] = 103 μM, 6% MeOH, I = 0.1 M KCl, pH = 1.84–11.63.

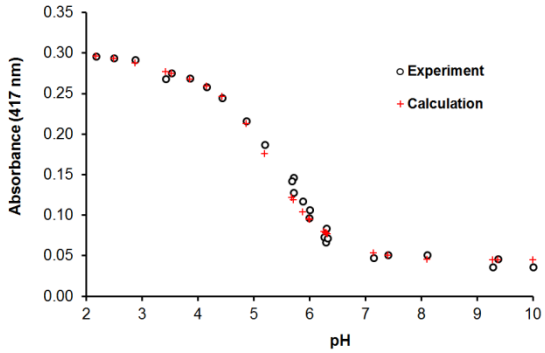

Figure S11. Changes of absorbance with pH at 417 nm.

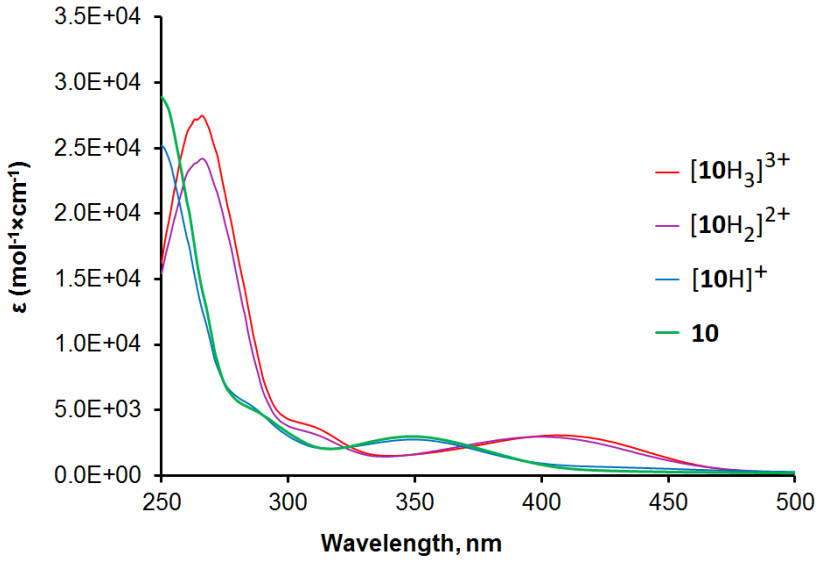

Figure S12. Calculated with the Specfit/32 program UV–vis spectra of **10**, $[\mathbf{10}H]^{+}$, $[\mathbf{10}H_2]^{2+}$ and $[\mathbf{10}H_3]^{3+}$ in water.

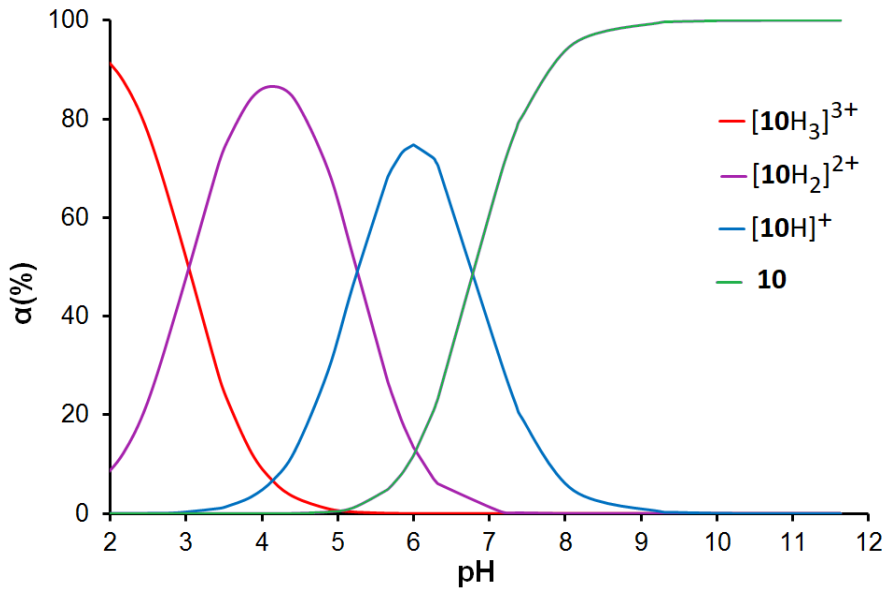

Figure S13. Distribution diagram of the protonated species of **10** calculated with the Specfit/32 program

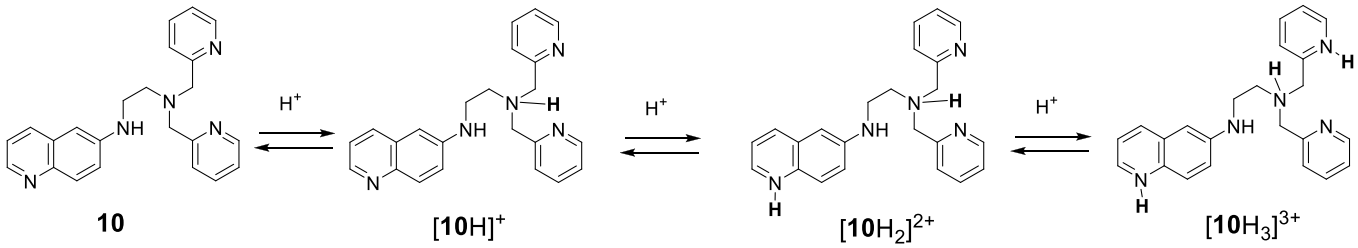

Scheme S3. Protonation sequence for ligand **10**.

2.2 Fluorescence studies

Fluorimetric studies of protonation of compound **5**

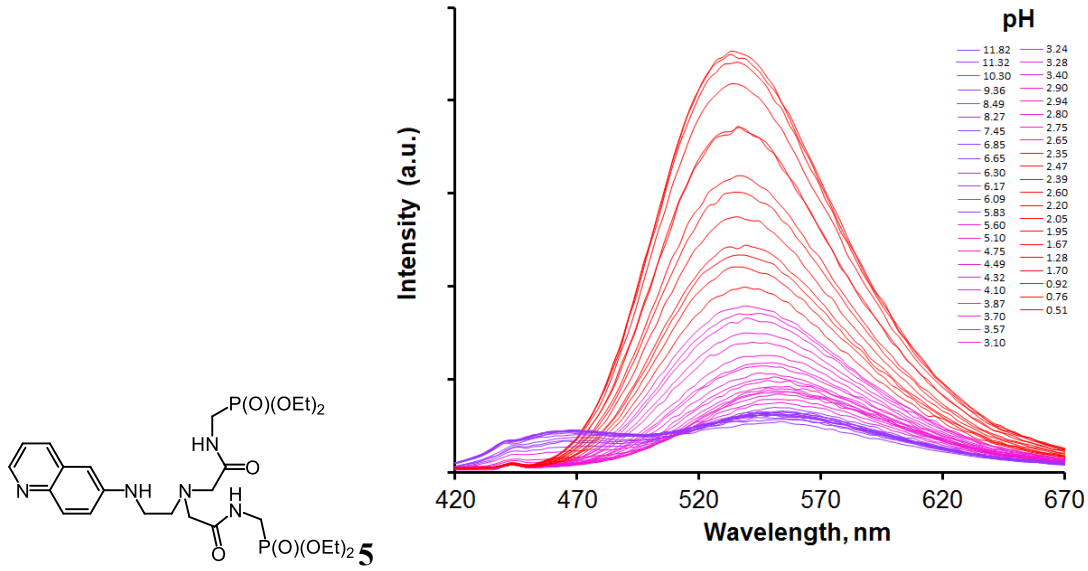

Figure S14. Fluorimetric titration of **5** as a function of pH. [**5**] = 27 μM, I = 0.1 M KCl, λ_{ex} = 375 nm, pH = 0.51–11.82.

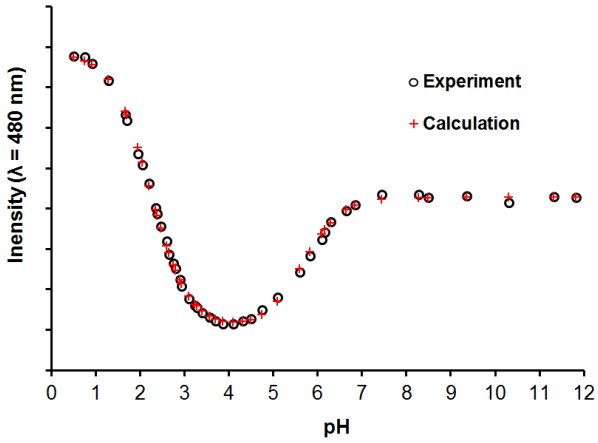

Figure S15. Changes of fluorescence intensity with pH at 480 nm

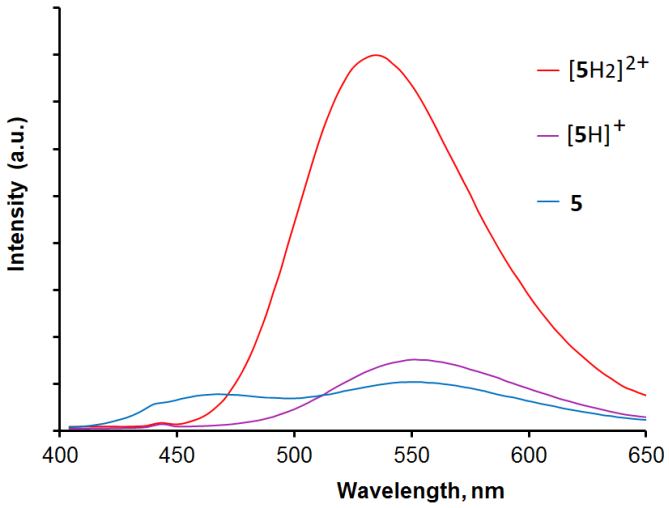

Figure S16. Calculated with the Specfit/32 program fluorescence spectra of **5**, $[\mathbf{5}H]^{+}$ and $[\mathbf{5}H_2]^{2+}$ in water.

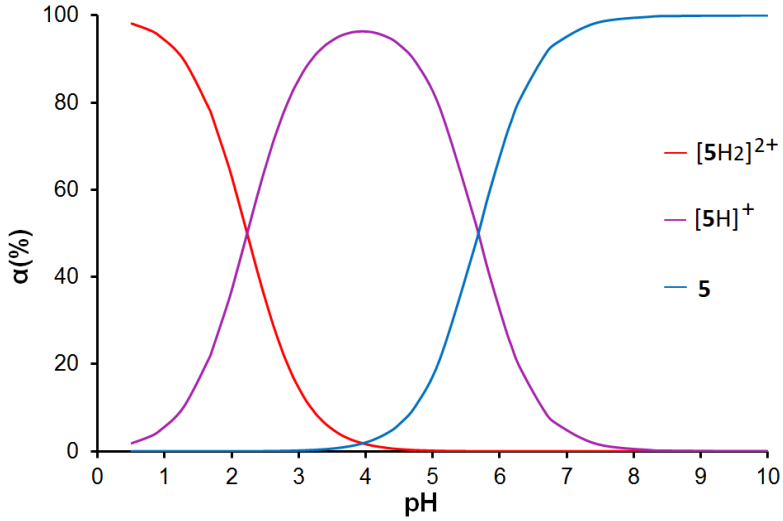

Figure S17. Distribution diagram of the protonated species of **5** calculated with the Specfit/32 program.

Fluorimetric studies of protonation of compound **6**

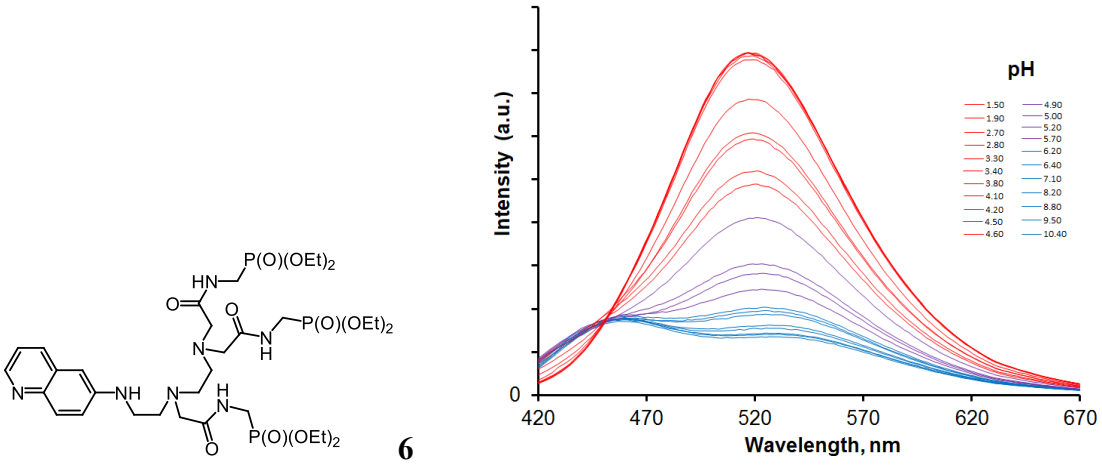

Figure S18. Fluorimetric titration of **6** as a function of pH. [**6**] = 20 μM, I = 0.1 M KCl, λ_{ex} = 356 nm, pH = 1.50–10.40

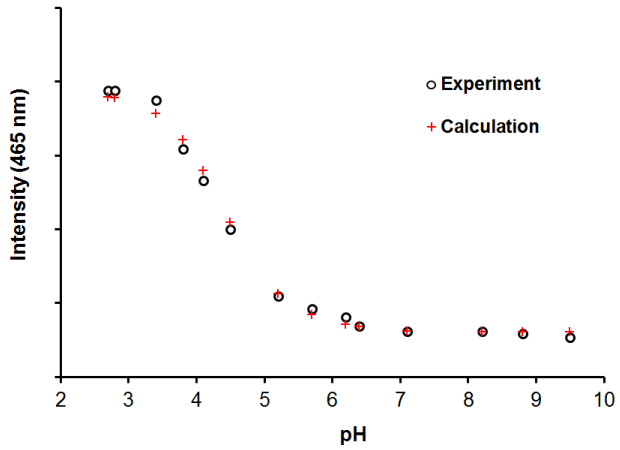

Figure S29. Evolution of fluorescence intensity with pH at 465 nm.

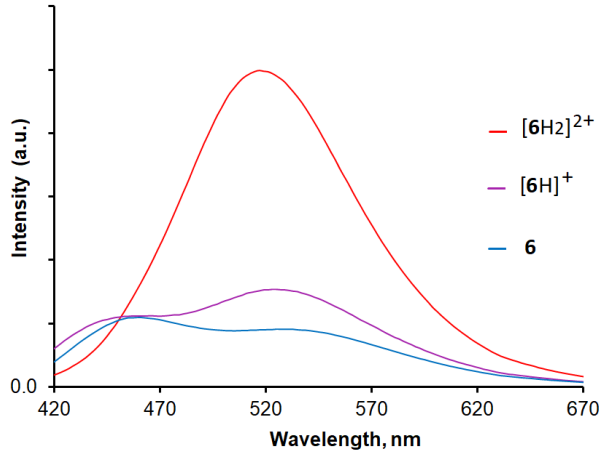

Figure S20. Calculated with the Specfit/32 program fluorescence spectra of **6**, $[\mathbf{6}H]^{+}$ and $[\mathbf{6}H_2]^{2+}$ in water.

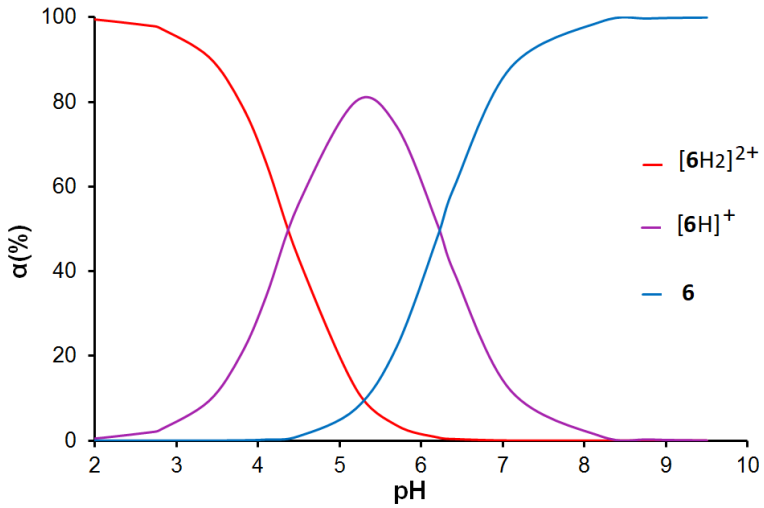

Figure S21. Distribution diagram of the protonated species of **6** calculated with the Specfit/32 program.

Fluorimetric studies of protonation of compound **10**

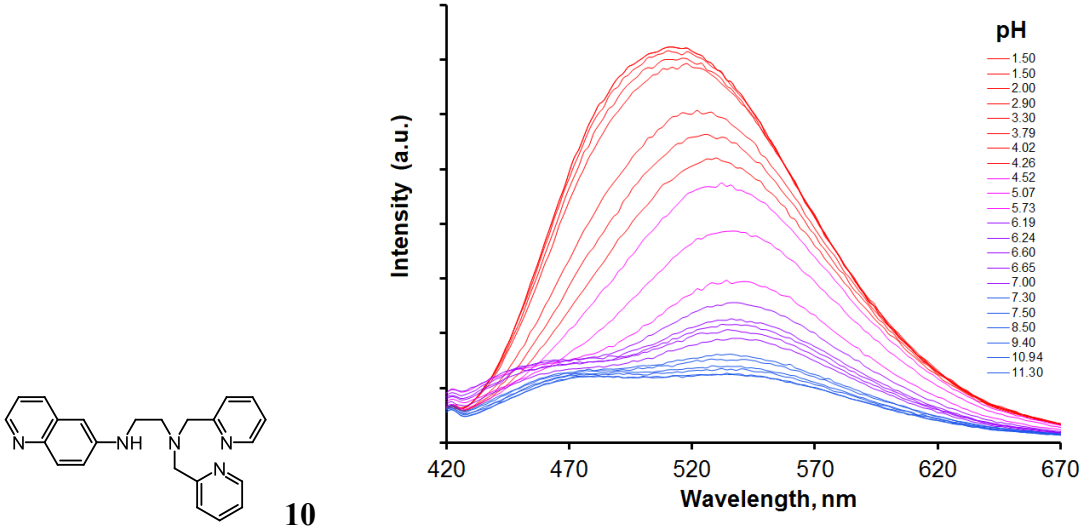

Figure S22. Fluorimetric titration of **10** as a function of pH. [**10**] = 26 μM, 2% MeOH, I = 0.1 M KCl, λ_{ex} = 345 nm, pH = 1.50–11.30.

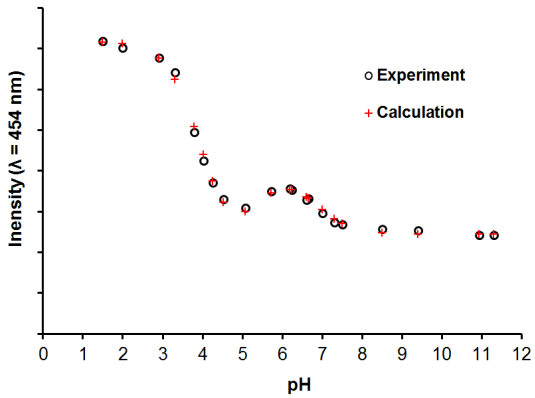

Figure S23. Changes of fluorescence intensity with pH at 454 nm.

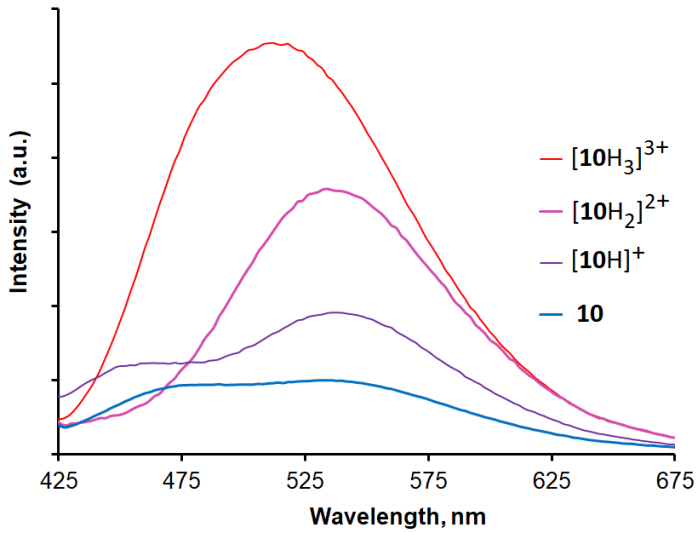

Figure S24. Calculated with the Specfit/32 program fluorescence spectra of **10**, $[\mathbf{10}H]^{+}$, $[\mathbf{10}H_2]^{2+}$ and $[\mathbf{10}H_3]^{3+}$ in water.

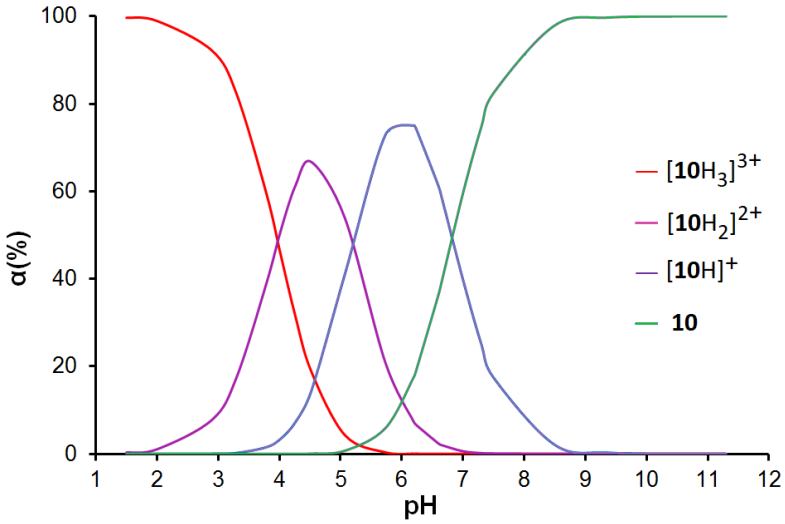

Figure S25. Distribution diagram of the protonated species of **10** calculated with the Specfit/32 program.

2.3 NMR studies of the compound 6

A

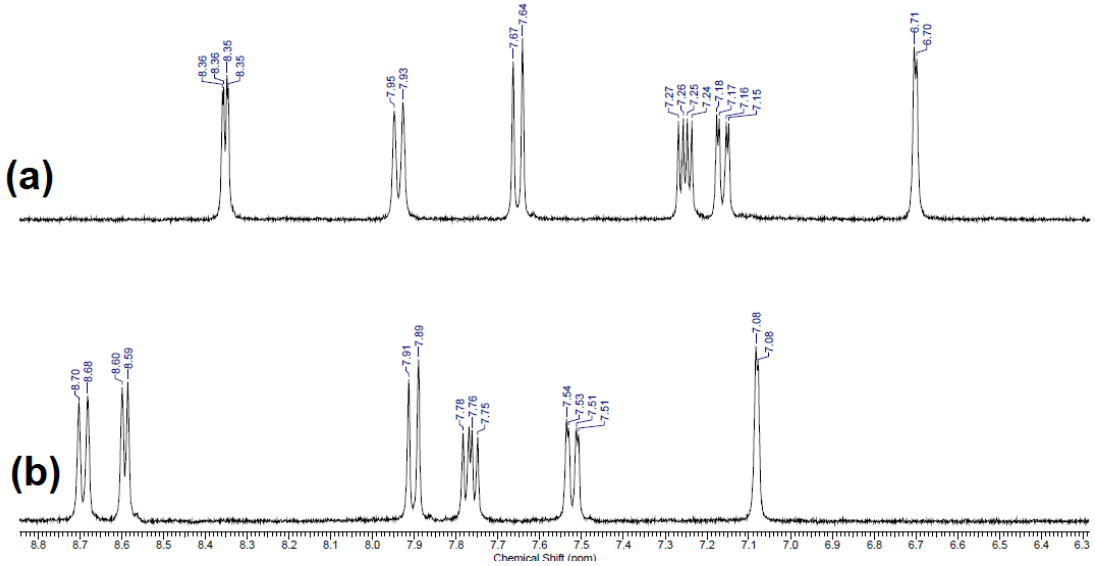

B

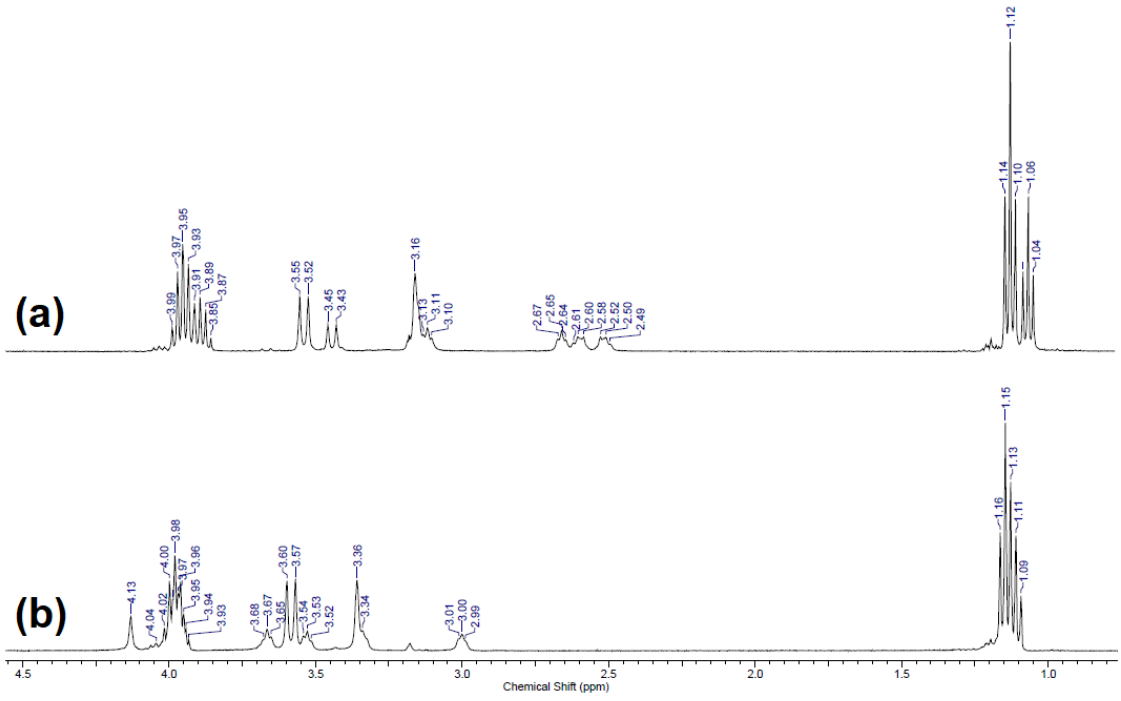

Figure S26. Aromatic (A) and aliphatic (B) regions of ^{1}H NMR (400 MHz) spectra of **6** in D_2O/MeOD (5:1 v/v, [**6**] = 0.04 M) at 298 K before (a) and after addition (b) addition of gaseous HCl.

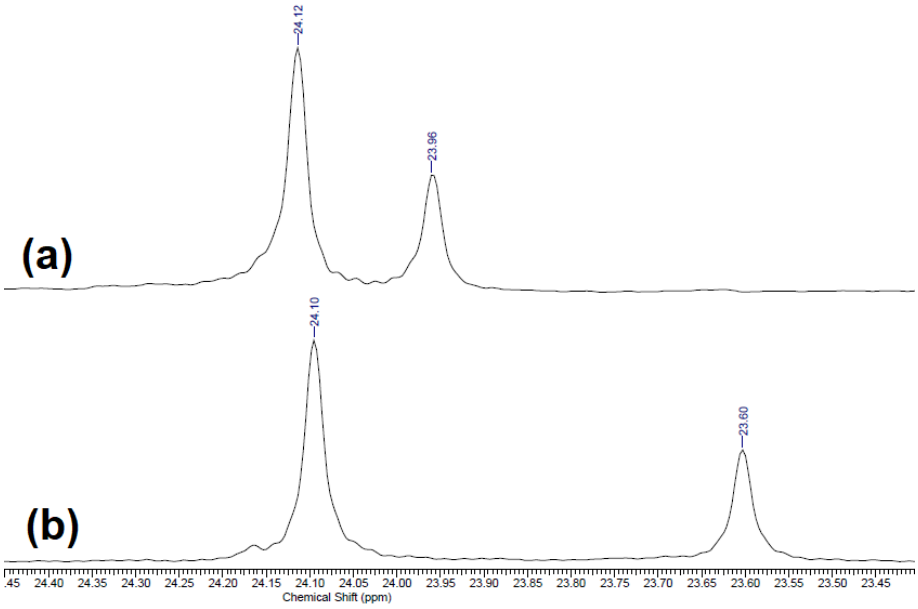

Figure S27. $^{31}P\{^{1}H\}$ NMR (162.5 MHz) spectra (a) of **6** in D_2O-MeOD (5:1 v/v, [**6**] = 0.04 M) at 298 K before (a) and after addition (b) addition of gaseous HCl.

3. Metal binding studies of compounds 5, 6 and 10

3.1 Fluorimetric and spectrophotometric studies of metal binding by compound 10

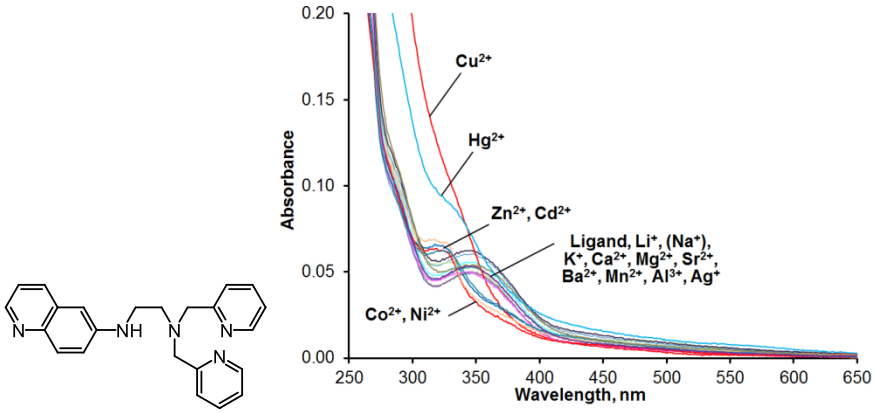

Figure S28. UV–vis spectra of **10** ([**10**] = 20 μM, 0.03M HEPES buffer, 2% MeOH, pH = 7.4) before and after addition of 5 equiv. of metal perchlorates.

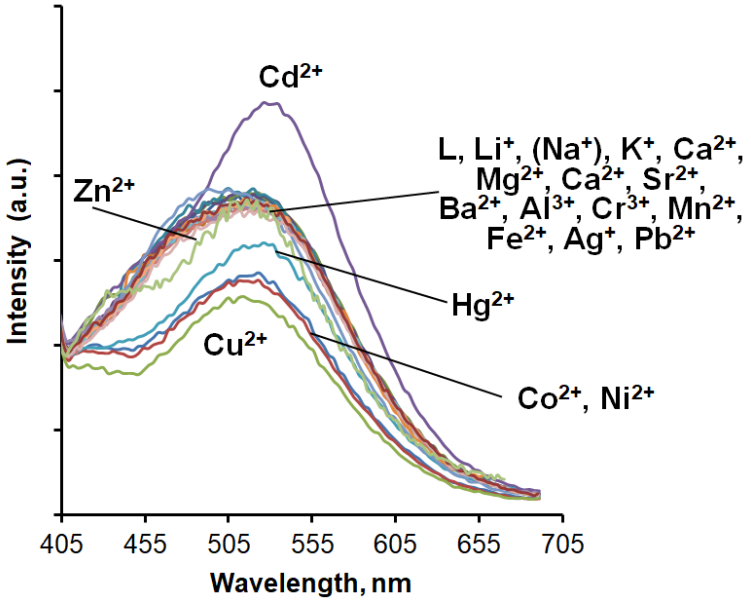

Figure S29. Fluorescence spectra of **10** ([**10**] = 20 μM, 0.03M HEPES buffer, 2% MeOH, pH = 7.4, λ_{ex} = 345 nm) before and after addition of 5 equiv. of metal perchlorates.

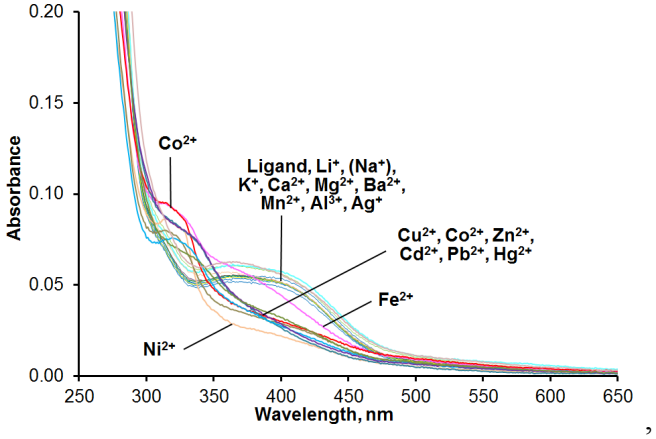

Figure S30. UV–vis spectra of **10** ([**10**] = 27 μM, 0.03M acetate buffer, 2% MeOH pH = 5.0) before and after addition of 5 equiv. of metal perchlorates.

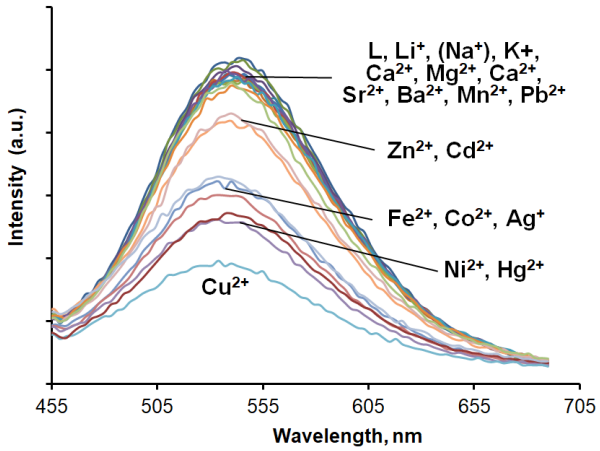

Figure S31. Fluorescence spectra of **10** ([**10**] = 27 μM, 0.03M acetate buffer, 2% MeOH, pH = 5.0, λ_{ex} = 385 nm) before and after addition of 5 equiv. of metal perchlorates.

3.2 Fluorimetric and spectrophotometric studies of metal binding by compound 5

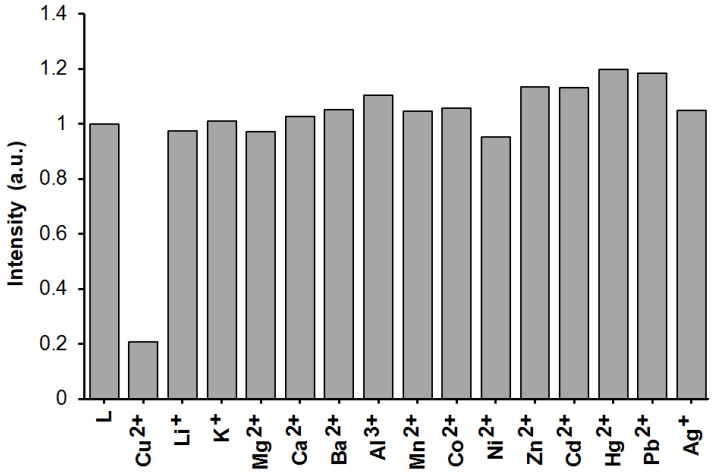

Figure S32. Normalized (to the ligand emission) fluorescence intensity (λ = 551 nm) of ligand **5** ([**5**] = 27 μM in 0.03 M HEPES buffer at pH = 7.4 (λ_{ex} = 355 nm) and solutions obtained after addition of 1 equiv of metal perchlorates.

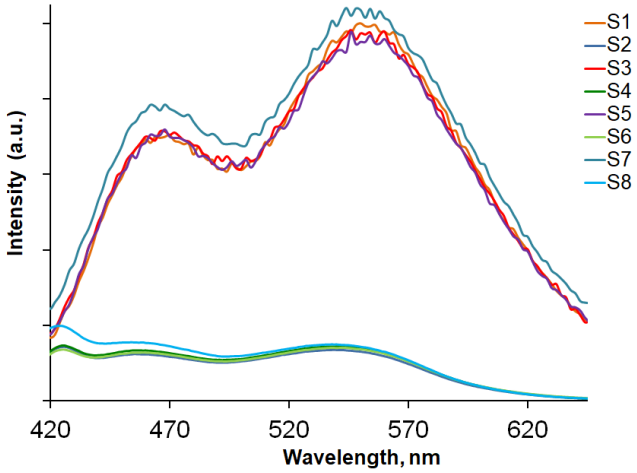

Figure S33. Cross-selectivity studies of metal ion binding by ligand **5** ([**5**] = 27 μM, 0.03M HEPES buffer, pH =7.4, λ_{ex} = 355 nm) using fluorescence spectroscopy:

(S1) emission spectrum of **5**,

(S2) emission spectrum of **5** after addition of Cu^{2+} (1 equiv),

(S3) emission spectrum of **5** after addition of Li^{+}, (Na^{+}), K^{+}, Mg^{2+}, Ca^{2+}, Ba^{2+}, Al^{3+} (1 equiv of each metal ion),

(S4) emission spectrum of **5** after addition of Li^{+}, (Na^{+}), K^{+}, Mg^{2+}, Ca^{2+}, Ba^{2+}, Al^{3+} (1 equiv of each metal ion) and Cu^{2+} (1 equiv)

(S5) emission spectrum of **5** after addition of Mn^{2+}, Co^{2+}, Ni^{2+}, Zn^{2+} (1 equiv of each metal ion),

(S6) emission spectrum of **5** after addition of Mn^{2+}, Co^{2+}, Ni^{2+}, Zn^{2+} (1 equiv of each metal ion) and Cu^{2+} (1 equiv)

(S7) emission spectrum of **5** after addition of Ag^{+}, Hg^{2+}, Cd^{2+}, Pb^{2+} (1 equiv of each metal ion),

(S8) emission spectrum of **5** after addition of Ag^{+}, Hg^{2+}, Cd^{2+}, Pb^{2+} (1 equiv of each metal ion) and Cu^{2+} (1 equiv)

Determination of stability constants

Spectrophotometric titration

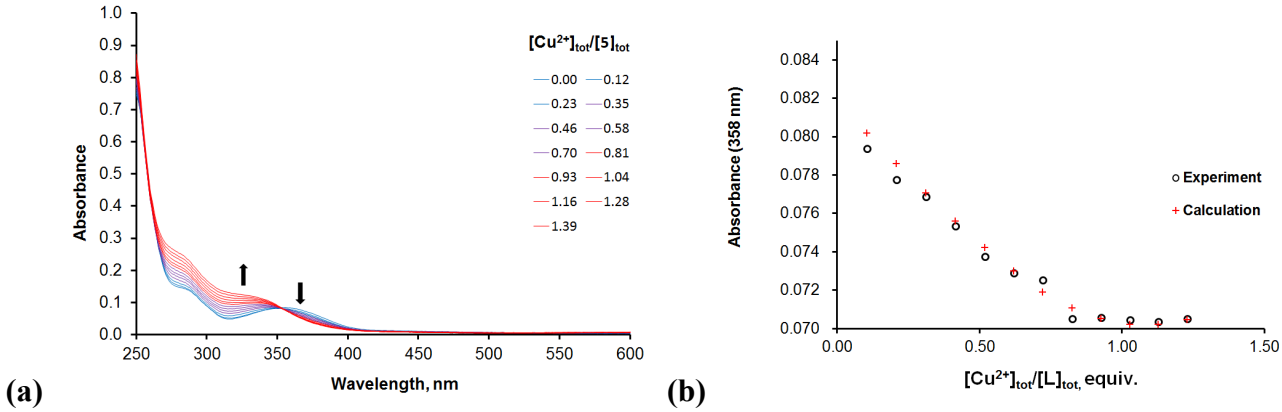

Figure S34. (a) Evolution of UV–vis spectrum of **5** ([**5**] = 27 μM, 0.03M HEPES buffer, pH = 7.4) upon addition of $Cu(ClO_4)_2$ (0–1.4 equiv.). **(b)** Changes of absorbance against $[Cu^{2+}]_{tot}$ /$[\mathbf{5}]_{tot}$ ratio at 358 nm.

Model for calculation:

$L \leftrightarrow LH^{+} \leftrightarrow LH_2^{2+}$, $Cu^{2+} + L \leftrightarrow [CuL]^{2+}$, $Cu^{2+} \leftrightarrow Cu(OH)^{+} \leftrightarrow Cu_2(OH)_2^{2+} \leftrightarrow Cu(OH)_2$

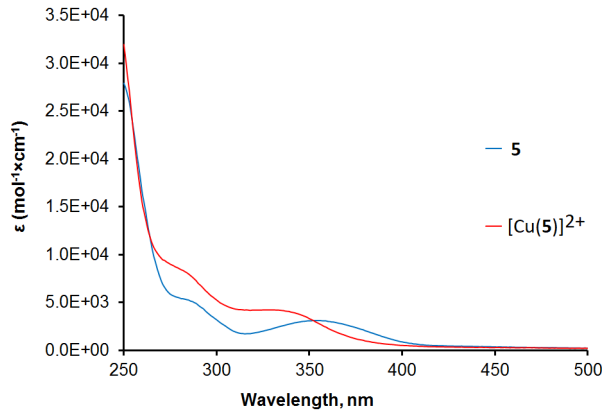

Figure S35. Calculated with the Specfit/32 program UV–vis spectra of **5** and $[Cu(\mathbf{5})]^{2+}$ in 0.03M HEPES buffer at pH = 7.4.

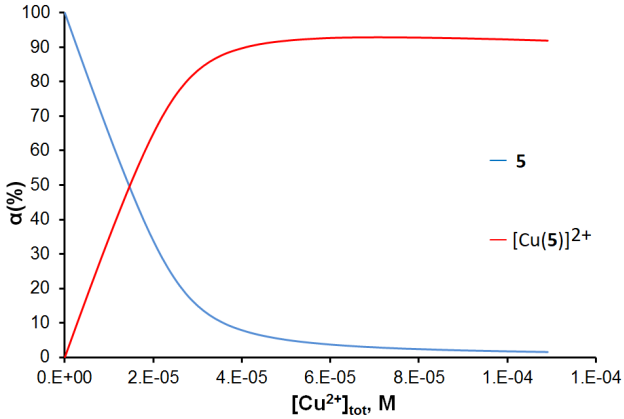

Figure S36. Distribution diagram of **5** complexes formed with Cu^{II} ([**5**] = 27 μM, 0.03M HEPES buffer, pH = 7.4) calculated with the Specfit/32 program.

Fluorescence titration

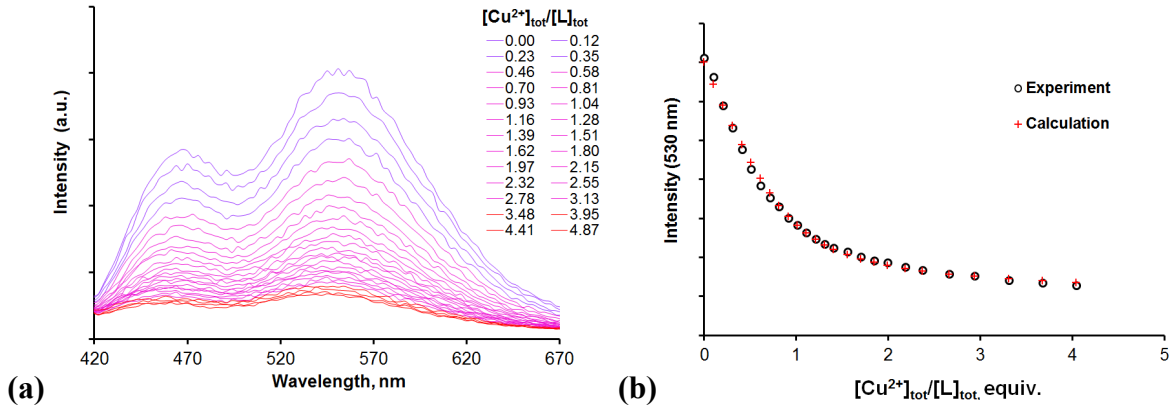

Figure S37. (a) Evolution of fluorescence spectrum of **5** ([**5**] = 27 μM, 0.03M HEPES buffer, pH=7.4, λ_{ex} = 355 nm) upon addition of $Cu(ClO_4)_2$ (0 – 4.87 equiv.). **(b)** Changes of fluorescence intensity against $[Cu^{2+}]_{tot}/[\mathbf{5}]_{tot}$ ratio at 550 nm.

Model for calculation:

$L \leftrightarrow LH^{+} \leftrightarrow LH_2^{2+}$, $Cu^{2+} + L \leftrightarrow [CuL]^{2+}$, $Cu^{2+} \leftrightarrow Cu(OH)^{+} \leftrightarrow Cu_2(OH)_2^{2+} \leftrightarrow Cu(OH)_2$

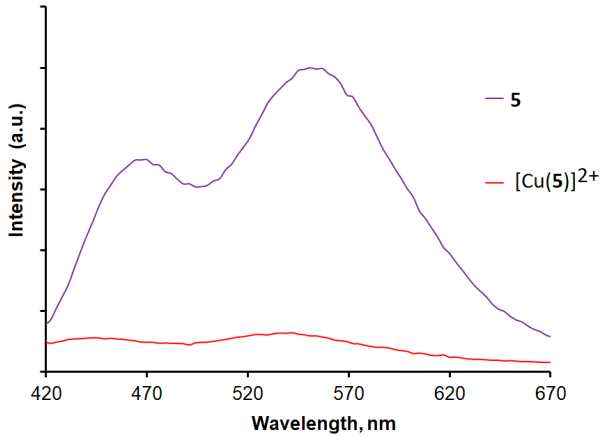

Figure S38. Calculated with the Specfit/32 program fluorescence spectra of **5** and $[Cu(\mathbf{5})]^{2+}$ in water.

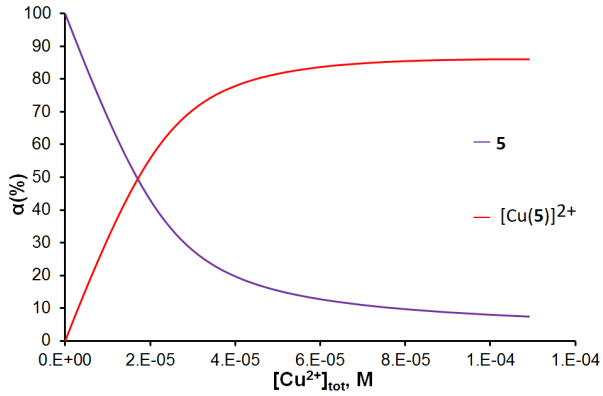

Figure S39. Species distribution diagram for the **5**/Cu^{2+} system in water calculated with the Specfit/32 program.

3.3. Fluorimetric and spectrophotometric studies of metal binding by the compound 6

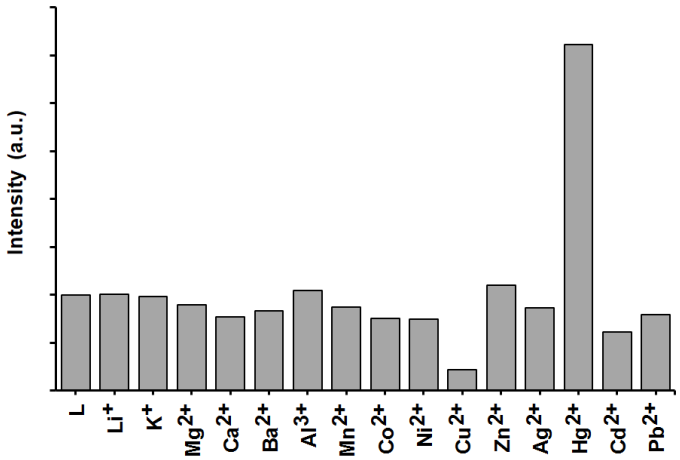

Figure S40. Fluorescence intensity of **6** ([**6**] = 20 μM, 0.03M HEPES buffer, pH=7.4, λ_{ex} = 356 nm) before and after addition of 1 equiv of metal perchlorates solutions at 548 nm.

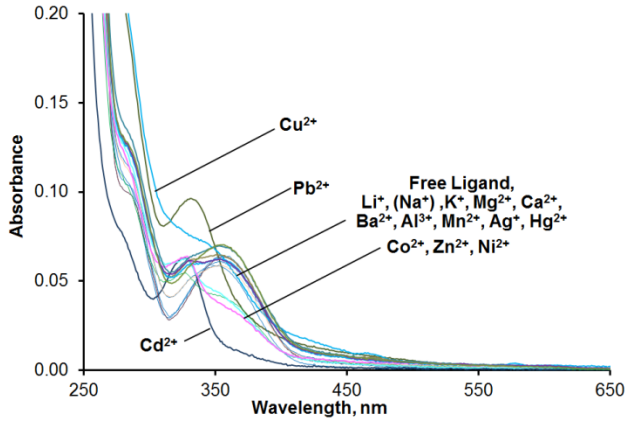

Figure S41. UV–vis spectra of **6** ([**6**] = 20 μM, 0.03M HEPES buffer, pH=7.4) before and after addition of 1 equiv of metal perchlorates.

Cross-selectivity studies

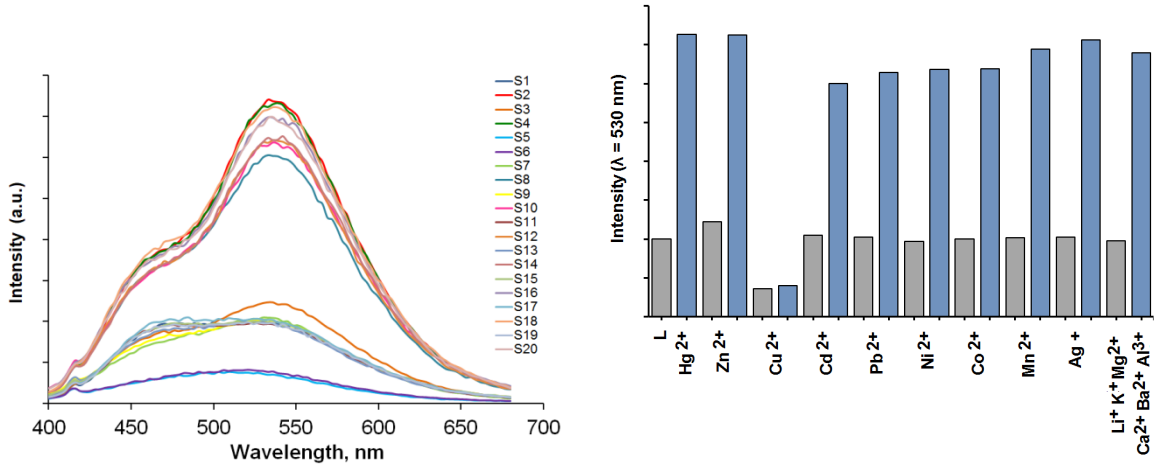

Figure S42. Cross-selectivity studies of metal ion binding by ligand **8** ([**8**] = 20 μM, 0.03M HEPES buffer, pH=7.4, λ_{ex} = 356 nm) using fluorescence spectroscopy:

(S1) emission spectrum of **6**,

(S2) emission spectrum of **6** after addition of Hg^{2+} (1 equiv.),

(S3) emission spectrum of **6** after addition of Zn^{2+} (1 equiv.),

(S4) emission spectrum of **6** after addition of Zn^{2+} (1 equiv.), and Hg^{2+} (1 equiv.)

(S5) emission spectrum of **6** after addition of Cu^{2+} (1 equiv.),

(S6) emission spectrum of **6** after addition of Cu^{2+} (1 equiv.), and Hg^{2+} (1 equiv.)

(S7) emission spectrum of **6** after addition of Cd^{2+} (1 equiv.),

(S8) emission spectrum of **6** after addition of Cd^{2+} (1 equiv.), and Hg^{2+} (1 equiv.)

(S9) emission spectrum of **6** after addition of Pb^{2+} (1 equiv.),

(S10) emission spectrum of **6** after addition of Pb^{2+} (1 equiv.), and Hg^{2+} (1 equiv.)

(S11) emission spectrum of **6** after addition of Ni^{2+} (1 equiv.),

(S12) emission spectrum of **6** after addition of Ni^{2+} (1 equiv.), and Hg^{2+} (1 equiv.)

(S13) emission spectrum of **6** after addition of Co^{2+} (1 equiv.),

(S14) emission spectrum of **6** after addition of Co^{2+} (1 equiv.), and Hg^{2+} (1 equiv.)

(S15) emission spectrum of **6** after addition of Mn^{2+} (1 equiv.),

(S16) emission spectrum of **6** after addition of Mn^{2+} (1 equiv.), and Hg^{2+} (1 equiv.)

(S17) emission spectrum of **6** after addition of Ag^{+} (1 equiv.),

(S18) emission spectrum of **6** after addition of Ag^{+} (1 equiv.), and Hg^{2+} (1 equiv.)

(S19) emission spectrum of **6** after addition of Li^{+}, (Na^{+}), K^{+}, Mg^{2+}, Ca^{2+}, Ba^{2+}, Al^{3+} (1 equiv. of each metal ion),

(S20) emission spectrum of **6** after addition of Li^{+}, (Na^{+}), K^{+}, Mg^{2+}, Ca^{2+}, Ba^{2+}, Al^{3+} (1 equiv. of each metal ion) and Hg^{2+} (1 equiv.)

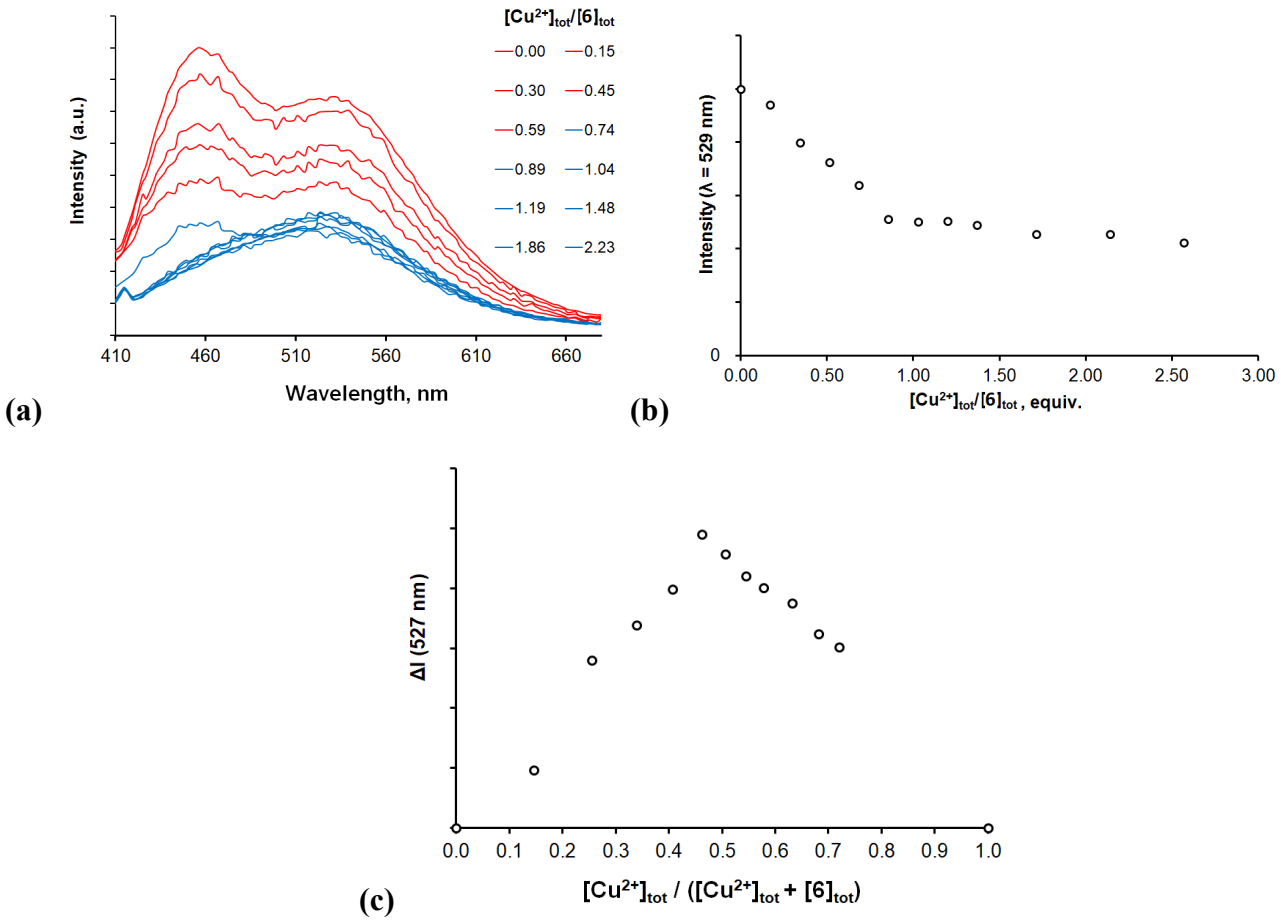

Figure S43. (a) Evolution of fluorescence spectrum of **6** ([**6**] = 13 μM, 0.03M HEPES buffer, pH=7.4, λ_{ex} = 356 nm) upon addition of $Cu(ClO_4)_2$ (0–2.5 equiv.). **(b)** Changes of fluorescence intensity against $[Cu^{2+}]_{tot}$ /$[\mathbf{6}]_{tot}$ ratio at 529 nm. **(c)** Job's plot derived from the titration curve {P. MacCarthy, *Anal. Chem.*, 1978, 50(14), 2165}.

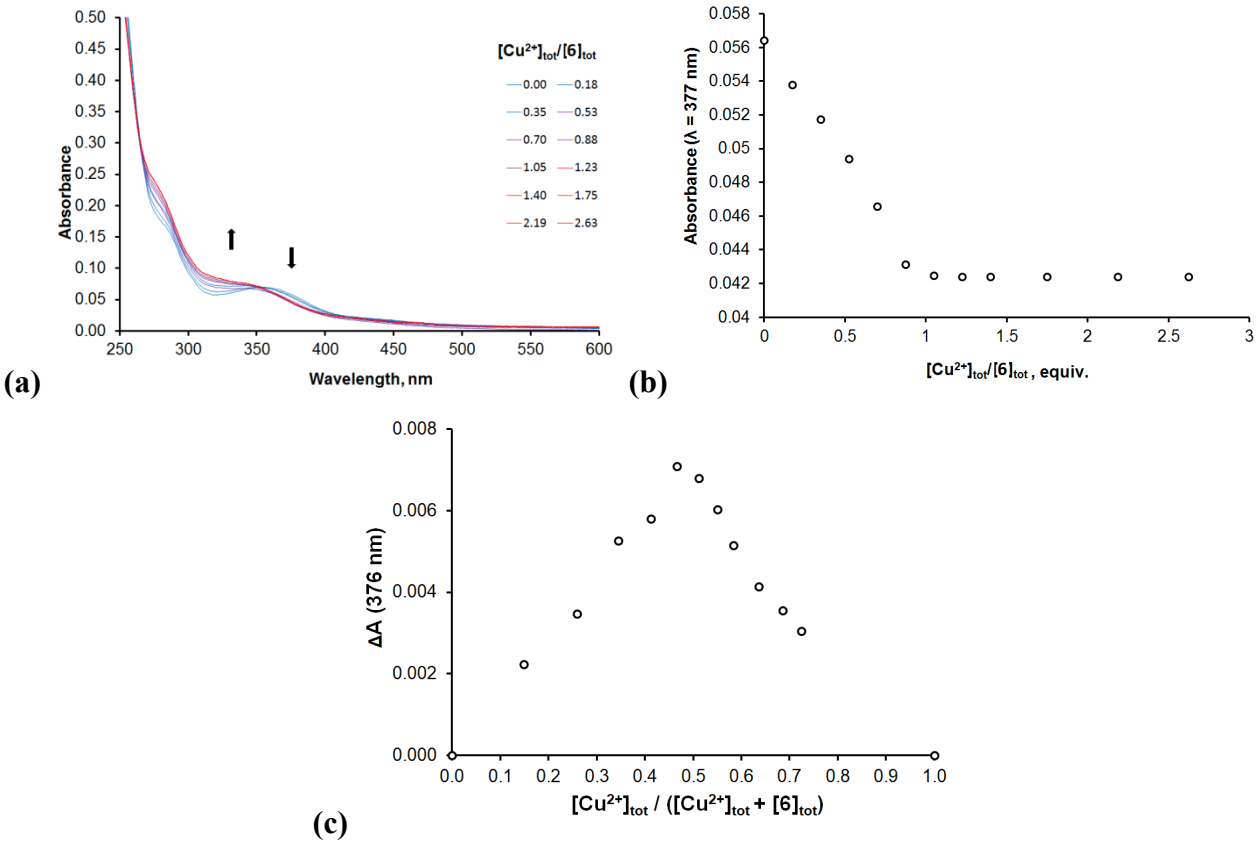

Figure S44. (a) Evolution of UV–vis spectrum of **6** ([**6**] = 15 μM, 0.03M HEPES buffer, pH=7.4) upon addition of $Cu(ClO_4)_2$ (0 – 2.5 equiv.). **(b)** Changes of absorbance against $[Hg^{2+}]_{tot}$ /$[\mathbf{6}]_{tot}$ ratio at 377 nm. **(c)** Job's plot derived from the titration curve {P. MacCarthy, *Anal. Chem.*, **1978**, *50*, 2165}.

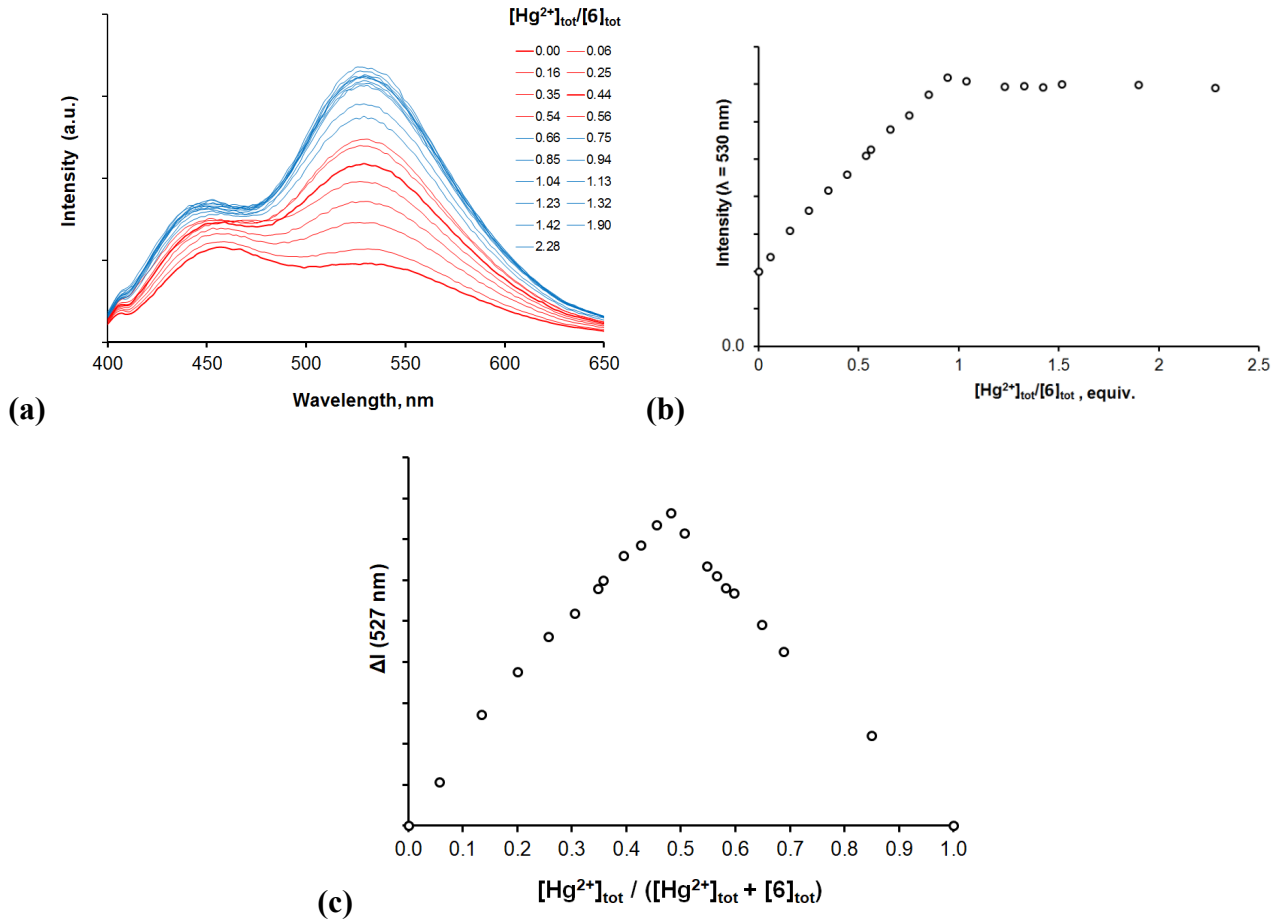

Figure S45. (a) Evolution of fluorescence spectrum of **6** ([**6**] = 20 μM, 0.03M HEPES buffer, pH=7.4, λ_{ex} = 356 nm) upon addition of $Hg(ClO_4)_2$ (0–2.5 equiv.); **(b)** Changes of fluorescence intensity against $[Hg^{2+}]_{tot}$ /$[\mathbf{6}]_{tot}$ ratio at 530 nm. **(c)** Job's plot derived from the titration curve {P. MacCarthy, *Anal. Chem.*, **1978**, *50*, 2165}.

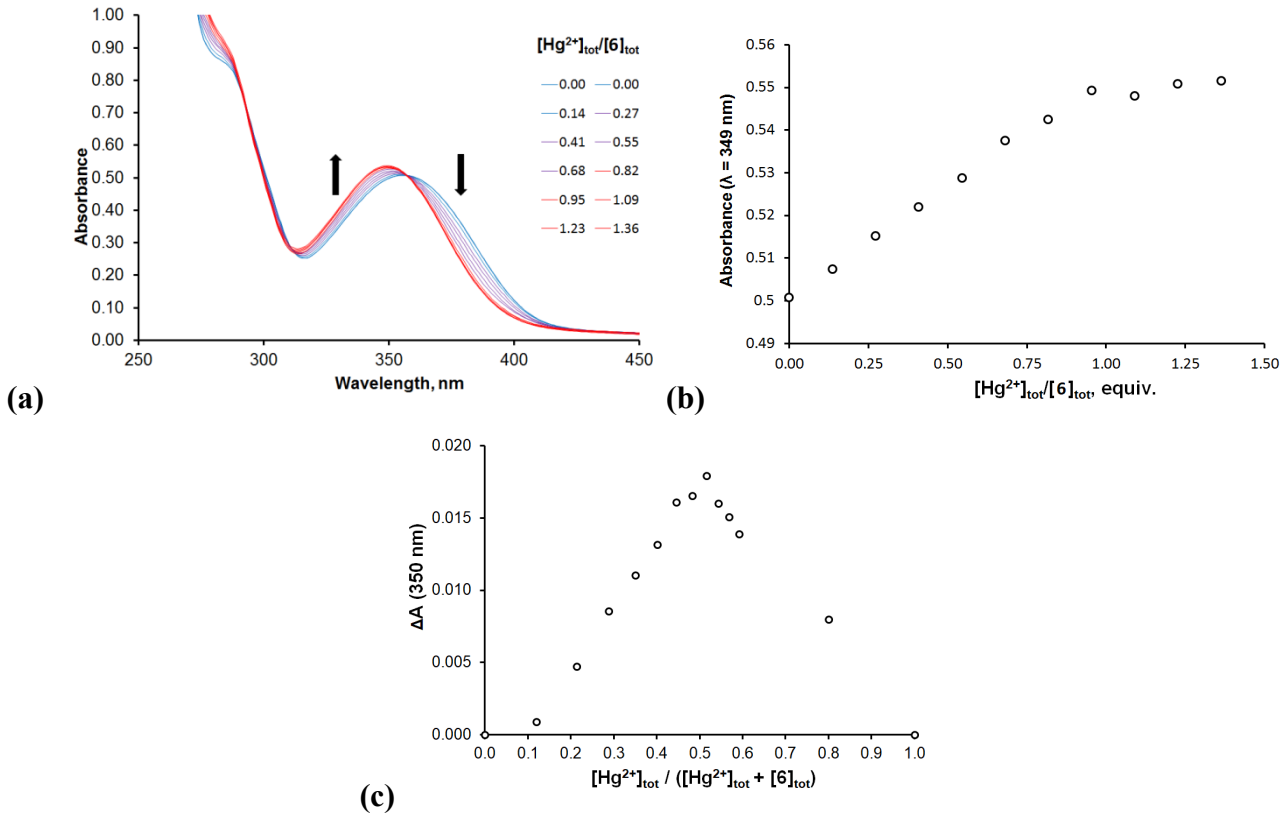

Figure S46. (a) Evolution of UV–vis spectrum of **6** ([**6**] = 196 μM, 0.03M HEPES buffer, pH=7.4) upon addition of $Hg(ClO_4)_2$ (0–1.5 equiv); **(b)** Changes of absorbance against $[Hg^{2+}]_{tot}$ /$[\mathbf{6}]_{tot}$ ratio at 349 nm. **(c)** Job's plot derived from the titration curve {P. MacCarthy, *Anal. Chem.*, **1978**, *50*, 2165}.

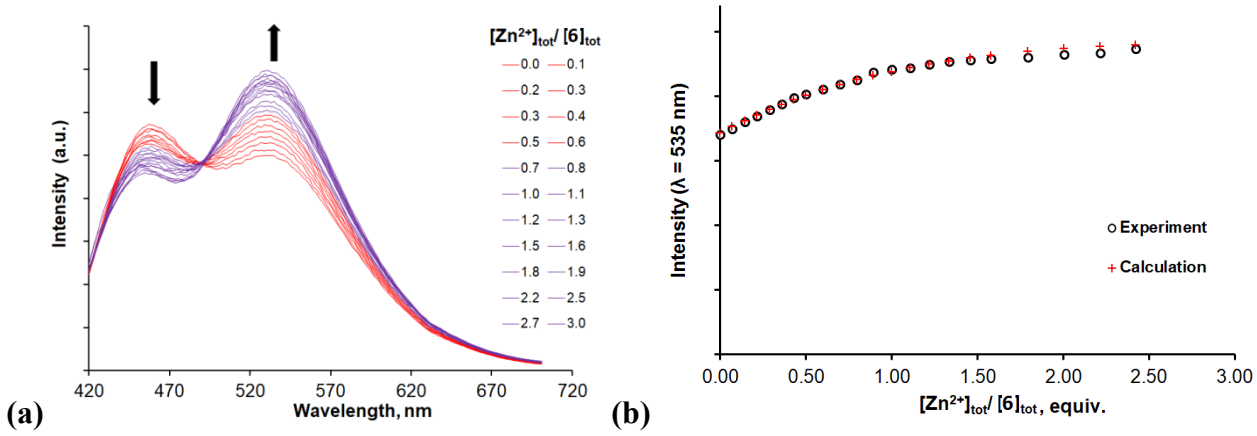

Figure S47. (a) Evolution of fluorescence spectrum of **6** ([**6**] = 20 μM, 0.03M HEPES buffer, pH=7.4, λ_{ex} = 356 nm) upon addition of $Zn(ClO_4)_2$ (0–3 equiv.); **(b)** Changes of fluorescence intensity against $[Zn^{2+}]_{tot}$ /$[\mathbf{6}]_{tot}$ ratio at 550 nm.

Model for calculation:

$L \leftrightarrow LH^{+} \leftrightarrow LH_2^{2+}$, $Zn^{2+} \leftrightarrow Zn(OH)^{+}$, $Zn^{2+} + L \leftrightarrow [ZnL]^{2+}$,

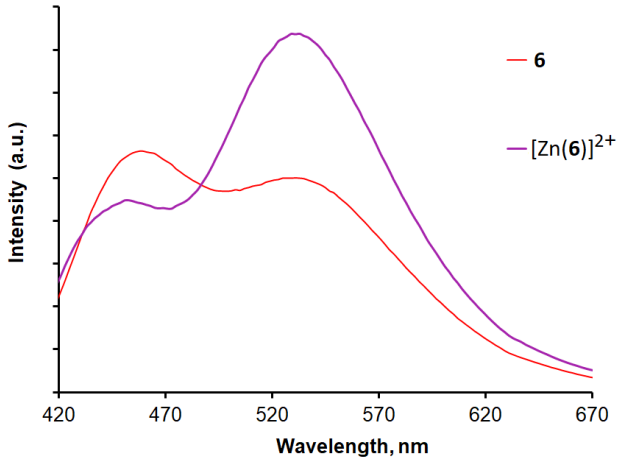

Figure S48. Calculated with the Specfit/32 program normalized fluorescence spectra of **6** and $[Zn(\mathbf{6})]^{2+}$ in water.

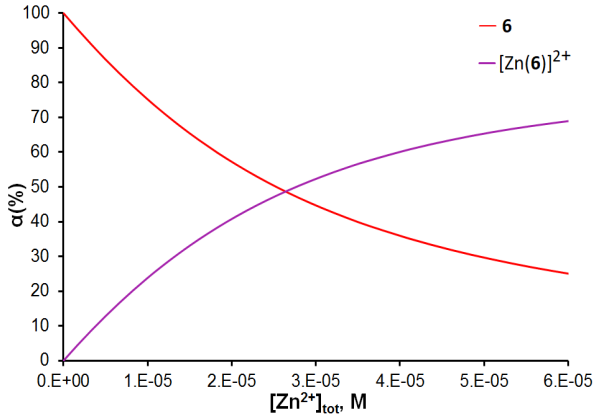

Figure S49. Species distribution diagram for the **6**/Zn^{2+} system in water calculated with the Specfit/32 program.

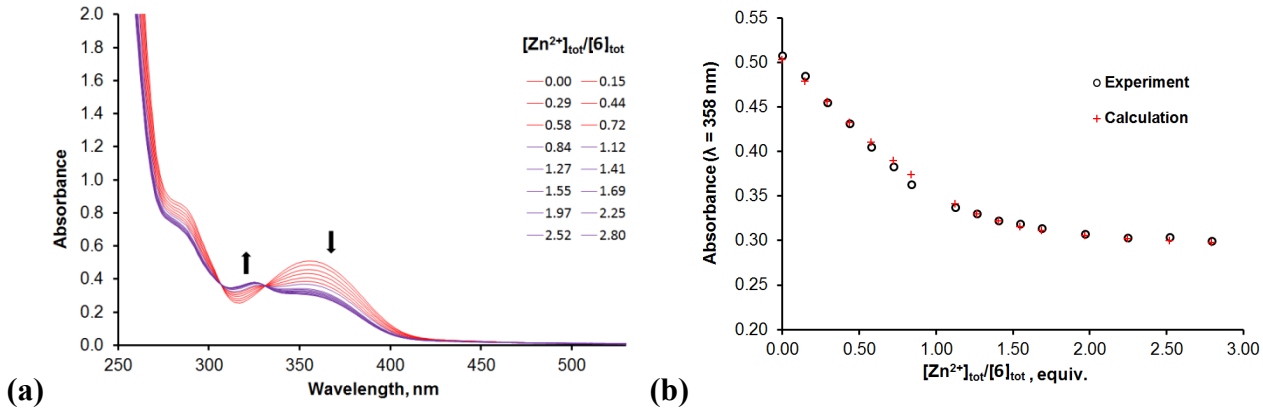

Figure S50. (a) Evolution of UV–vis spectrum of **6** ([**6**] = 160 μM, 0.03M HEPES buffer, pH=7.4) upon addition of $Cu(ClO_4)_2$ (0–2.8 equiv); (b) Changes of absorbance against $[Zn^{2+}]_{tot}/[\mathbf{6}]_{tot}$ ratio at 358 nm. Model for calculation: $L \leftrightarrow LH^+ \leftrightarrow LH_2^{2+}$, $Zn^{2+} \leftrightarrow Zn(OH)^+$, $Zn^{2+}+L \leftrightarrow [ZnL]^{2+}$.

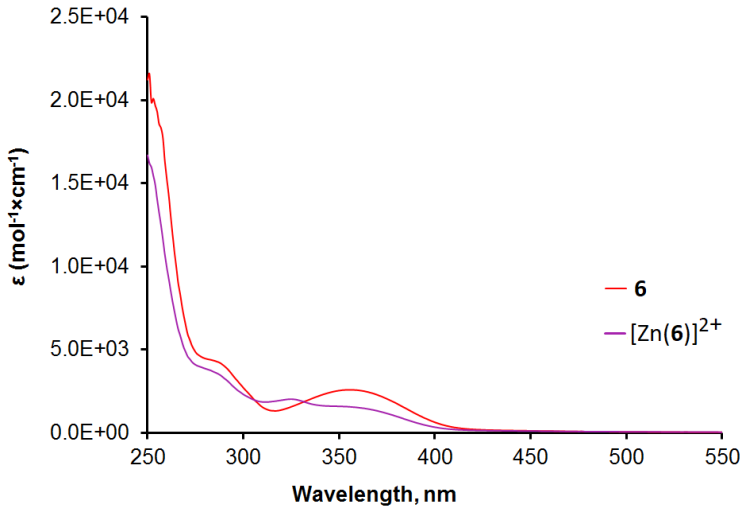

Figure S51. UV–vis spectra of **6** and $[Zn(\mathbf{6})]^{2+}$ in water calculated with the Specfit/32 program.

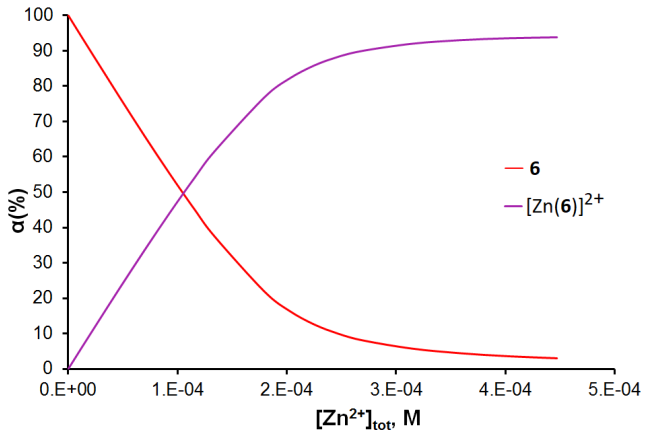

Figure S52. Species distribution diagram for the **6**/Zn^{2+} system in water calculated with the Specfit/32 program.

(a)

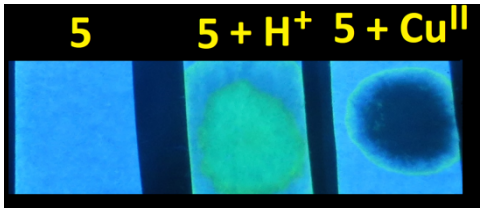

(b)

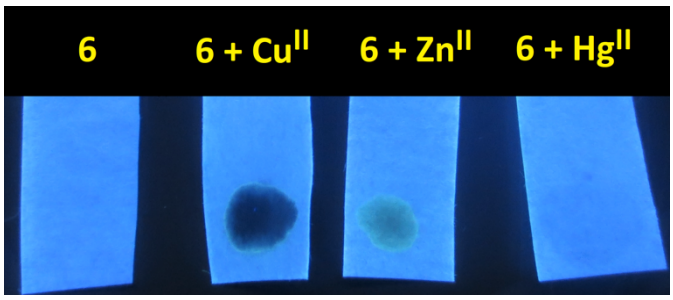

Figure S53. (a) Visual detection of Cu^{2+} and H^{+} using paper stripes with **5**. **(b)** Visual detection of Cu^{2+}, Zn^{2+}, Hg^{2+} and H^{+} using paper stripes with **6**.

4. Investigation of the structure of complexes

4.1. NMR-studies of $[Zn(6)]^{2+}$ complex

NMR-titration of ligand **6** with Zn(II) perchlorate

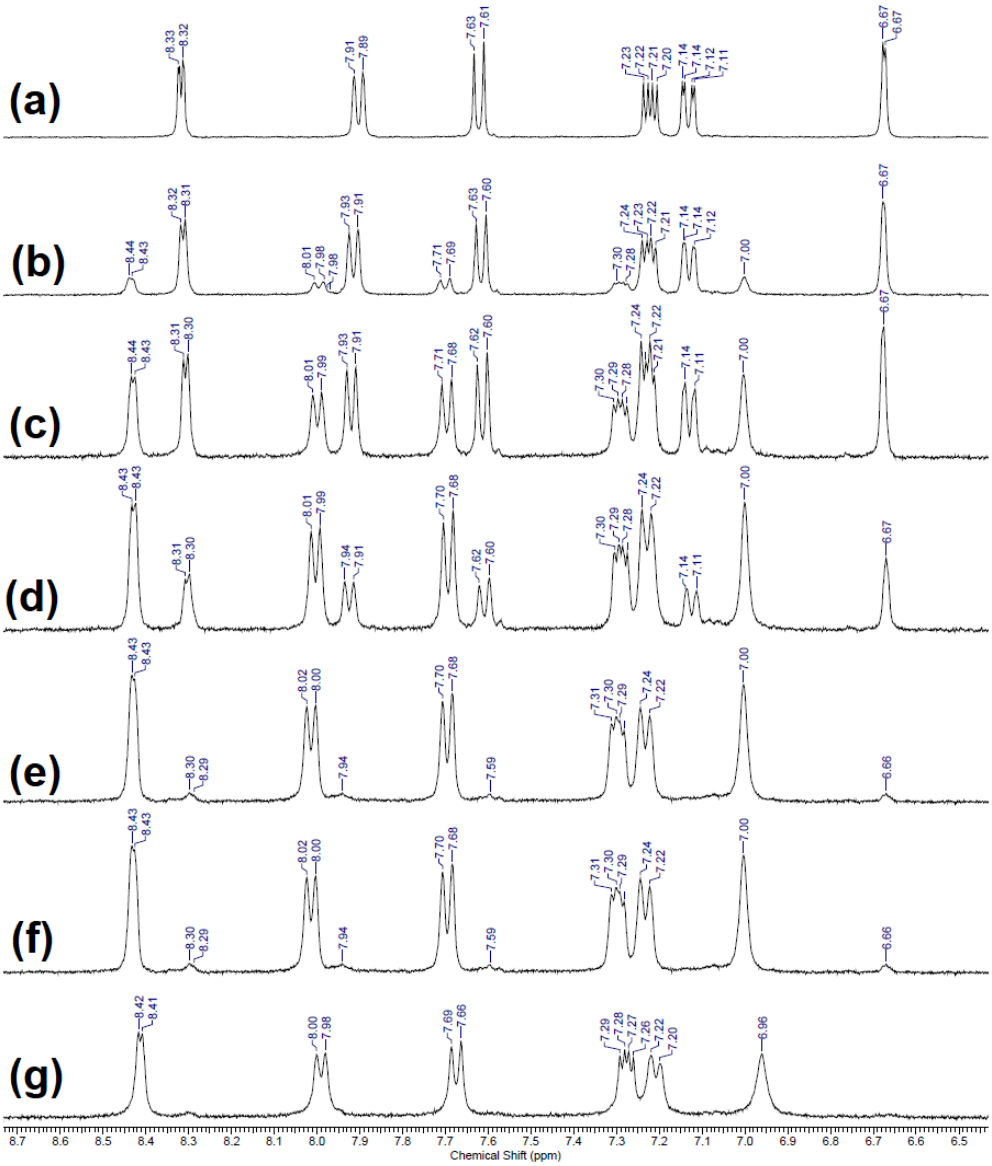

Figure S54. 400 MHz ^{1}H NMR spectra (aromatic) of **6** in D_2O/MeOD (5:1 v/v, [**6**] = 0.04 M) at 298 K before (a) and after addition of 0.2 (b), 0.4 (c), 0.6 (d), 0.8 (e), 1.0 (f) and 2.0 (g) equiv of zinc(II) perchlorate.

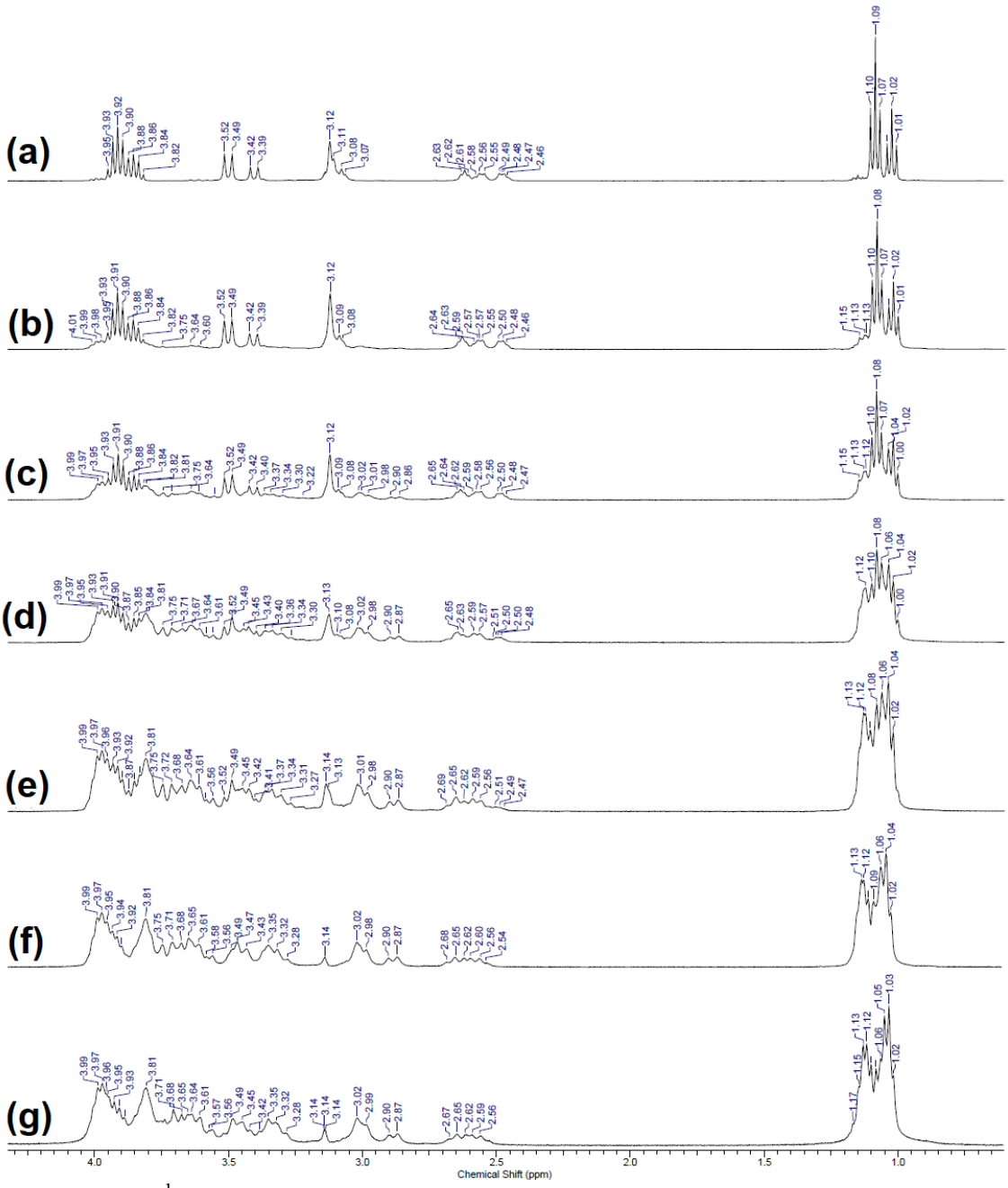

Figure S55. 400 MHz ^{1}H NMR spectra (aliphatic) of **6** in D_2O/MeOD (5:1 v/v, [**6**] = 0.04 M) at 298 K before (a) and after addition of 0.2 (b), 0.4 (c), 0.6 (d), 0.8 (e), 1.0 (f) and 2.0 (g) equiv of zinc(II) perchlorate.

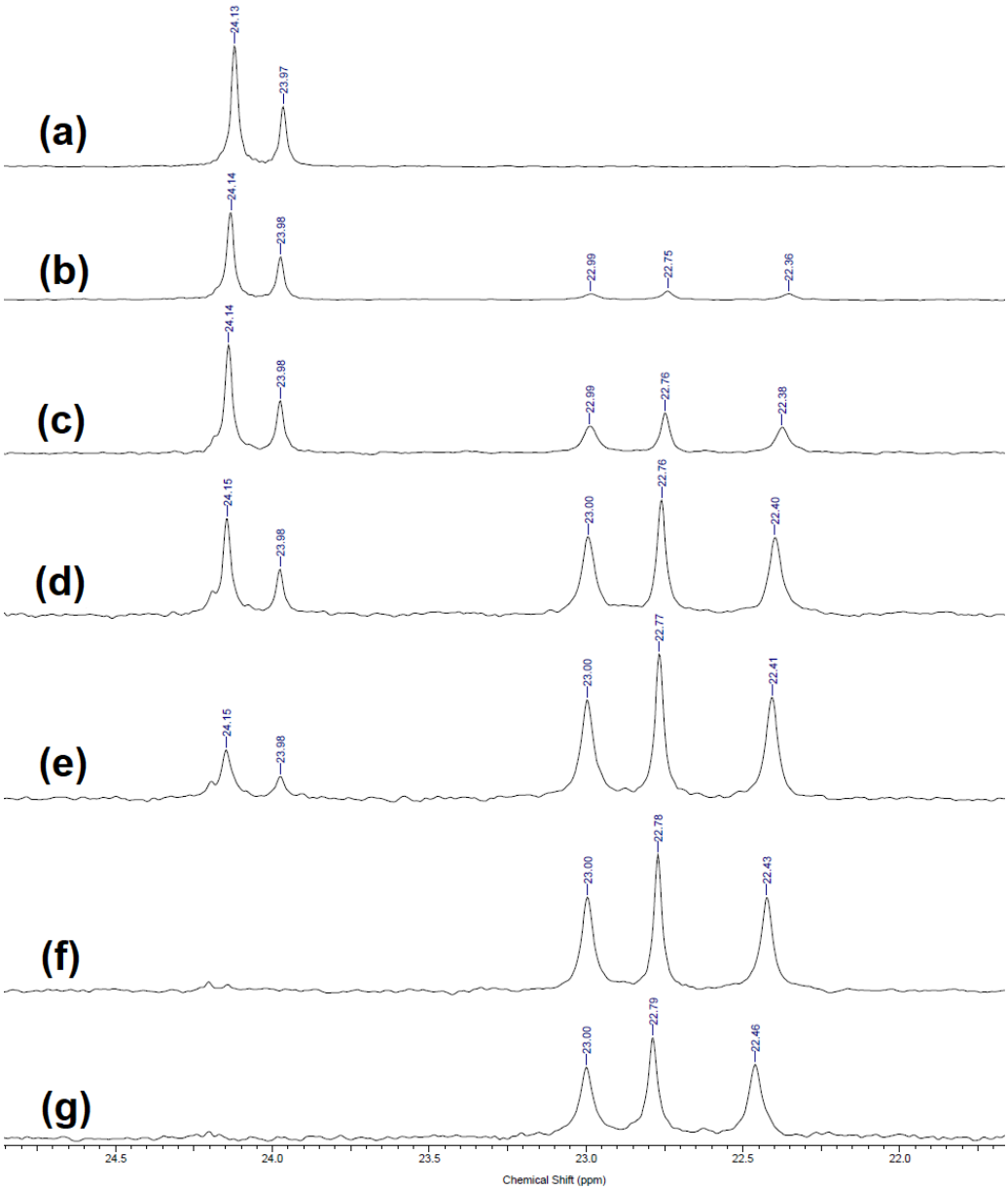

Figure S56. 162.5 MHz ^{31}P NMR spectra of **6** in D_2O/MeOD (5:1 v/v, [**6**] = 0.04 M) at 298 K before (a) and after addition of 0.2 (b), 0.4 (c), 0.6 (d), 0.8 (e), 1.0 (f), and 2.0 (g) equiv of zinc(II) perchlorate.

^{1}H–^{1}H COSY NMR spectra of [Zn(**6**)]$^{2+}$ complex

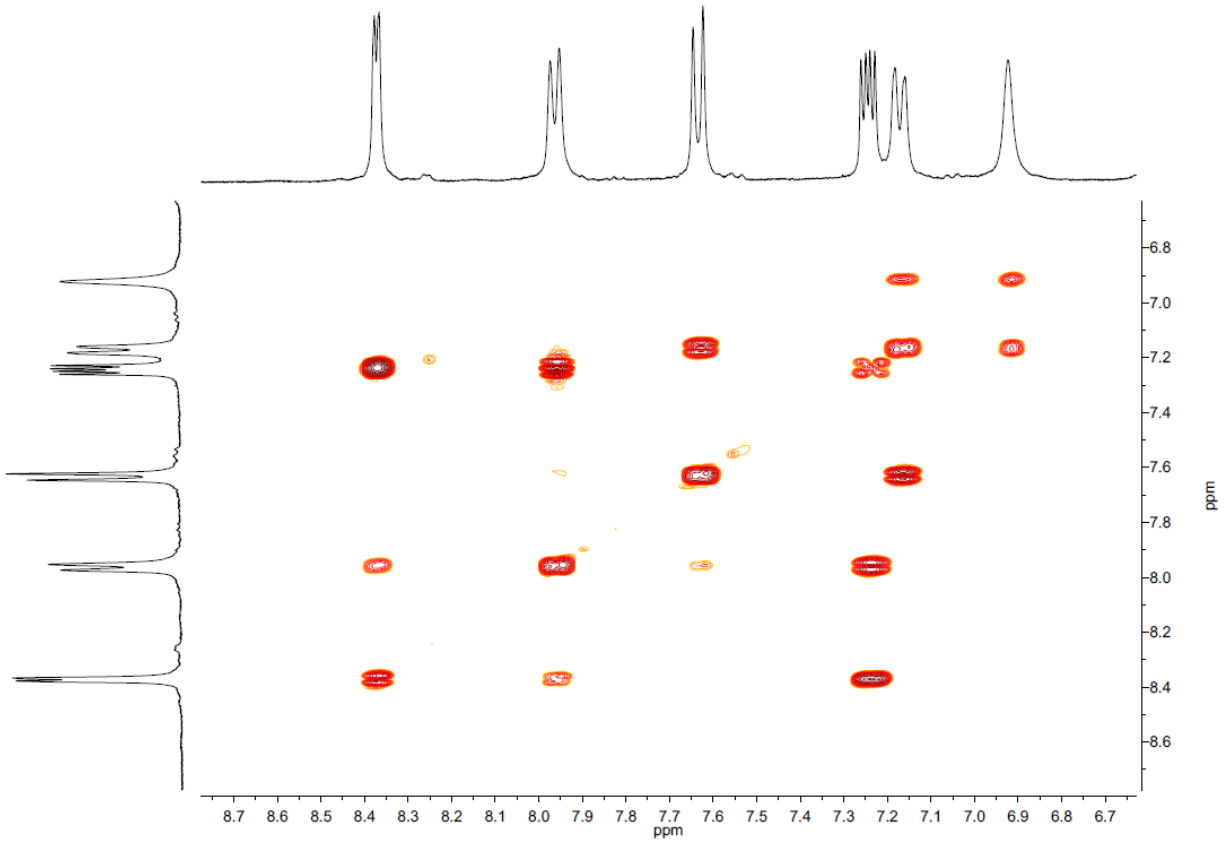

Figure S57. Aromatic region of ^{1}H–^{1}H COSY spectra (400 MHz) of complex [Zn(**6**)]$^{2+}$ in D_2O/MeOD (5:1 v/v) at 298 K.

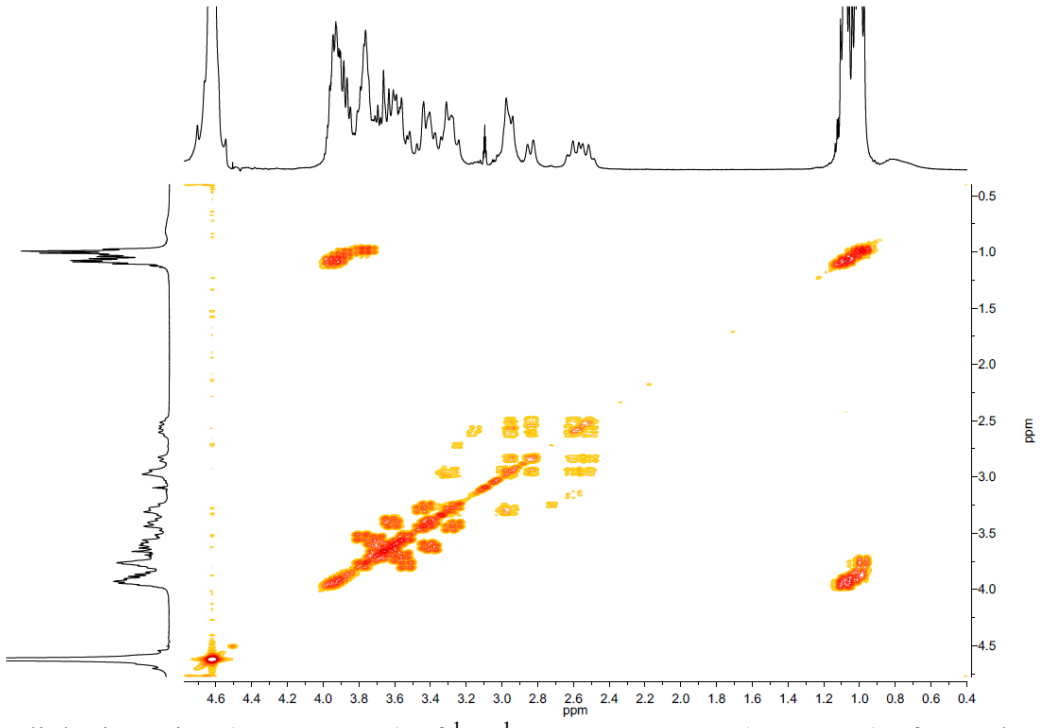

Figure S58. Aliphatic region (0.4–4.6 ppm) of ^{1}H–^{1}H COSY spectra (400 MHz) of complex [Zn(**6**)]$^{2+}$ in D_2O/MeOD (5:1 v/v) at 298 K.

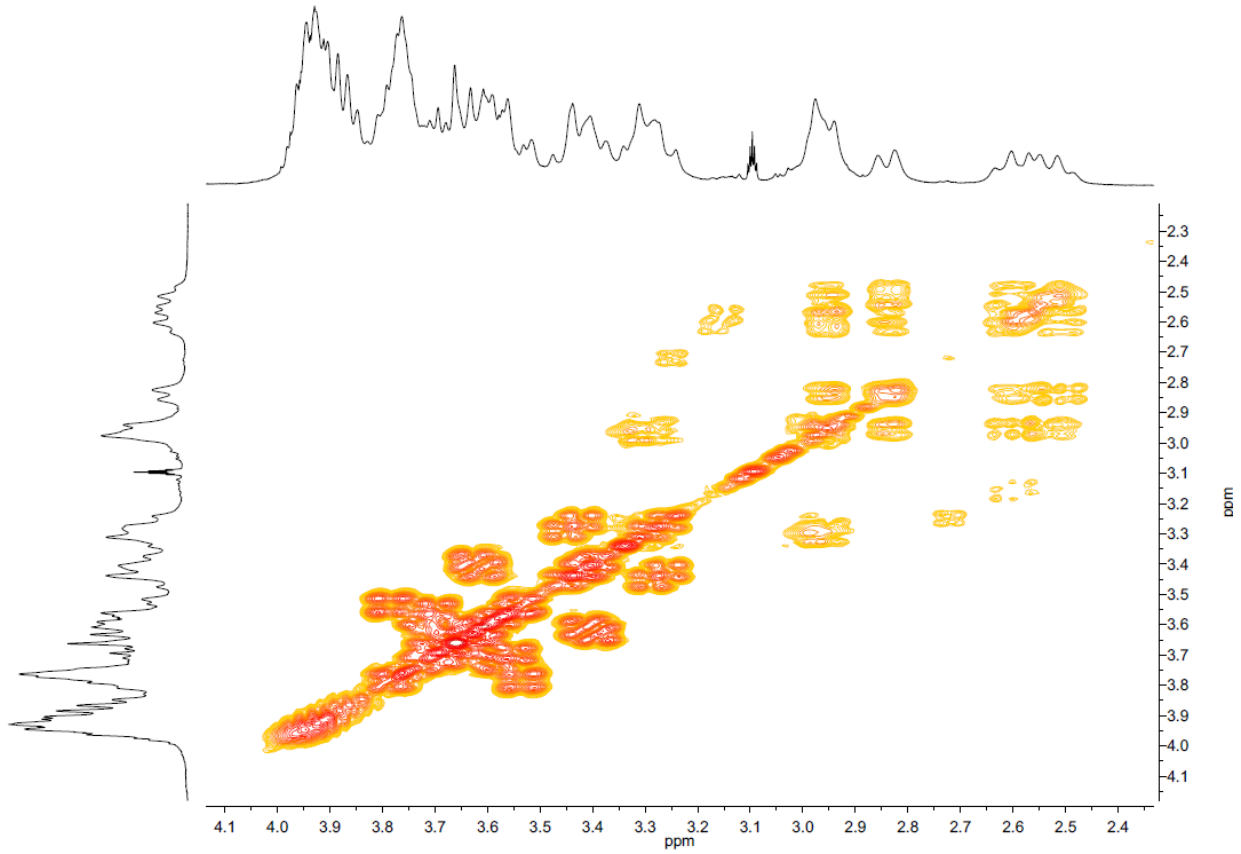

Figure S59. Aliphatic region (2.35–4.1 ppm) of ^{1}H–^{1}H COSY spectra (400 MHz) of complex [Zn(**6**)]$^{2+}$ in D_2O/MeOD (5:1 v/v) at 298 K.

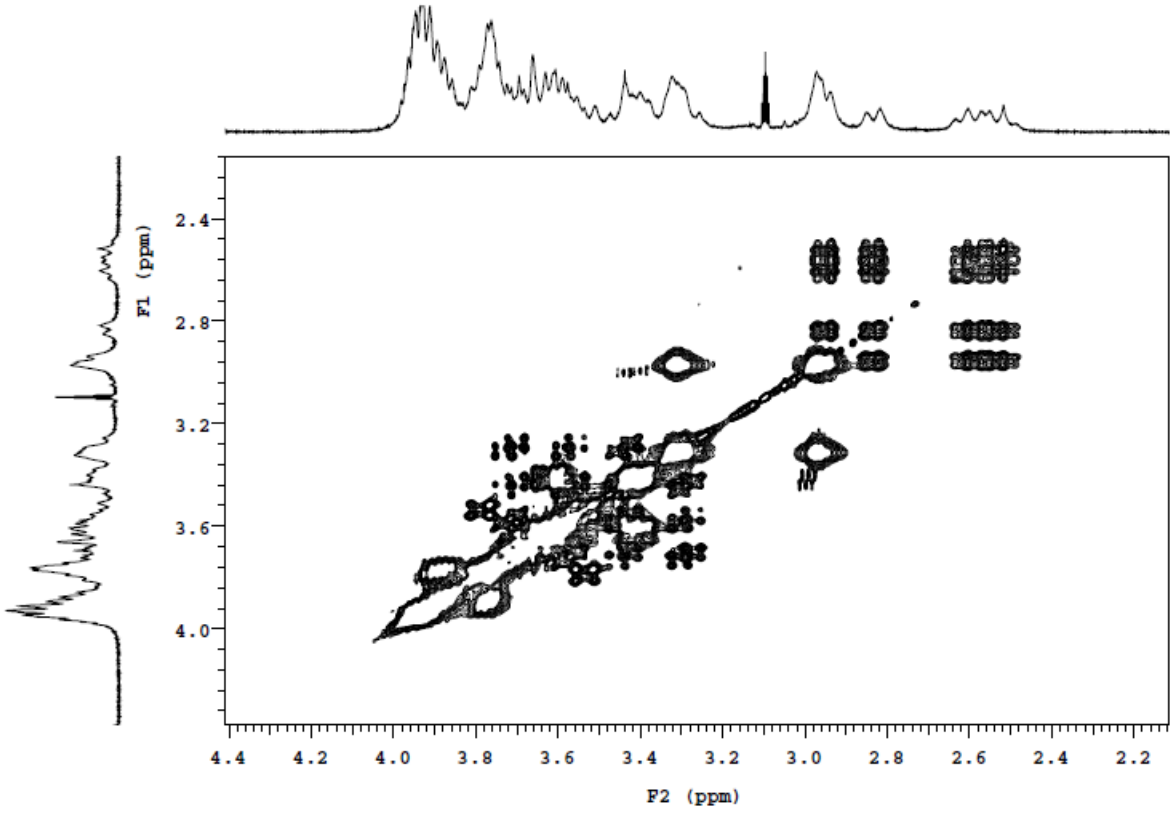

Figure S60. Aliphatic region of TOCSY spectra (400 MHz) of complex [Zn(**6**)]$^{2+}$ in D_2O/MeOD (5:1 v/v) at 298 K.

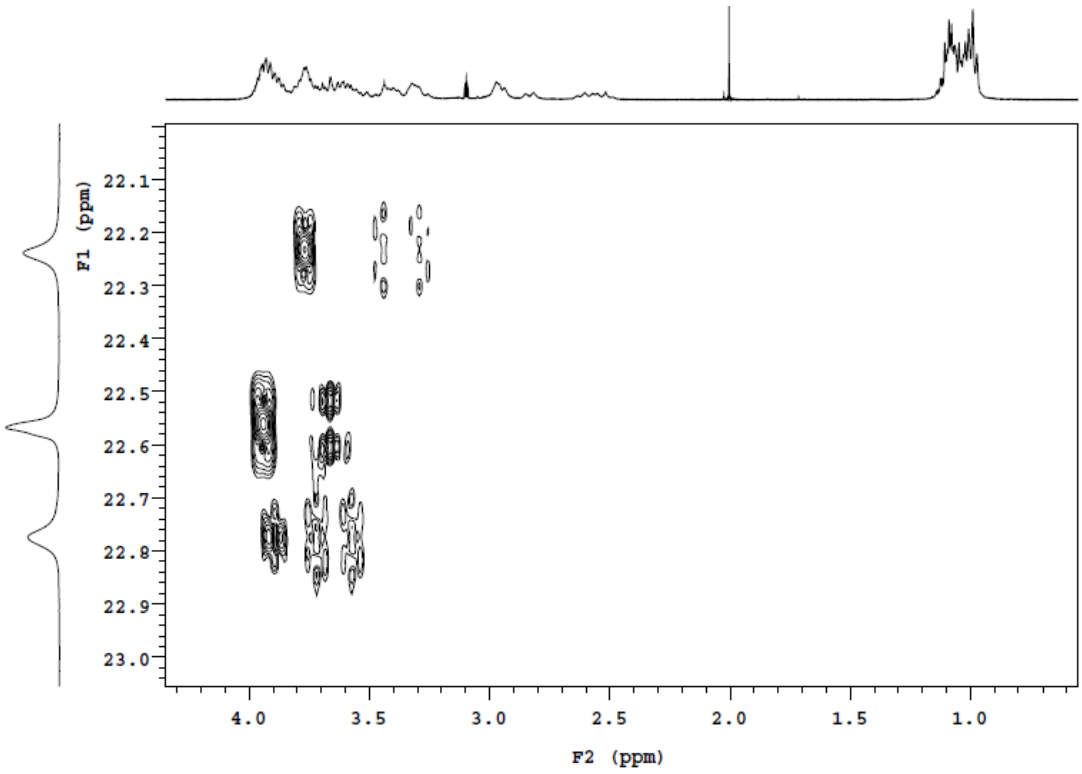

Figure S61. Aliphatic region (0.5–4.3 ppm) of gHMBCAD–{^{1}H–^{31}P} NMR spectra of [Zn(**6**)]$^{2+}$ complex in D_2O/MeOD (5:1 v/v) at 298 K.

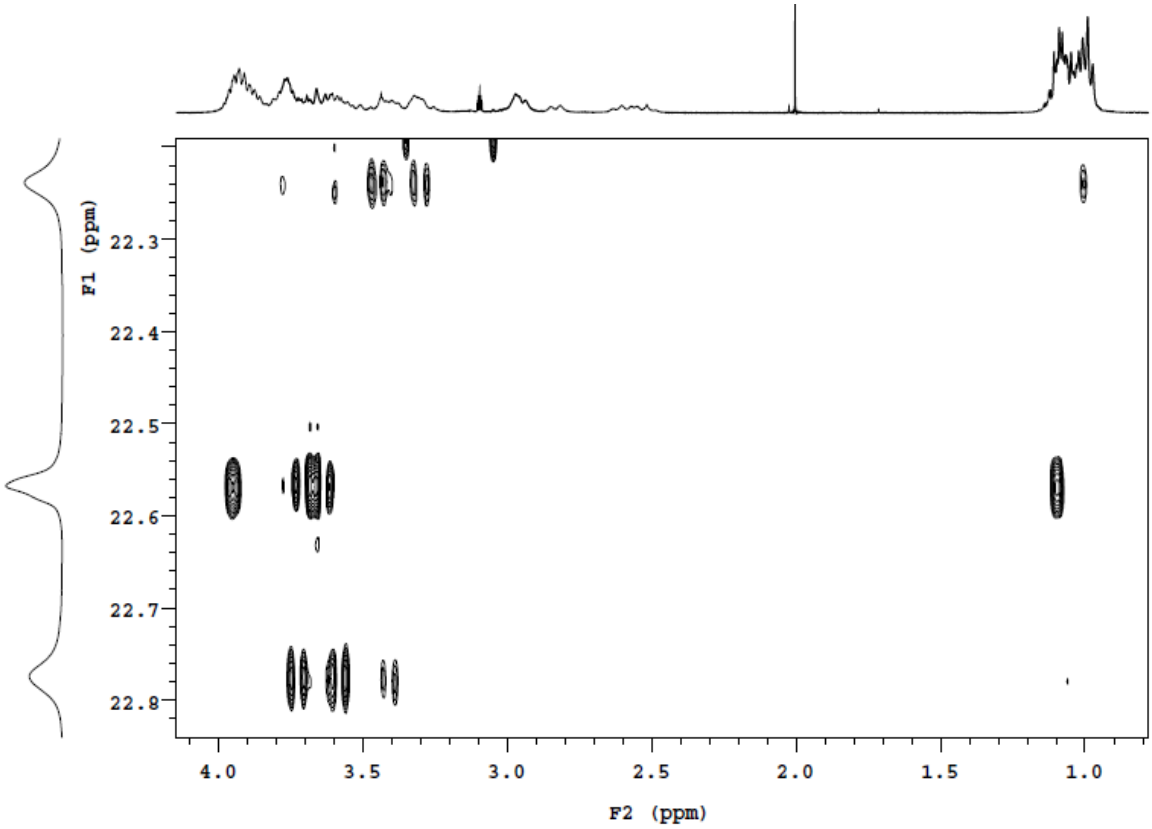

Figure S62. Aliphatic region (0.8–4.1 ppm) of LR-HMBCAD–{^{1}H–^{31}P} NMR spectra of [Zn(**6**)]$^{2+}$ complex in D_2O/MeOD (5:1 v/v) at 298 K. {R.T. Williamson, A.V. Buevich, G.E. Martin and T. Parella, *J. Org. Chem.*, **2014**, *79*, 3887-3894}.

(a)

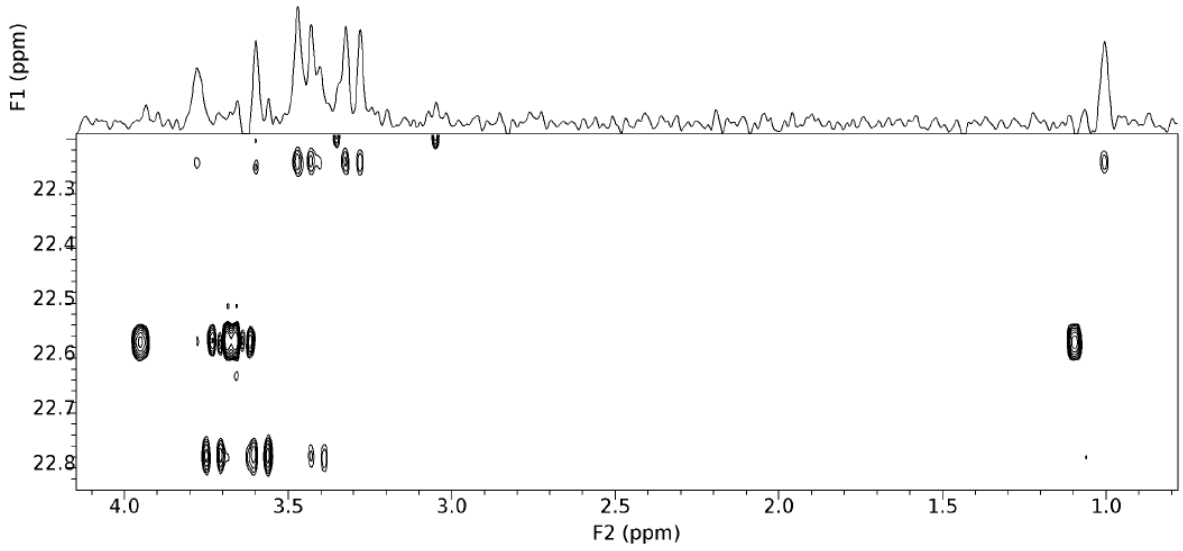

(b)

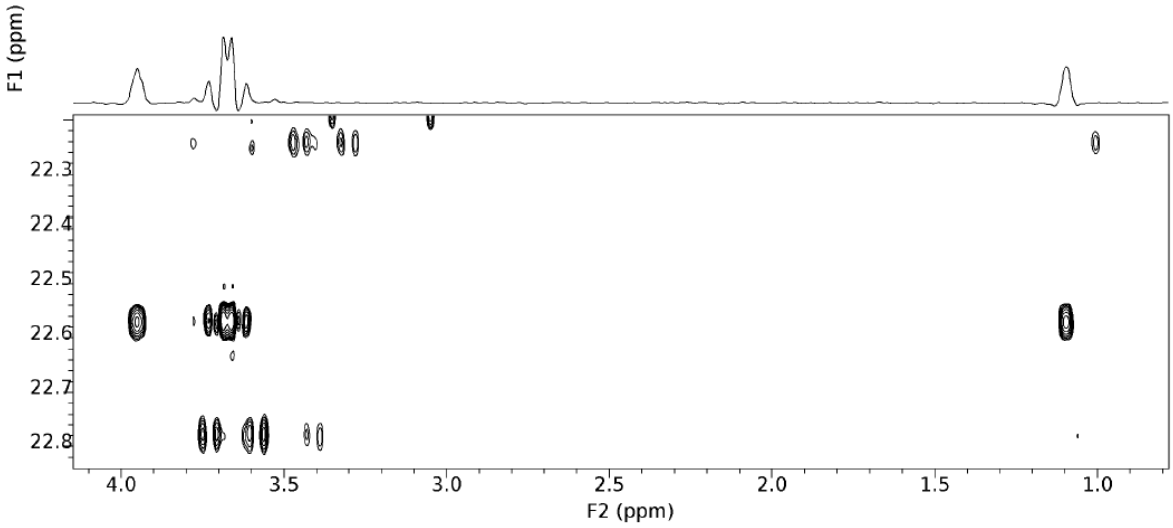

(c)

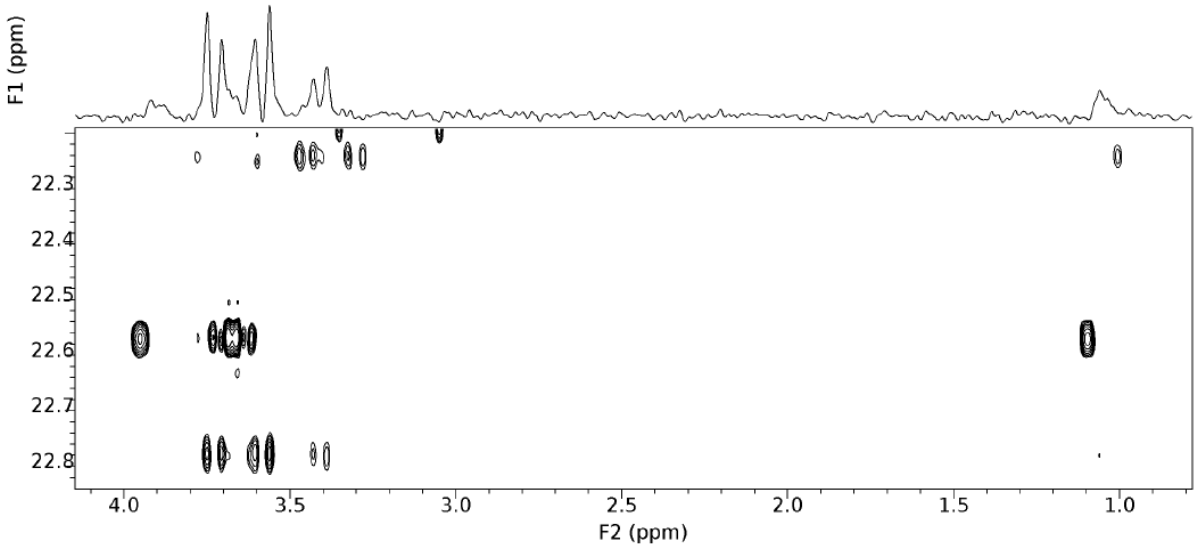

Figure S63. Aliphatic region (0.8–4.1 ppm) of LR-HMBCAD–{^{1}H–^{31}P} NMR spectra of [Zn(**6**)]$^{2+}$ complex in D_2O/MeOD (5:1 v/v) at 298 K: correlations of ^{31}P spectra with Sections of 2D-spectra at ^{31}P shift 22.2 (a), 22.6 (b) and 22.8 (c) ppm.

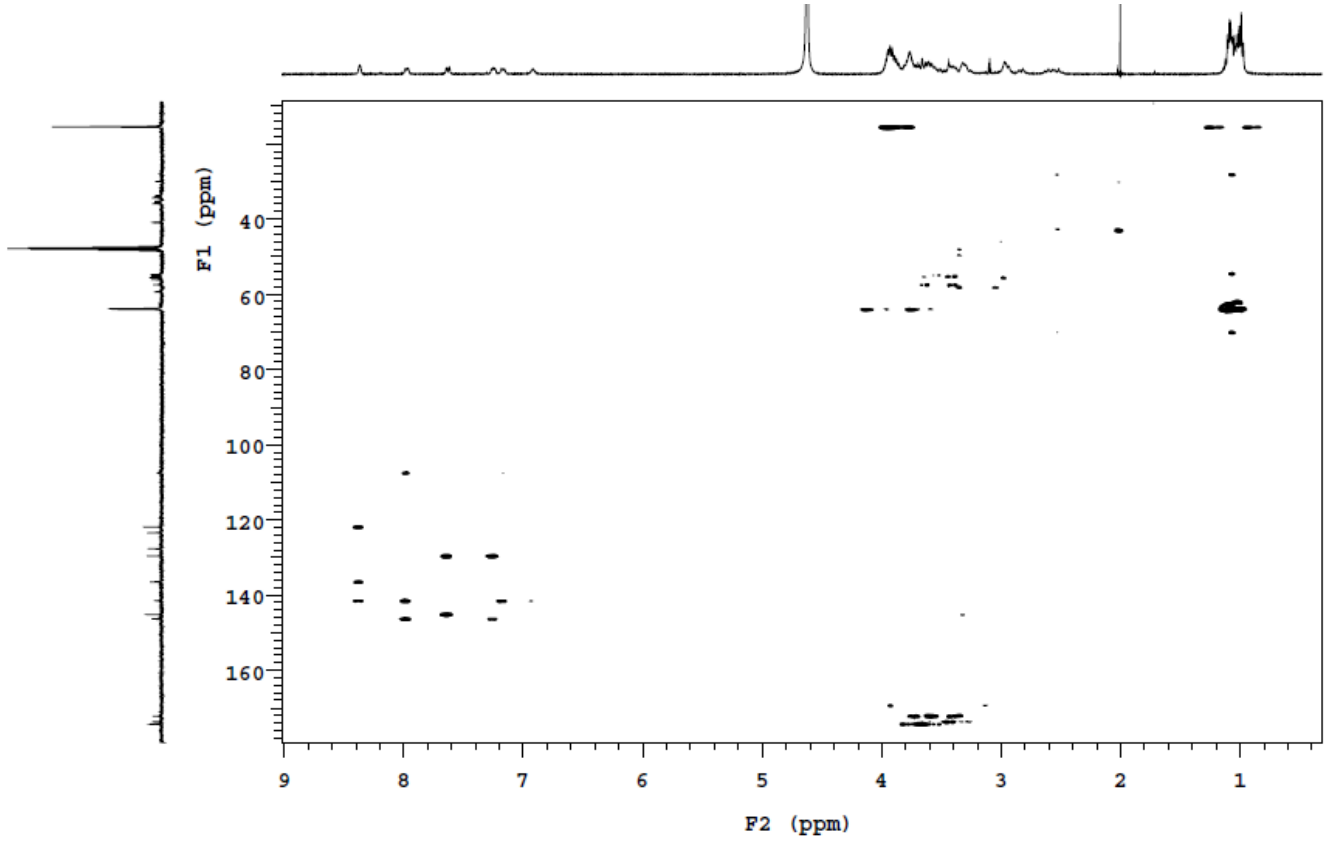

Figure S64. gHMBCAD-{^{1}H–^{13}C} NMR spectra of [Zn(**6**)]$^{2+}$ complex in D_2O/MeOD (5:1 v/v) at 298 K.

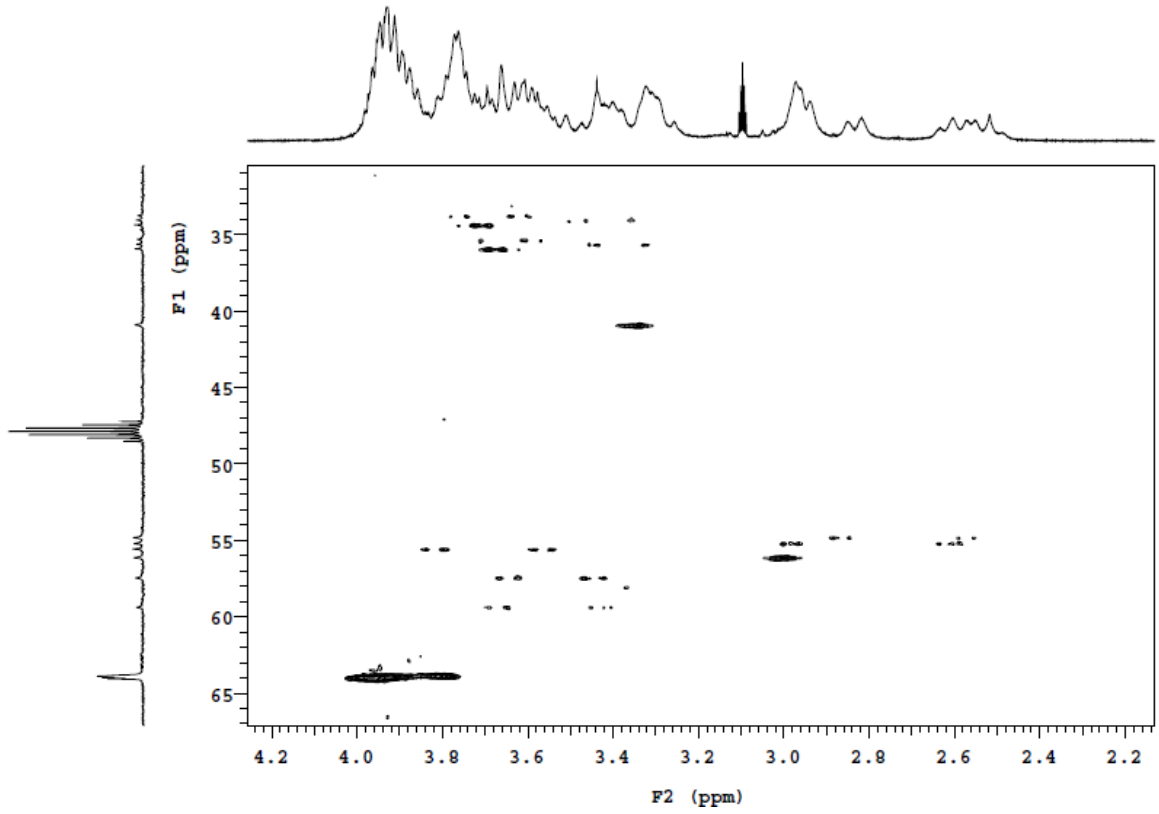

Figure S65. Aliphatic region (2.2–4.2 ppm) of gHMQCAD-{^{1}H–^{13}C} NMR spectra of [Zn(**6**)]$^{2+}$ complex in D_2O/MeOD (5:1 v/v) at 298 K.

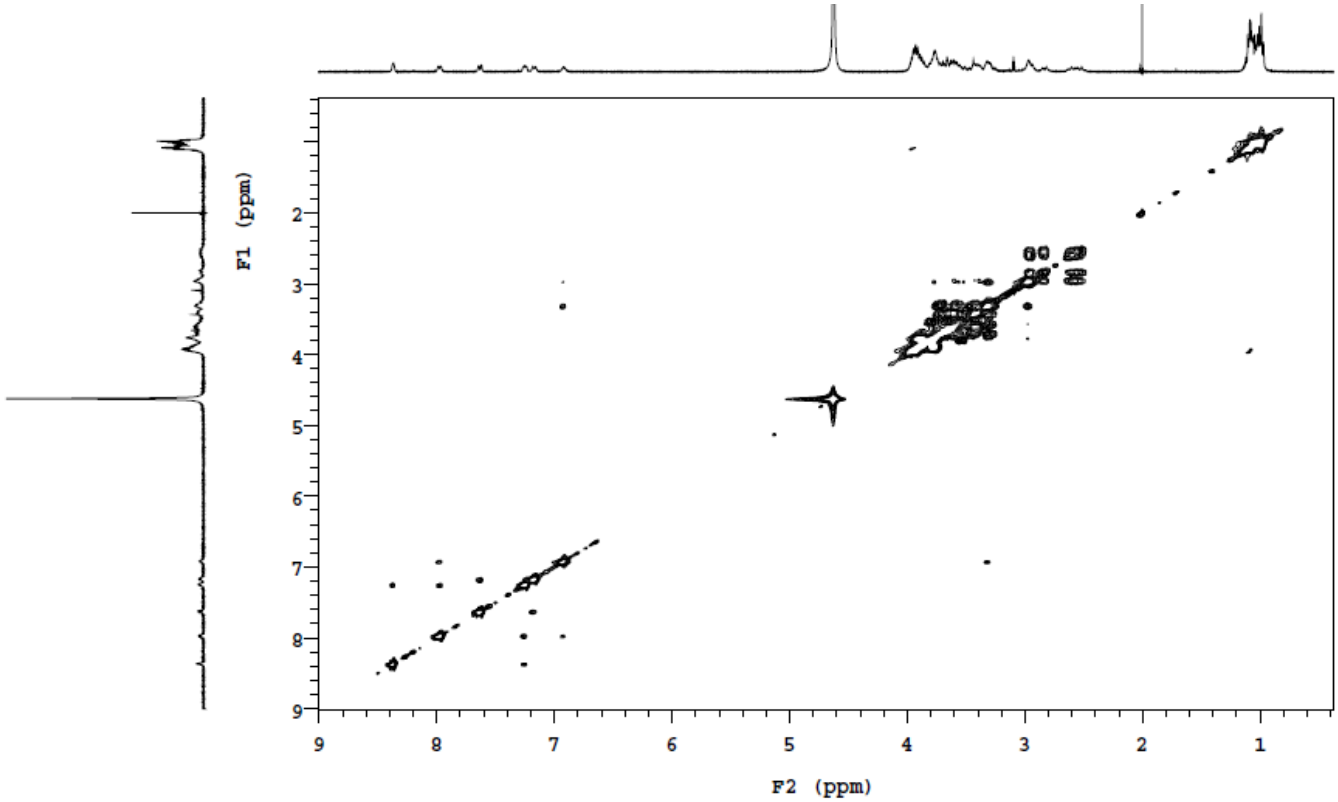

Figure S66. NOESY spectra of $[Zn(\mathbf{6})]^{2+}$ complex in D_2O/MeOD (5:1 v/v) at 298 K.

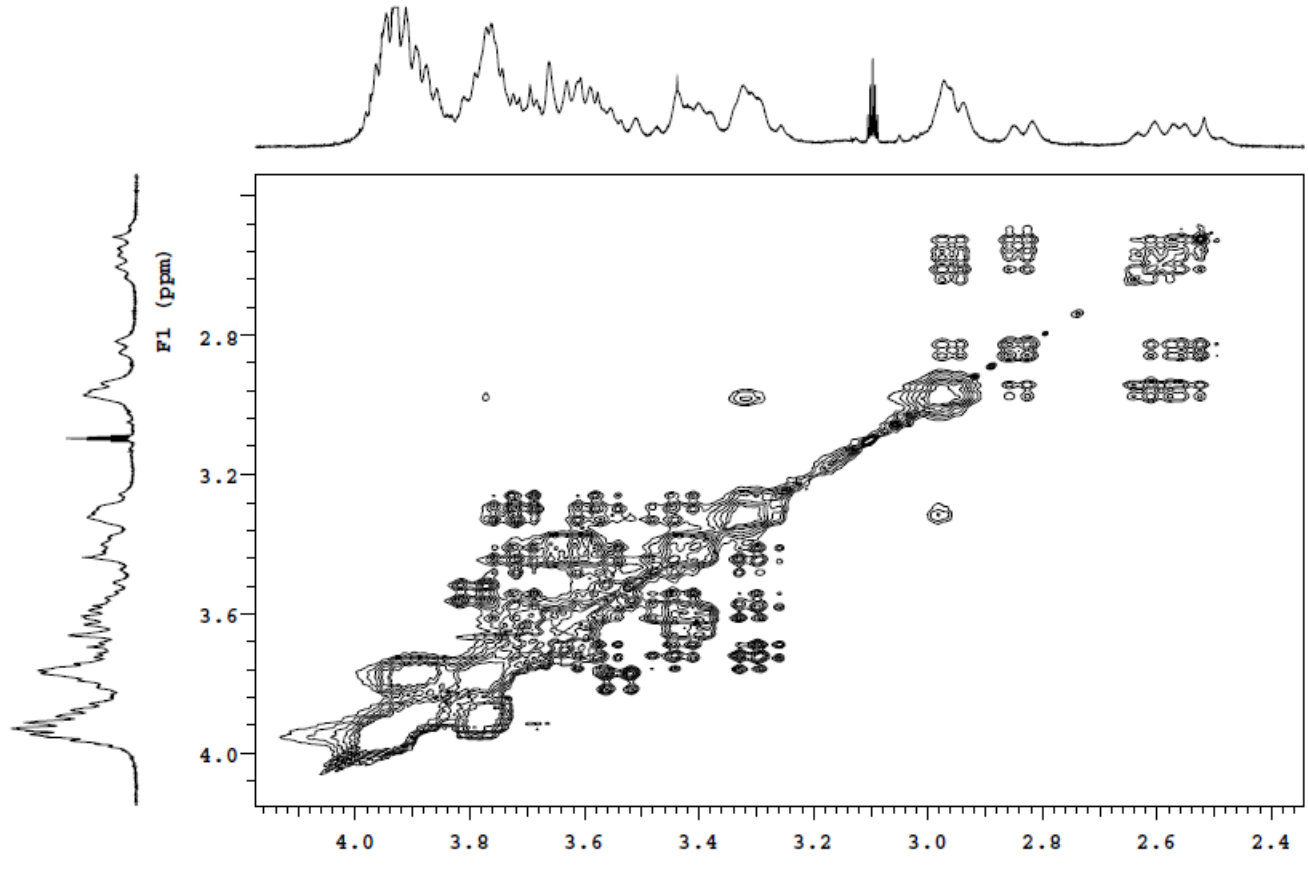

Figure S67. Aliphatic region (2.4–4.0 ppm) of NOESY spectra of $[Zn(\mathbf{6})]^{2+}$ complex in D_2O/MeOD (5:1 v/v) at 298 K.

Table S1. Assignment of signals in ^{1}H NMR spectrum of $[Zn(\mathbf{6})]^{2+}$.

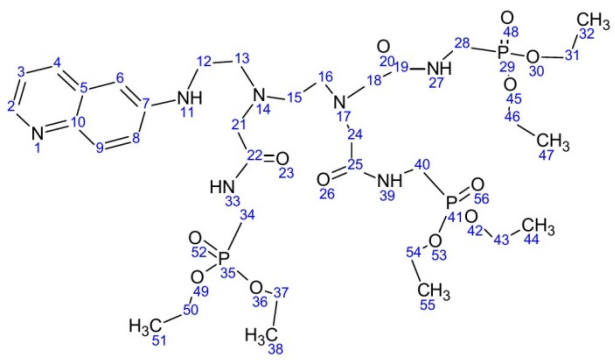

Assignment*	Chemical shift (ppm)				*J* (Hz)		
	^{1}H		^{13}C	^{31}P	H-H	H-P	C-P
2	8.38		146.32		-		
3	7.27		121.89		-		
4	7.99		136.51		-		
5			129.61				
6	6.94		107.49		-		
7			145.18				
8	7.18		123.43		-		
9	7.65		127.68		-		
10			141.5				
12	3.32	3.32	40.924		<0.1		
13	2.98	2.98	56.138		<0.1		
15	2.84	2.54	54.833		14.8		
16	2.96	2.59	55.205		12.8		
18	3.62	3.42	57.47		17.2		
19			173.67				
21	3.79	3.54	55.57		17.4		
22			174.31				4.14
24	3.64	3.40	59.39		16.8		
25			172.21				
28	3.44	3.30	34.85		14.4	12.2	157
29				22.22			
31,46	3.77		63.89				
32,47	0.99		15.5				
34	3.69	3.64	35.15		15.6	12.4	157
35				22.57			
37,50	3.94		64.03				6.95
38,51	1.08		15.5				
40	3.7	3.58	34.55		16	11.6	157
41				22.85			
43,54	3.90		63.92				
44,55	1.03		15.5				

* Chemical shifts of the proton and carbon atoms were obtained from gHSQCAD (at = 0.5s) and LR-HSQMBC (at=0.3s). The assignment was provided using gHMBCAD, NOESY and gCOSY-spectra (Figs. S59-67).

4.2. DFT-calculation studies of $[Zn(6)]^{2+}$ complex

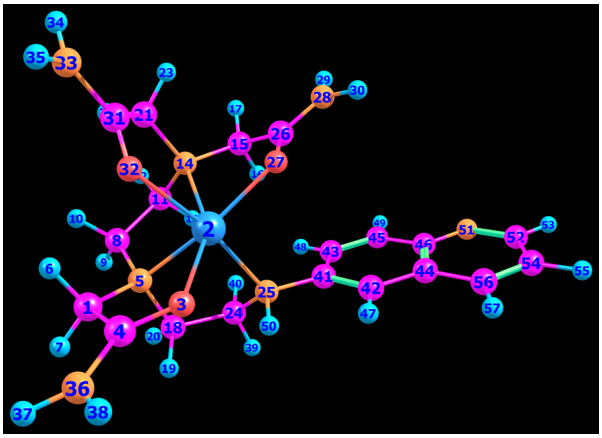

Figure S68. The structure of model **M1** (hydrogen atoms and phosphonate pendant arms are omitted) of Zn complex of ligand **6** obtained by full geometry optimization at B3LYP/6-31G(d,p) level.

COORD 1 — NUCLEAR COORDINATES

VIB 1

	ATOM	X	Y	Z
1	CARBON	28.567741	5.070436	15.070565
2	ZINC	23.810598	7.899411	14.818165
3	OXYGEN	24.209790	4.068907	14.128771
4	CARBON	26.445092	3.307599	14.175834
5	NITROGEN	27.486915	7.091643	16.662026
6	HYDROGEN	29.397535	5.902003	13.371504
7	HYDROGEN	30.057261	4.002057	16.042027
8	CARBON	28.993470	9.462507	16.631239
9	HYDROGEN	30.421591	9.470384	18.134982
10	HYDROGEN	30.024969	9.534807	14.842254
11	CARBON	27.364915	11.860490	16.892788
12	HYDROGEN	28.614266	13.514983	16.798386
13	HYDROGEN	26.457499	11.911473	18.743713
14	NITROGEN	25.348080	11.972107	14.944429
15	CARBON	23.090692	13.437974	15.650325
16	HYDROGEN	22.777242	13.280493	17.688059
17	HYDROGEN	23.263618	15.456989	15.209334
18	CARBON	26.918724	6.097611	19.246462
19	HYDROGEN	26.768281	4.041063	19.105071
20	HYDROGEN	28.491252	6.485273	20.540012
21	CARBON	26.289528	12.669092	12.411826
22	HYDROGEN	28.229143	13.392239	12.524368
23	HYDROGEN	25.150894	14.203631	11.616215
24	CARBON	24.462303	7.122604	20.375034
25	NITROGEN	22.356033	6.895581	18.531550
26	CARBON	20.753281	12.278084	14.380956
27	OXYGEN	20.757410	9.997473	13.771079
28	NITROGEN	18.762461	13.759222	14.006525
29	HYDROGEN	18.740152	15.598580	14.519111
30	HYDROGEN	17.145064	12.995789	13.323340
31	CARBON	26.246105	10.446160	10.553899
32	OXYGEN	25.592897	8.298375	11.252794
33	NITROGEN	26.983945	10.924681	8.194682
34	HYDROGEN	27.517891	12.663781	7.604729
35	HYDROGEN	26.941950	9.515491	6.900942
36	NITROGEN	27.084856	0.993364	13.439054
37	HYDROGEN	28.881313	0.350377	13.516631
38	HYDROGEN	25.742587	-0.165547	12.717686
39	HYDROGEN	24.044101	6.092793	22.123173
40	HYDROGEN	24.673697	9.103979	20.893811
41	CARBON	19.914766	7.862138	19.377096
42	CARBON	17.758303	6.547756	18.733411
43	CARBON	19.734616	10.160587	20.747311
44	CARBON	15.336846	7.484009	19.395310
45	CARBON	17.400664	11.110155	21.404475
46	CARBON	15.147152	9.822623	20.736887
47	HYDROGEN	17.886172	4.772163	17.702660
48	HYDROGEN	21.415048	11.155093	21.373647
49	HYDROGEN	17.220045	12.843807	22.483825
50	HYDROGEN	22.100742	5.013880	18.185896
51	NITROGEN	12.897740	10.867204	21.428398
52	CARBON	10.822640	9.622673	20.840565
53	HYDROGEN	9.045731	10.482956	21.414893
54	CARBON	10.796792	7.277059	19.530863
55	HYDROGEN	9.007449	6.363479	19.125069

56	CARBON	13.047930	6.212121	18.802489
57	HYDROGEN	13.100220	4.424057	17.795396

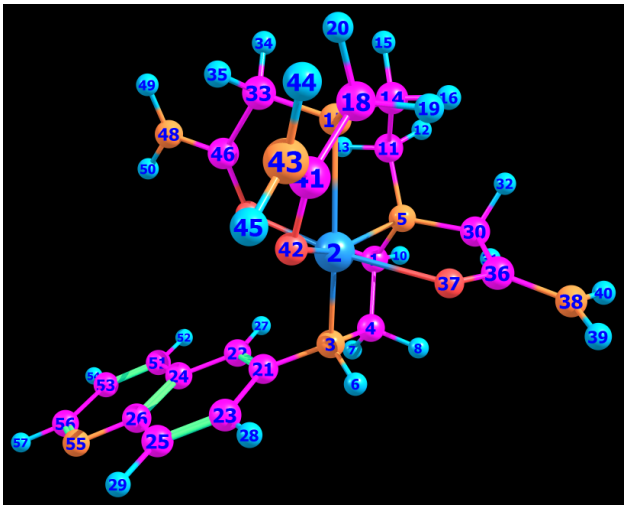

Figure S69. The structure of model **M2** (hydrogen atoms and phosphonate pendant arms are omitted) of Zn complex of ligand **6** obtained by full geometry optimization at B3LYP/6-31G(d,p) level.

COORD 3 NUCLEAR COORDINATES

VIB 1

	ATOM	X	Y	Z
1	CARBON	4.995841	6.172709	2.693548
2	ZINC	3.727122	8.611654	7.315908
3	NITROGEN	3.782732	4.654839	7.035271
4	CARBON	5.166810	4.038590	4.649561
5	NITROGEN	5.933712	8.600984	3.775121
6	HYDROGEN	4.895786	4.090178	8.501602
7	HYDROGEN	4.444615	2.287398	3.827388
8	HYDROGEN	7.140996	3.677389	5.145689
9	HYDROGEN	3.025511	6.461654	2.151884
10	HYDROGEN	6.054876	5.639507	0.991114
11	CARBON	5.113142	10.895263	2.383673
12	HYDROGEN	6.335093	11.280969	0.752563
13	HYDROGEN	3.223861	10.537069	1.635724
14	CARBON	5.090883	13.229625	4.118474
15	HYDROGEN	4.577148	14.898619	2.998734
16	HYDROGEN	6.992187	13.577583	4.848027
17	NITROGEN	3.377869	12.894840	6.314252
18	CARBON	4.191854	14.105375	8.677708
19	HYDROGEN	6.258058	14.106582	8.763989
20	HYDROGEN	3.568689	16.077368	8.845625
21	CARBON	1.328538	3.438447	7.445446
22	CARBON	-0.186508	2.603114	5.506238
23	CARBON	0.542361	3.210878	9.998637
24	CARBON	-2.565823	1.481425	6.052718
25	CARBON	-1.752392	2.139846	10.569587
26	CARBON	-3.370424	1.250111	8.621028
27	HYDROGEN	0.373123	2.775271	3.540161
28	HYDROGEN	1.775793	3.862793	11.508443
29	HYDROGEN	-2.380954	1.922097	12.507787
30	CARBON	8.682281	8.562019	4.235889
31	HYDROGEN	9.594215	7.013882	3.204902
32	HYDROGEN	9.557673	10.302316	3.535163
33	CARBON	0.704727	13.402407	5.731418
34	HYDROGEN	0.509738	14.754913	4.169847
35	HYDROGEN	-0.224817	14.259854	7.369907
36	CARBON	9.284903	8.356908	7.060866
37	OXYGEN	7.577465	8.616459	8.661910
38	NITROGEN	11.683951	7.941464	7.703635
39	HYDROGEN	12.154454	7.838865	9.555741
40	HYDROGEN	13.075149	7.715624	6.414330
41	CARBON	3.268072	12.528511	10.933905
42	OXYGEN	2.802898	10.229797	10.665397
43	NITROGEN	3.029453	13.685862	13.148835
44	HYDROGEN	3.377605	15.549523	13.377503
45	HYDROGEN	2.542902	12.663919	14.693206
46	CARBON	-0.738682	10.972604	5.111168
47	OXYGEN	0.258682	8.867567	5.447328
48	NITROGEN	-3.076450	11.218161	4.216753
49	HYDROGEN	-3.901530	12.917407	3.935062
50	HYDROGEN	-4.123268	9.647282	3.903048
51	CARBON	-4.218858	0.551651	4.156021
52	HYDROGEN	-3.679241	0.670880	2.177831
53	CARBON	-6.480419	-0.509220	4.864335
54	HYDROGEN	-7.789519	-1.253288	3.473512
55	NITROGEN	-5.622819	0.205071	9.294585
56	CARBON	-7.098987	-0.634777	7.472712

57	HYDROGEN	-8.886530	-1.467866	8.063967

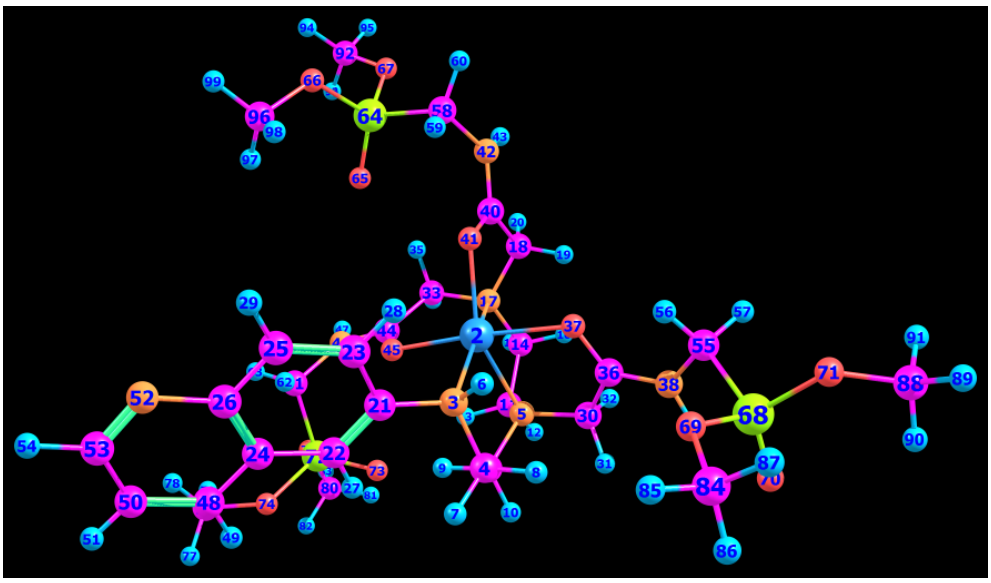

Figure S70. The optimized structure (B3LYP/6-31G(d,p)) of methyl analogue of Zn^{II} complex with ligand **6**.

COORD 2 NUCLEAR COORDINATES

VIB 1

	ATOM	X	Y	Z
1	CARBON	4.058382	4.690461	1.323544
2	ZINC	2.896477	7.117825	6.029103
3	NITROGEN	3.044570	3.097994	5.697966
4	CARBON	4.398986	2.583033	3.268971
5	NITROGEN	4.879492	7.166838	2.387838
6	HYDROGEN	4.228647	2.598604	7.130536
7	HYDROGEN	3.745344	0.787693	2.461424
8	HYDROGEN	6.400009	2.314272	3.719779
9	HYDROGEN	2.079404	4.874512	0.766010
10	HYDROGEN	5.143232	4.219167	-0.382641
11	CARBON	3.872846	9.381759	0.987064
12	HYDROGEN	5.014165	9.798833	-0.695389
13	HYDROGEN	1.984659	8.888114	0.311289
14	CARBON	3.814216	11.745701	2.679975
15	HYDROGEN	3.043520	13.335756	1.593246
16	HYDROGEN	5.737361	12.284106	3.211080
17	NITROGEN	2.364049	11.324341	5.040652
18	CARBON	3.391154	12.557988	7.309313
19	HYDROGEN	5.453594	12.413341	7.275437
20	HYDROGEN	2.894048	14.568526	7.443426
21	CARBON	0.690544	1.742976	6.130979
22	CARBON	-0.884922	1.000586	4.198594
23	CARBON	0.044259	1.239359	8.685203
24	CARBON	-3.166234	-0.302727	4.754099
25	CARBON	-2.160487	-0.001849	9.266050
26	CARBON	-3.828439	-0.808014	7.323763
27	HYDROGEN	-0.450238	1.401345	2.235348
28	HYDROGEN	1.323238	1.821129	10.185959
29	HYDROGEN	-2.670589	-0.432686	11.203763
30	CARBON	7.639117	7.283774	2.753794
31	HYDROGEN	8.631340	6.017756	1.445923
32	HYDROGEN	8.324127	9.192003	2.342320
33	CARBON	-0.383434	11.725757	4.770494
34	HYDROGEN	-0.799036	13.227402	3.401203
35	HYDROGEN	-1.218886	12.274620	6.590593
36	CARBON	8.363560	6.701673	5.494801
37	OXYGEN	6.770144	6.980319	7.223490
38	NITROGEN	10.730852	5.974418	5.908122
39	HYDROGEN	11.891574	5.576390	4.424269
40	CARBON	2.428084	11.084994	9.611068
41	OXYGEN	2.145841	8.744734	9.470461
42	NITROGEN	1.888157	12.390205	11.701308
43	HYDROGEN	2.033208	14.296742	11.627218
44	CARBON	-1.704677	9.268134	4.054129
45	OXYGEN	-0.745099	7.188167	4.604680
46	NITROGEN	-3.946530	9.437486	2.905252
47	HYDROGEN	-4.604447	11.160048	2.402756
48	CARBON	-4.851030	-1.169175	2.852756
49	HYDROGEN	-4.408792	-0.832883	0.876318
50	CARBON	-7.005907	-2.434894	3.561939
51	HYDROGEN	-8.326038	-3.157863	2.169285

52	NITROGEN	-5.984192	-2.044302	7.997868
53	CARBON	-7.491076	-2.820065	6.172682
54	HYDROGEN	-9.194978	-3.814663	6.753122
55	CARBON	11.746206	5.243488	8.374418
56	HYDROGEN	10.204742	4.963120	9.710686
57	HYDROGEN	13.000464	6.719321	9.104720
58	CARBON	0.283462	11.348610	13.691937
59	HYDROGEN	0.577168	9.311471	13.782922
60	HYDROGEN	0.758472	12.187346	15.514265
61	CARBON	-5.299828	7.217450	1.989599
62	HYDROGEN	-4.937919	5.640496	3.270128
63	HYDROGEN	-7.325264	7.611045	1.960132
64	PHOSPHORUS	-3.040700	12.016089	12.838324
65	OXYGEN	-3.508790	11.672990	10.073827
66	OXYGEN	-4.767501	10.371368	14.698127
67	OXYGEN	-3.260946	14.819048	13.949390
68	PHOSPHORUS	13.601856	2.338944	7.849470
69	OXYGEN	11.557144	0.227096	8.590756
70	OXYGEN	14.609662	2.365276	5.221259
71	OXYGEN	15.617196	2.161096	10.092285
72	PHOSPHORUS	-4.140492	6.332503	-1.176224
73	OXYGEN	-1.332912	6.278990	-1.351523
74	OXYGEN	-5.363192	3.636052	-1.826028
75	OXYGEN	-5.558611	8.430444	-2.860328
76	CARBON	-8.034583	3.230420	-2.295668
77	HYDROGEN	-8.161006	1.725968	-3.696440
78	HYDROGEN	-8.951077	2.630297	-0.545521
79	HYDROGEN	-8.929838	4.939105	-3.028082
80	CARBON	-4.850574	8.813373	-5.490023
81	HYDROGEN	-2.804377	9.014886	-5.652814
82	HYDROGEN	-5.497684	7.225175	-6.638872
83	HYDROGEN	-5.795039	10.540514	-6.089577
84	CARBON	12.295554	-2.420432	8.636307
85	HYDROGEN	10.585717	-3.482909	9.064927
86	HYDROGEN	13.040465	-2.989304	6.797280
87	HYDROGEN	13.704069	-2.726856	10.112026
88	CARBON	18.273377	2.772016	9.733210
89	HYDROGEN	19.325438	1.536416	10.999774
90	HYDROGEN	18.831953	2.446416	7.775942
91	HYDROGEN	18.592529	4.743576	10.255690
92	CARBON	-5.659193	16.159260	13.975212
93	HYDROGEN	-6.450380	16.249561	12.070557
94	HYDROGEN	-6.967767	15.214889	15.259637
95	HYDROGEN	-5.241871	18.054613	14.658761
96	CARBON	-5.993110	8.052997	13.902925
97	HYDROGEN	-6.684497	8.230306	11.968820
98	HYDROGEN	-4.666242	6.476212	14.043911
99	HYDROGEN	-7.559795	7.760360	15.205624

4.3. IR-studies

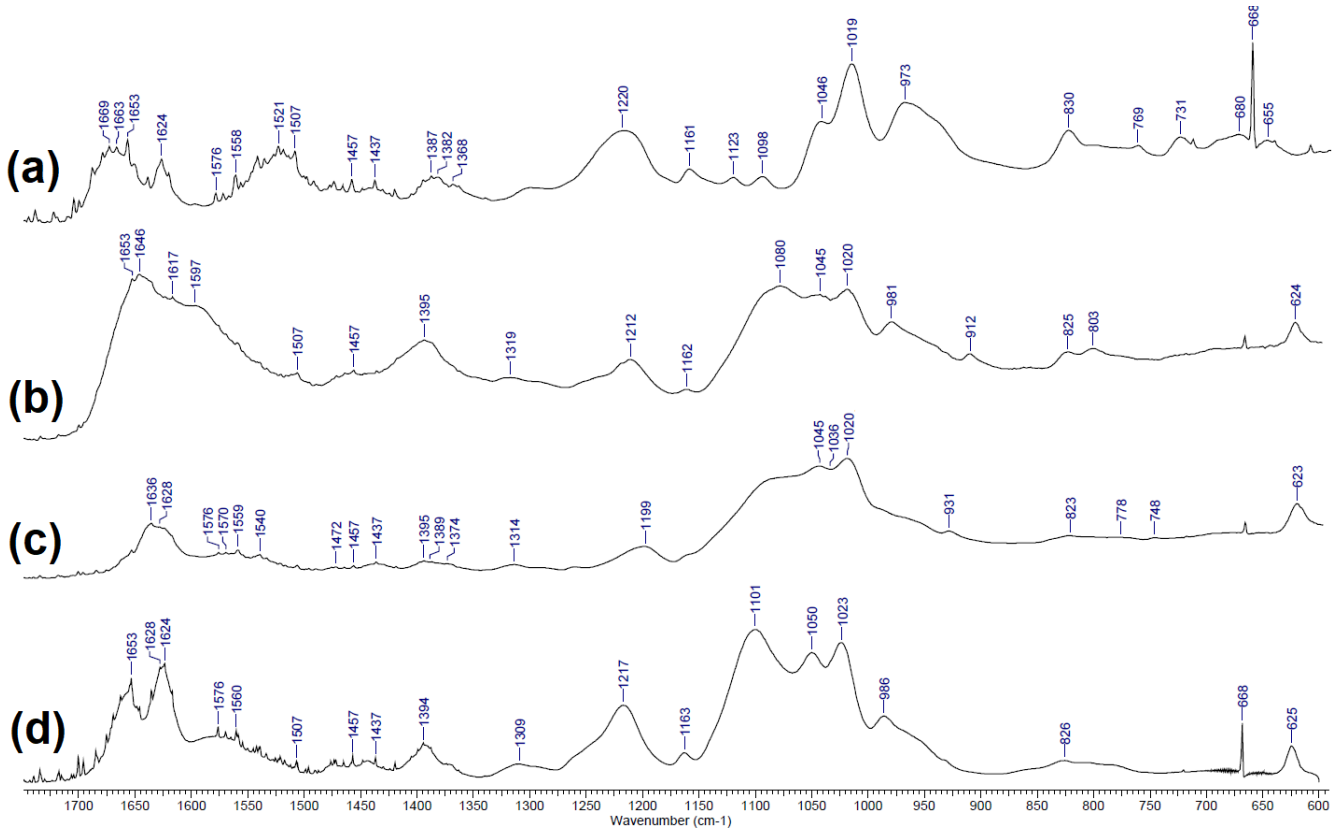

Figure S71. FT−IR-spectra (neat, ZnSe) of **6** **(a)**, $[Hg(\mathbf{6})](ClO_4)_2$ **(b)**, $[Zn(\mathbf{6})](ClO_4)_2$ **(c)** and $[Cu(\mathbf{6})](ClO_4)_2$ **(d)**.

4.4. ESI-spectra of $[Hg(6)]^{2+}$ complex

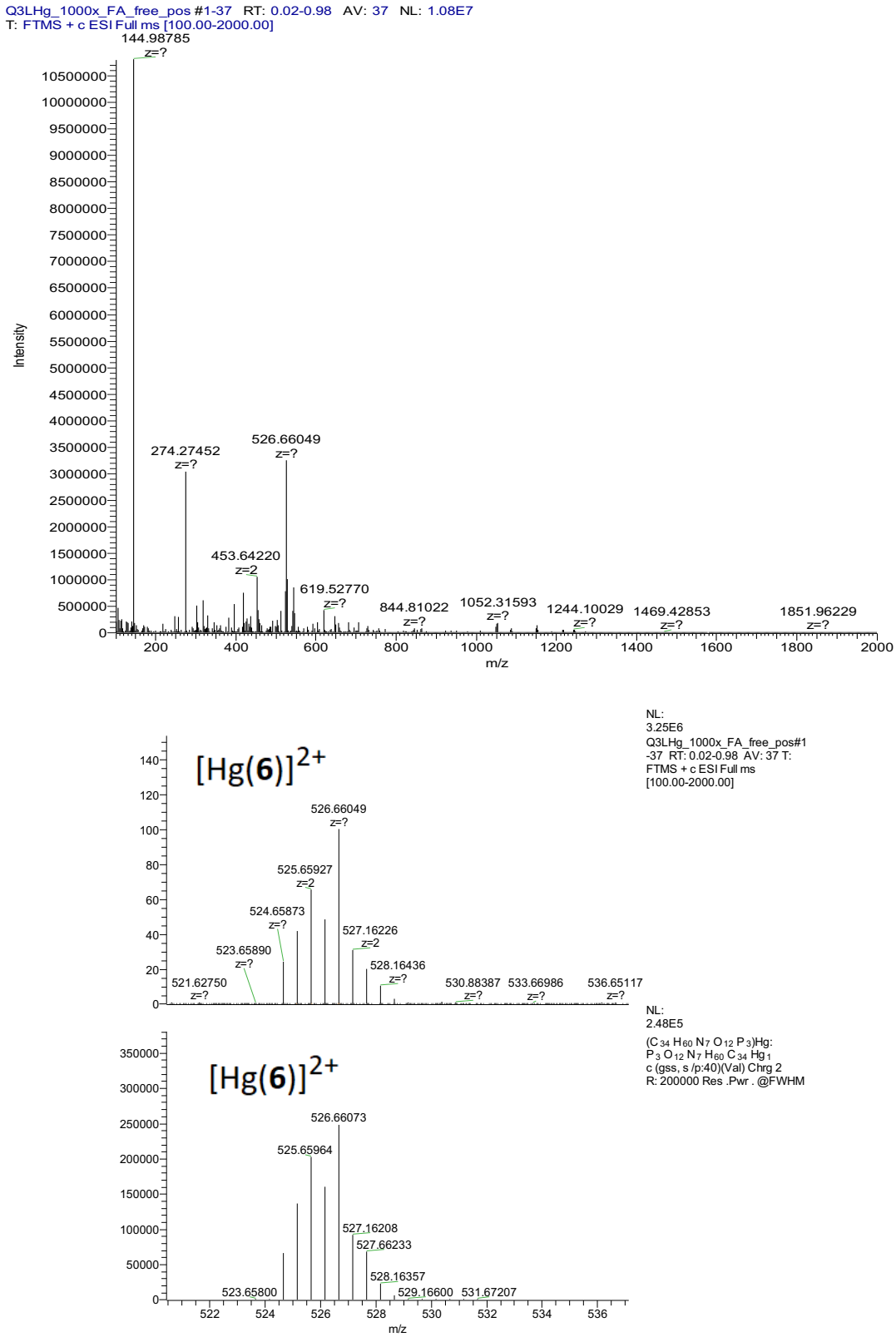

Scheme S72. HRMS ESI spectra of the aqueous solution of **6** and $Hg(ClO_4)_2$ (1:1 molar ratio).

4.5. NMR-studies of $[Hg(6)]^{2+}$ complex

NMR-titration of ligand **6** with Hg(II) perchlorate

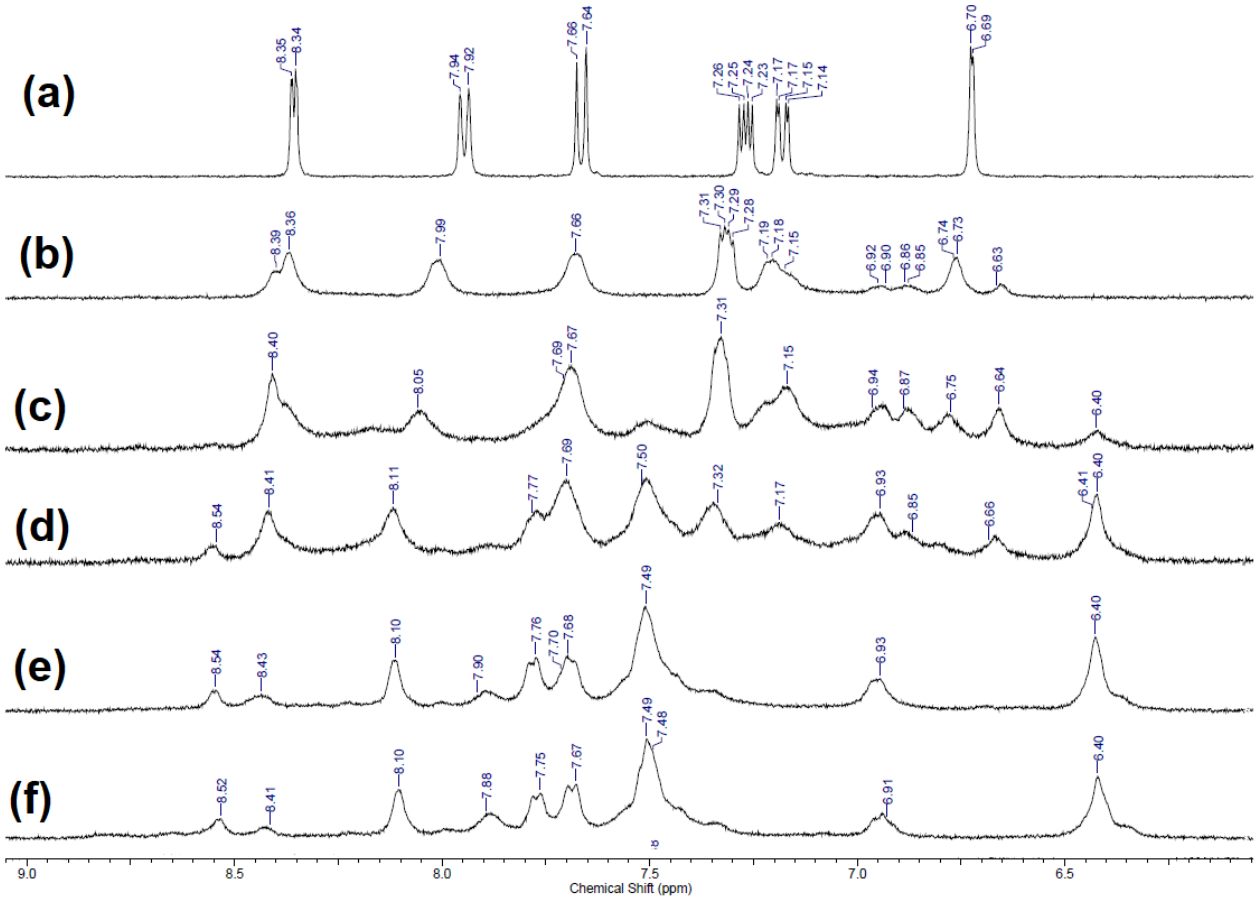

Figure S73. Aromatic region of ^{1}H NMR spectra (400 MHz) of **6** in D_2O/MeOD (5:1 v/v, [**6**] = 0.04 M) at 298 K before (a) and after addition of 0.2 (b), 0.4 (c), 0.6 (d), 0.8 (e) and 1.0 (f) equiv of mercury(II) perchlorate.

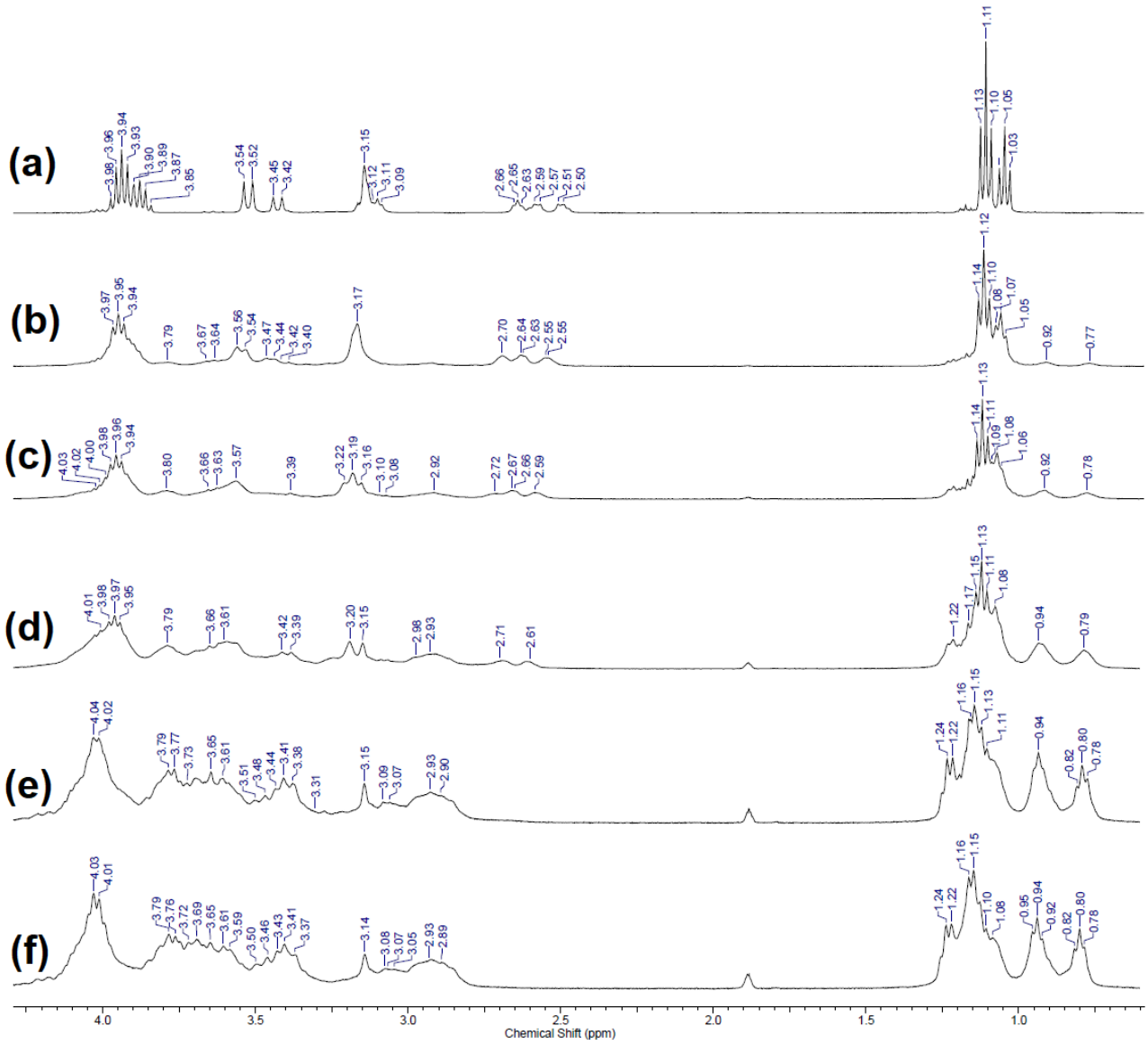

Figure S74. Aromatic region of ^{1}H NMR spectra (400 MHz)) of **6** in D_2O/MeOD (5:1 v/v, [**6**] = 0.04 M) at 298 K before **(a)** and after addition of 0.2 **(b)**, 0.4 **(c)**, 0.6 **(d)**, 0.8 **(e)** and 1.0 **(f)** equiv of mercury(II) perchlorate.

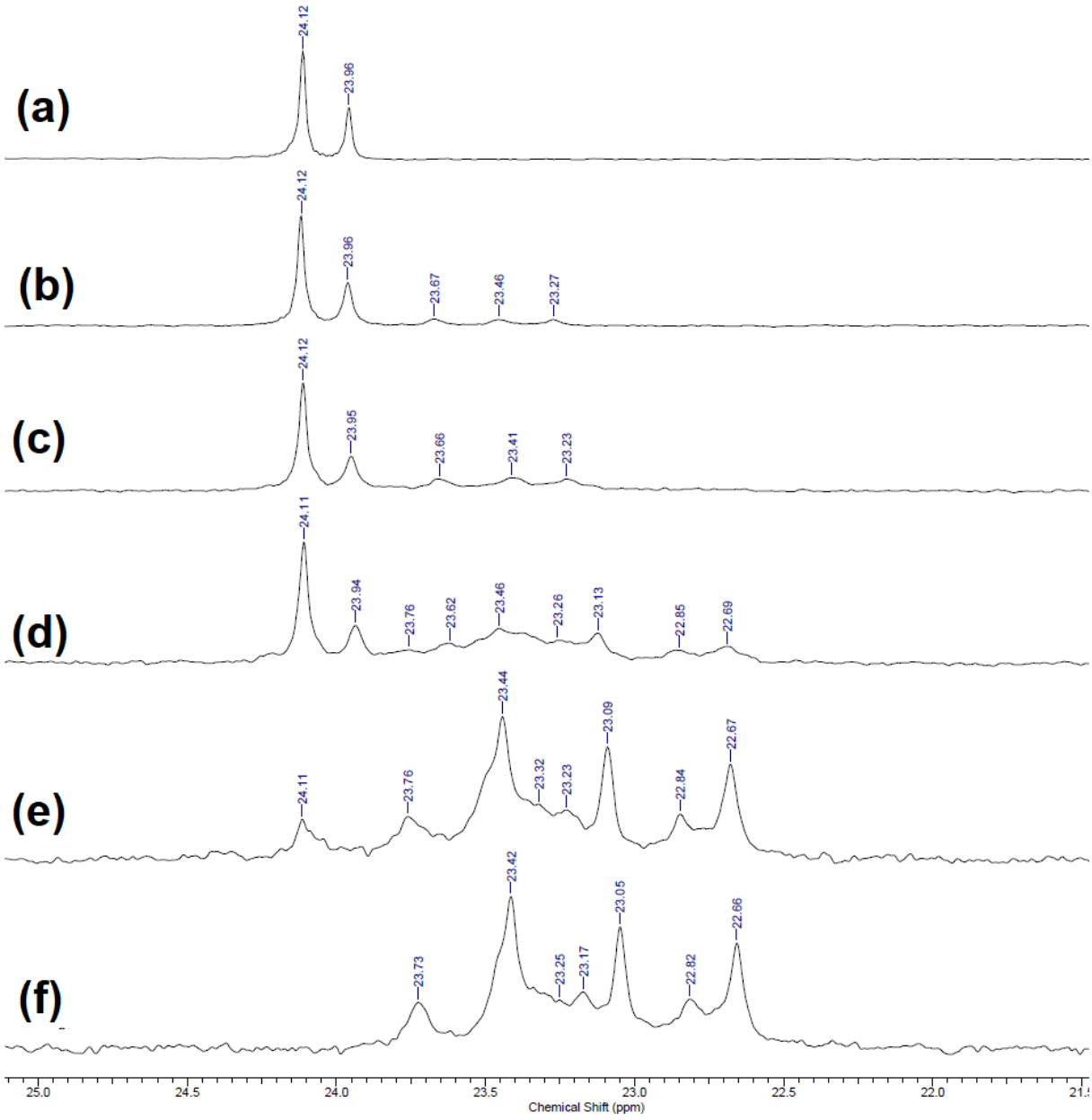

Figure S75. 162.5 MHz ^{31}P NMR spectra of **6** in D_2O/MeOD (5:1 v/v, [**6**] = 0.04 M) at 298 K before **(a)** and after addition of 0.2 **(b)**, 0.4 **(c)**, 0.6 **(d)**, 0.8 **(e)** and 1.0 **(f)** equiv of mercury(II) perchlorate.

5. Detection of sulfide anions

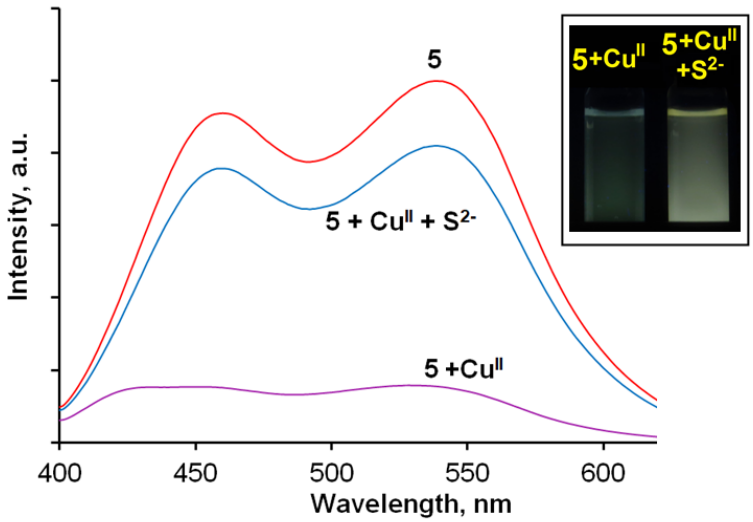

Figure S76. Changes in emission of an aqueous solution of ligand **5** (red line) (26.6 mM, pH = 7.4, 0.03M HEPES, λ_{ex} = 356 nm) after addition of Cu^{II} ions (1 equiv) (rose line) followed by S^{2-} ions (excess) (blue line). Inset: Visual detection of S^{2-} ions (excess) under UV light (λ = 365 nm) in the aqueous solution of ligand **5** (26.6 mM, pH = 7.4, 0.03M HEPES) and copper(II) perchlorate (1 equiv).

6. Characterization of compounds 5, 6, 9a-f, 10

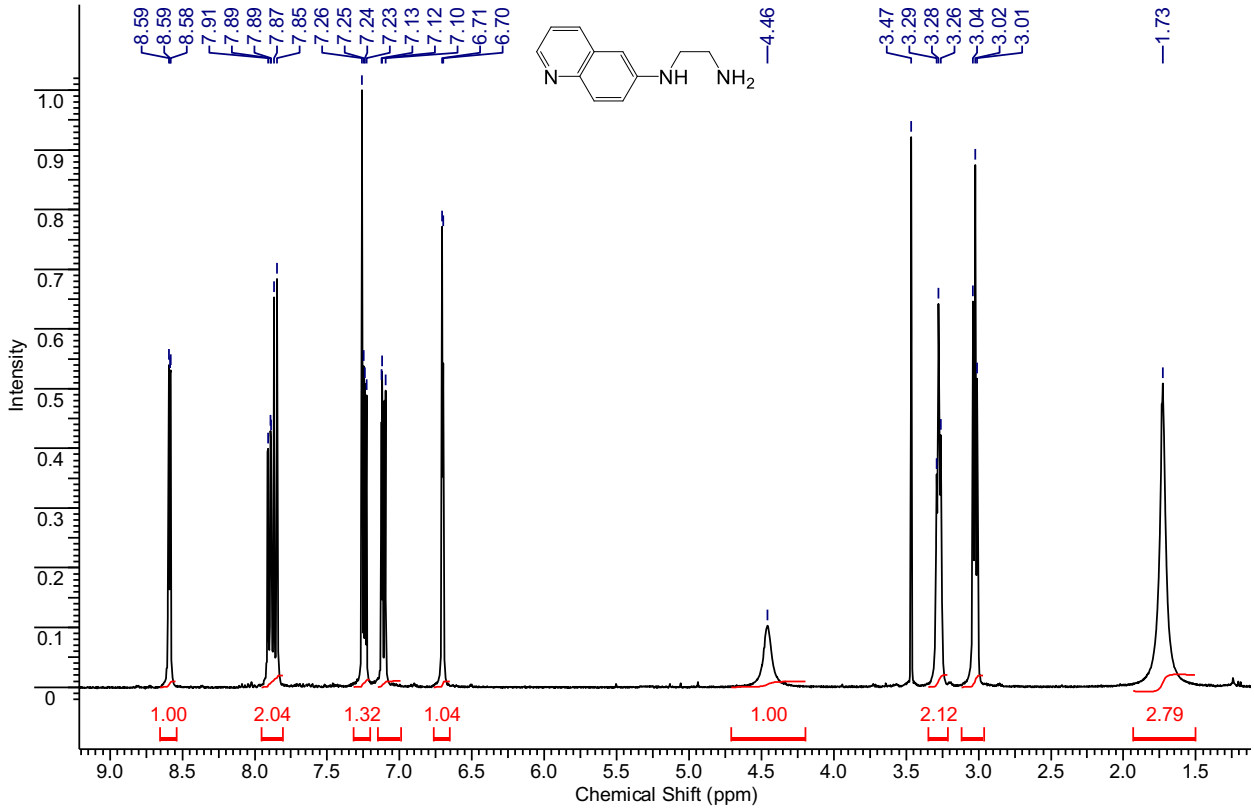

Figure S77. ^{1}H NMR spectrum of **9a** ($CDCl_3$, 400MHz, 300K).

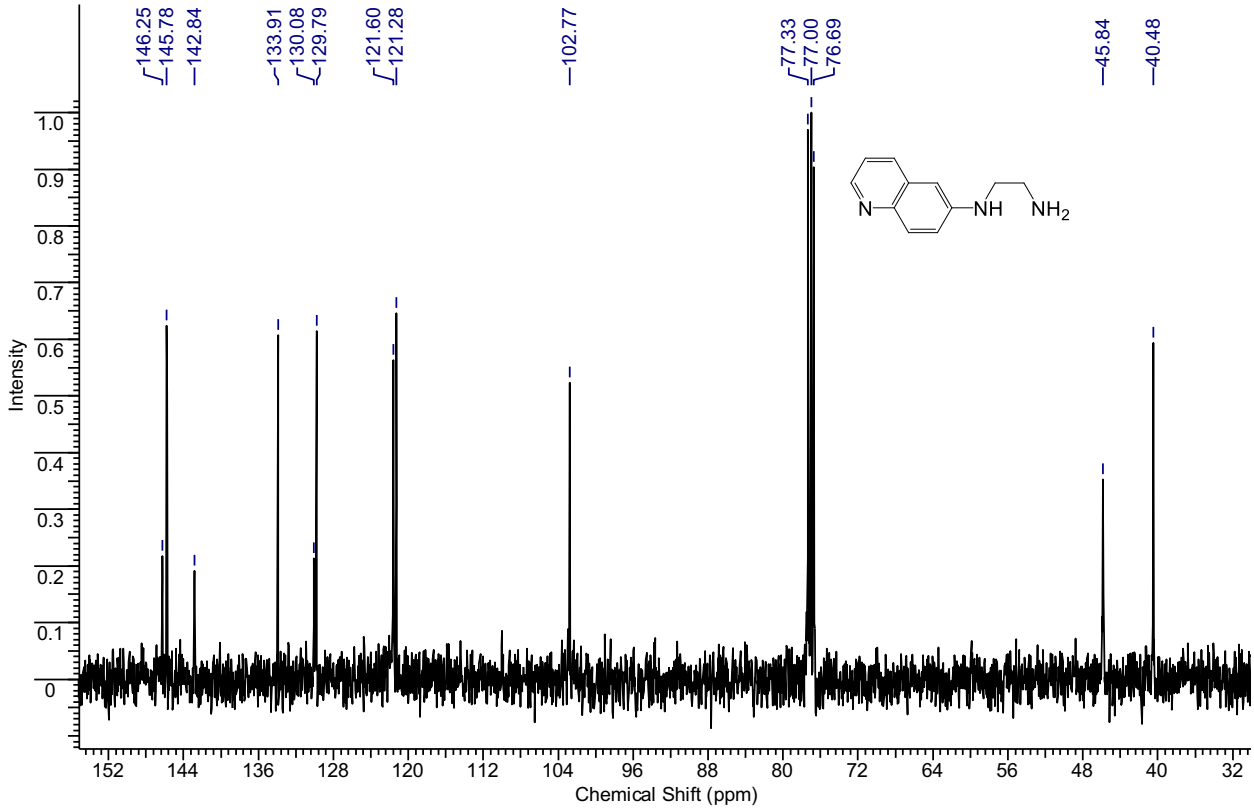

Figure S78. ^{13}C NMR spectrum of **9a** ($CDCl_3$, 100.6 MHz, 300K).

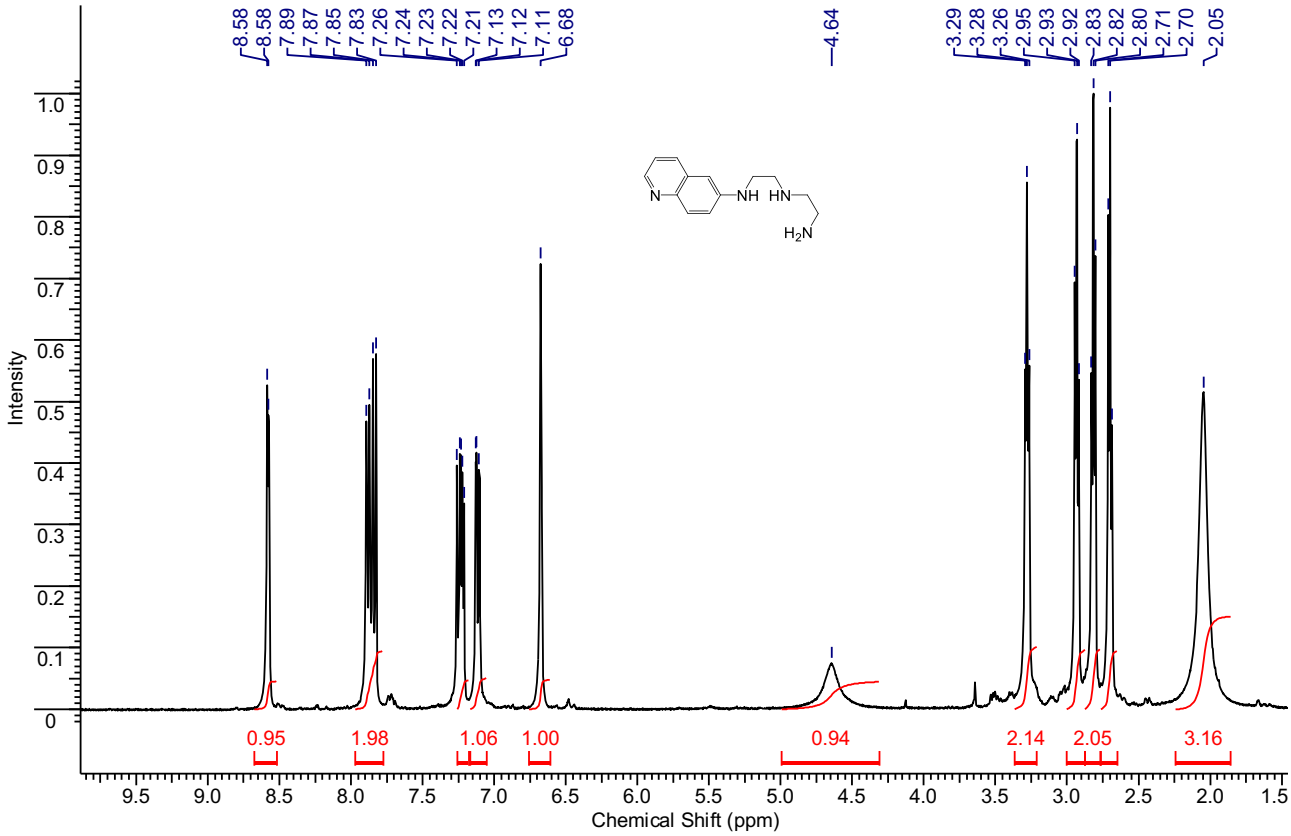

Figure S79. ^{1}H NMR spectrum of **9b** ($CDCl_3$, 400MHz, 300K).

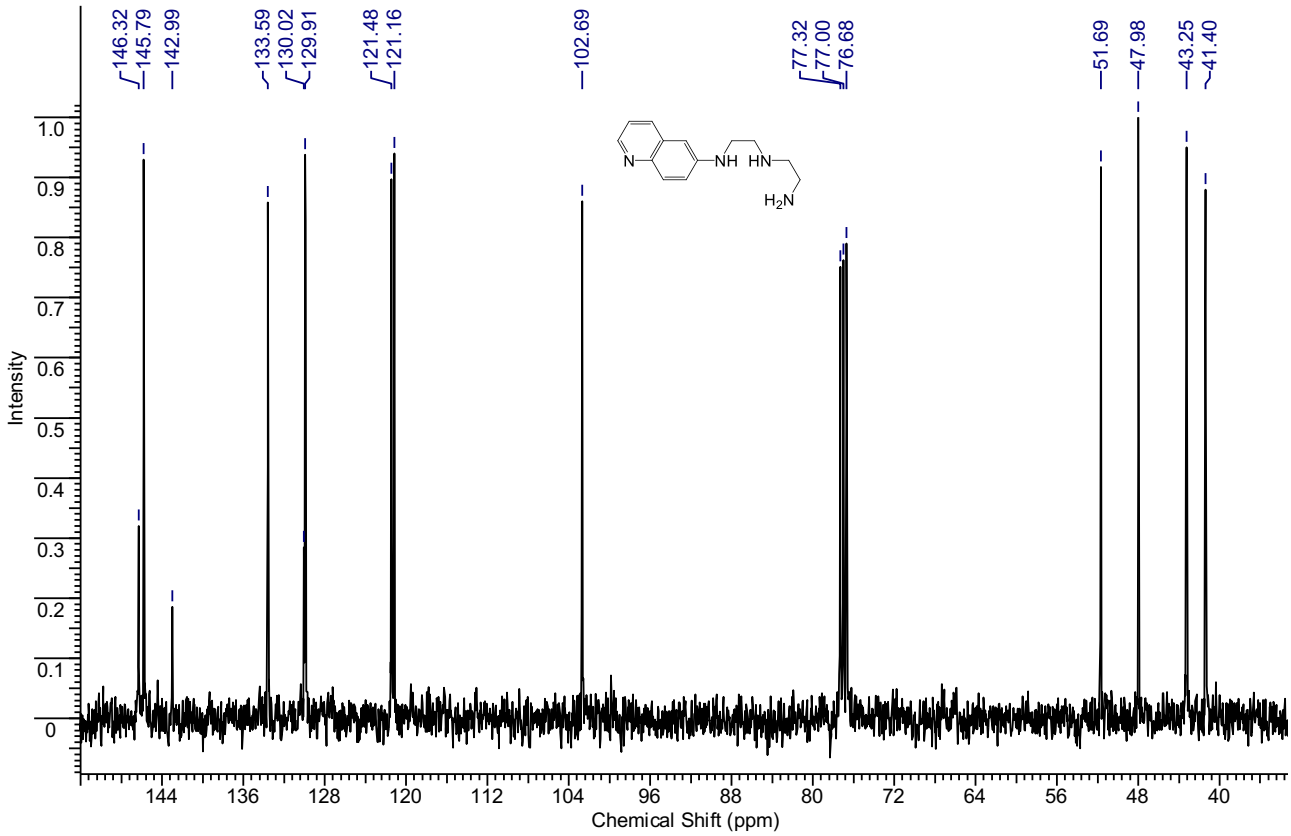

Figure S80. ^{13}C NMR spectrum of **9b** ($CDCl_3$, 100.6 MHz, 300K).

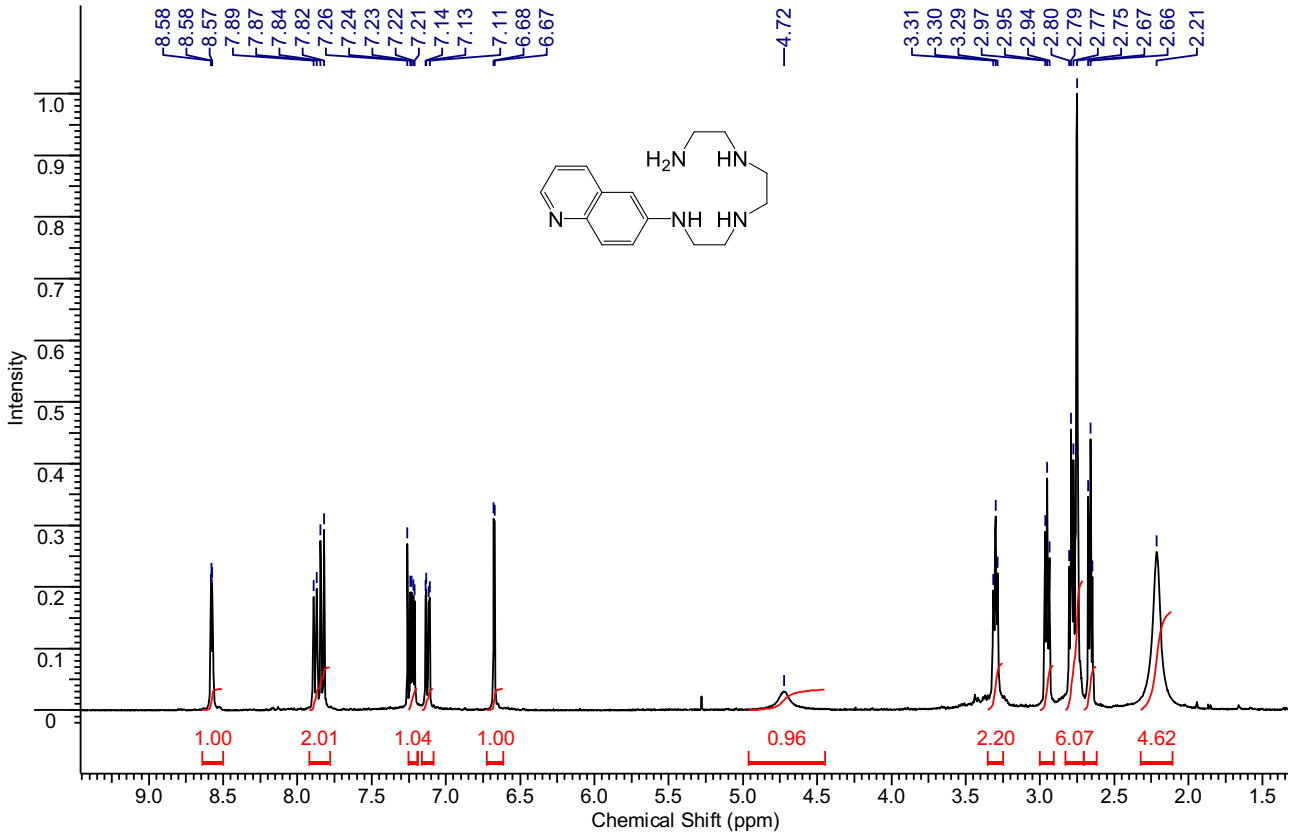

Figure S81. ^{1}H NMR spectrum of **9c** ($CDCl_3$, 400MHz, 300K).

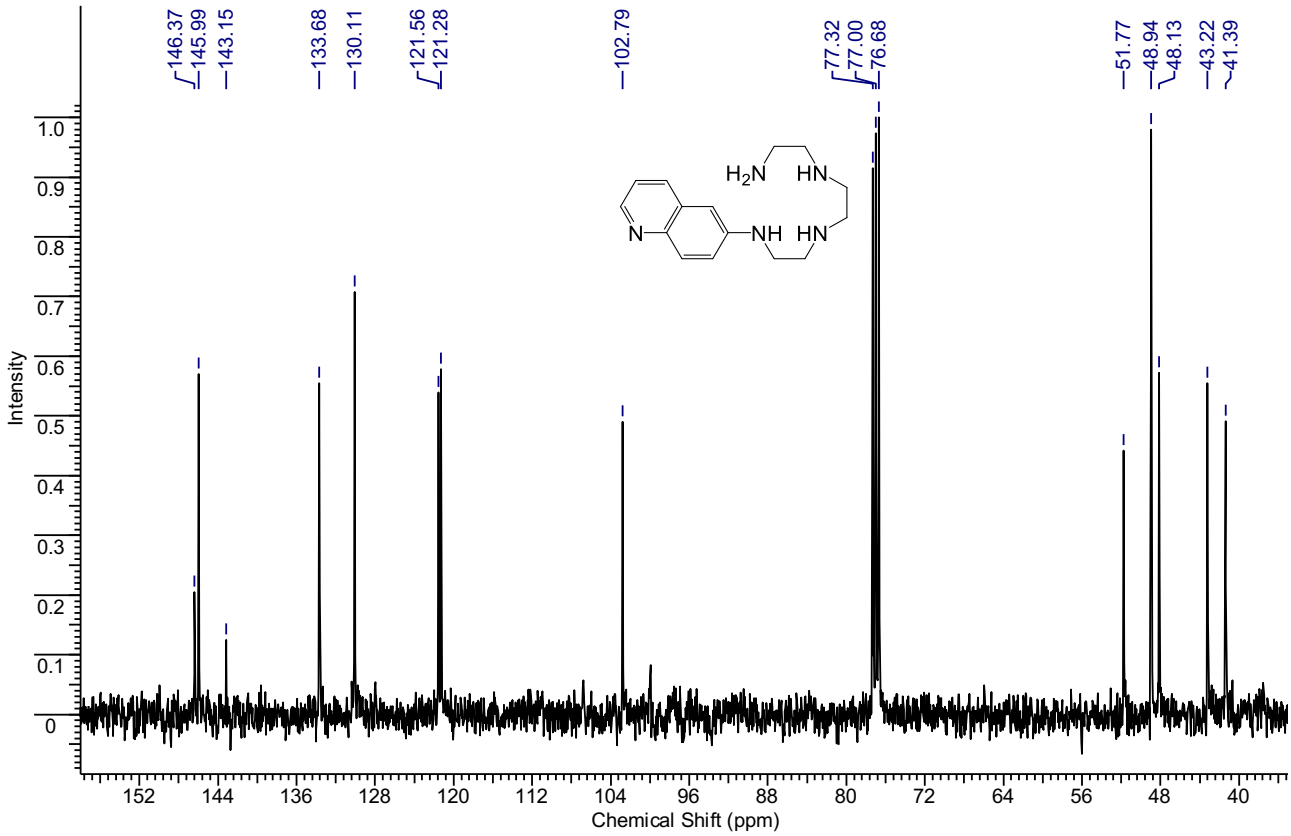

Figure S82. ^{13}C NMR spectrum of **9c** ($CDCl_3$, 100.6 MHz, 300K).

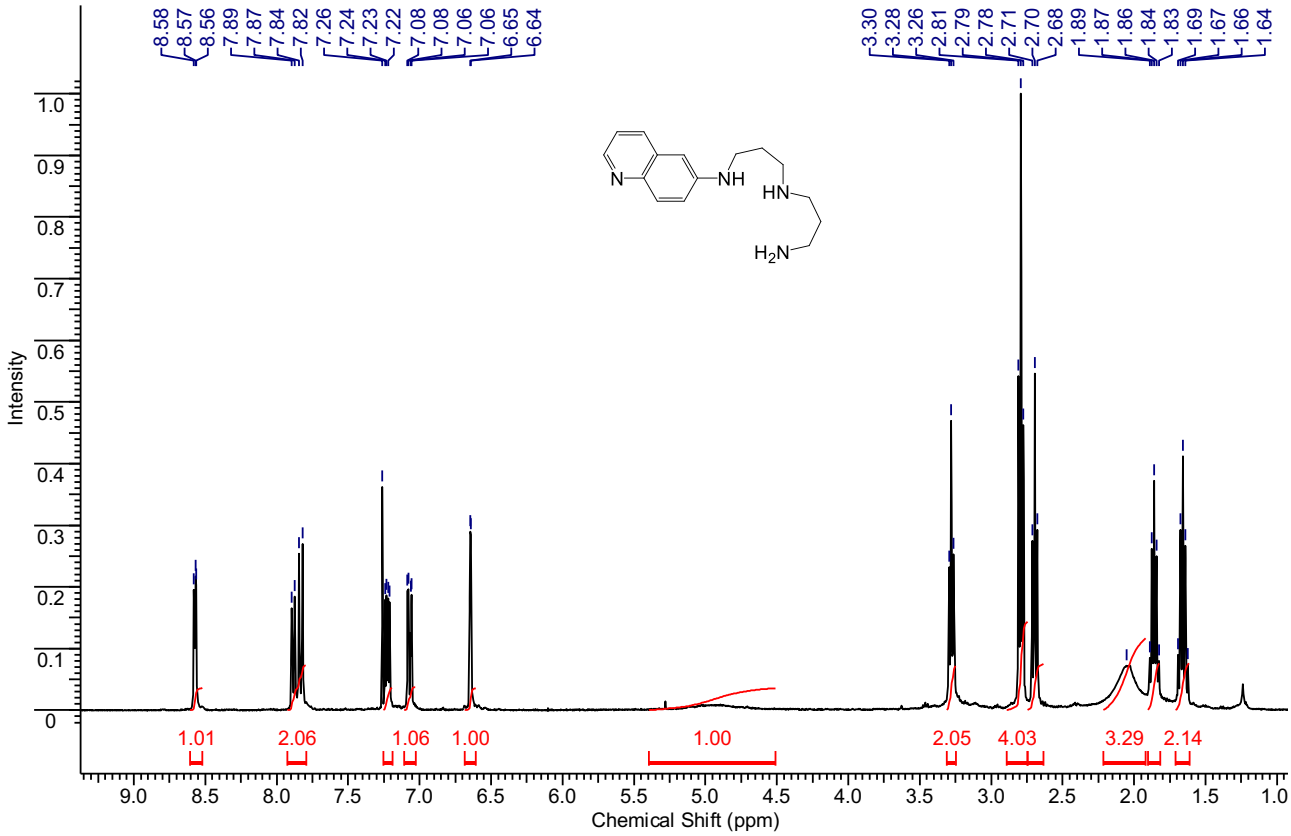

Figure S83. ^{1}H NMR spectrum of **9d** ($CDCl_3$, 400MHz, 300K).

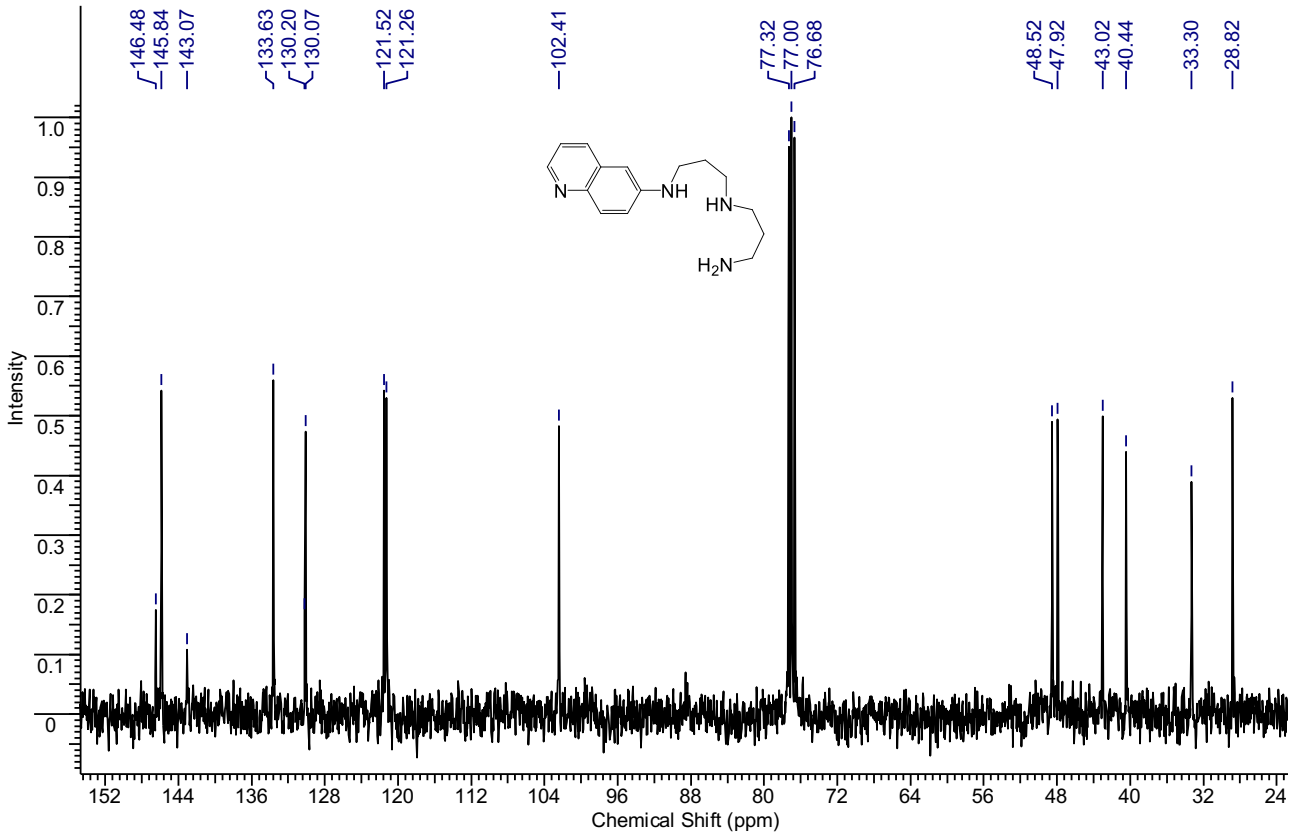

Figure S84. ^{13}C NMR spectrum of **9d** ($CDCl_3$, 100.6 MHz, 300K).

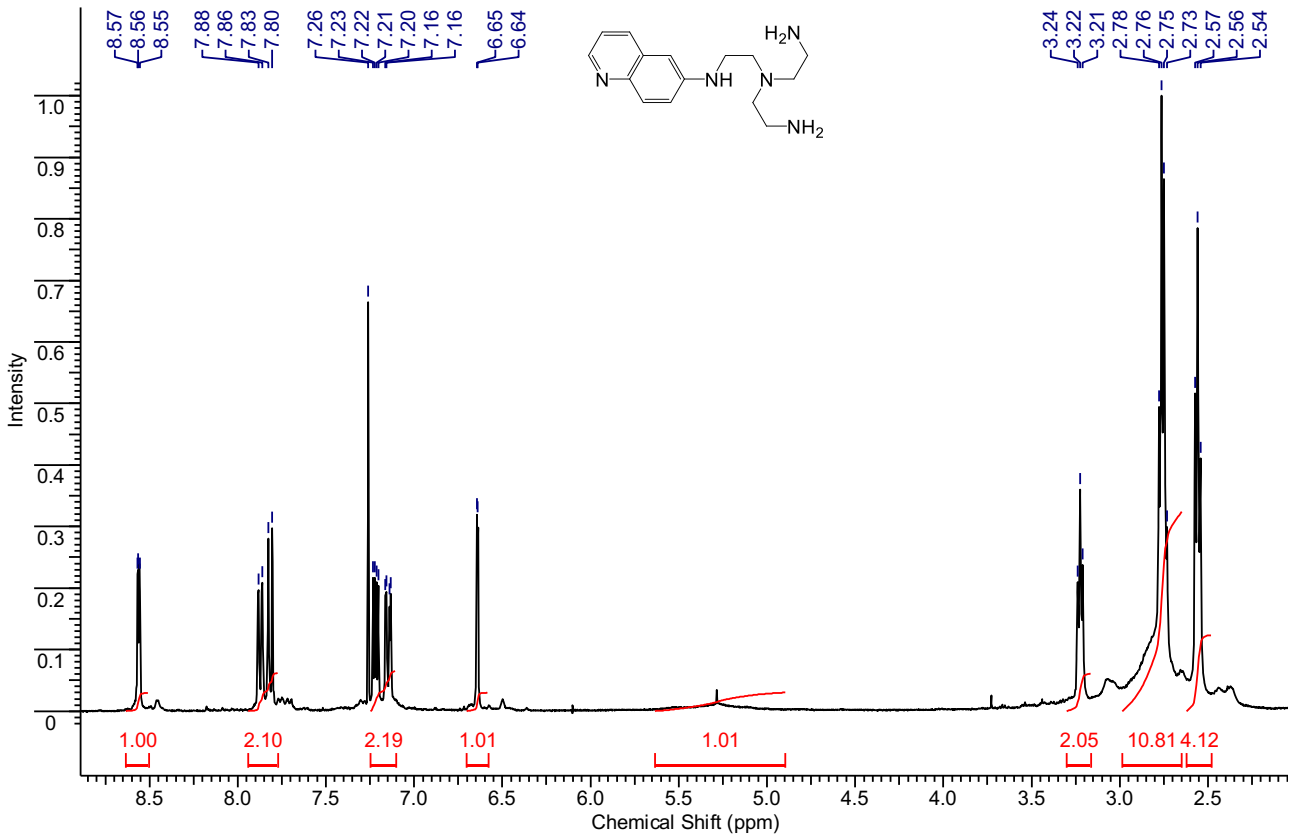

Figure S85. ^{1}H NMR spectrum of **9e** ($CDCl_3$, 400MHz, 300K).

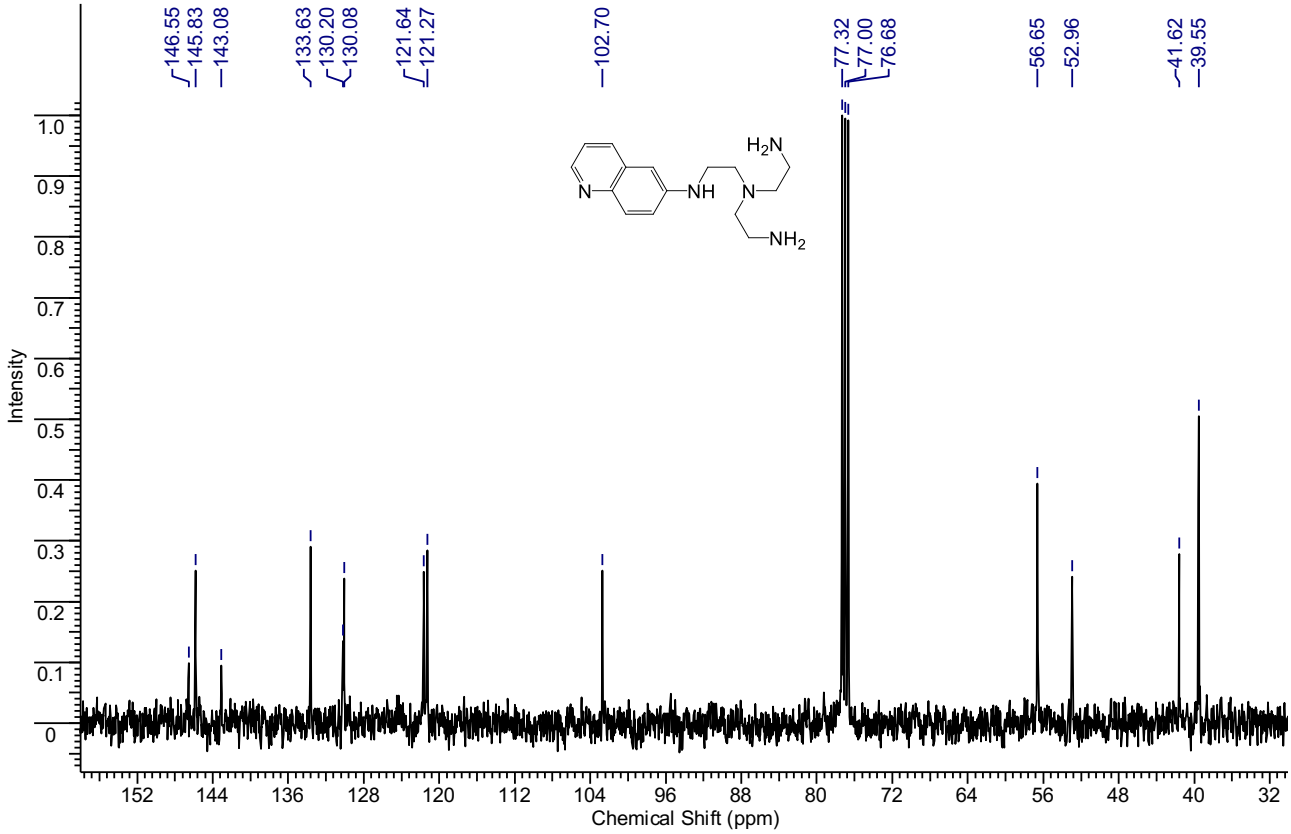

Figure S86. ^{13}C NMR spectrum of **9e** ($CDCl_3$, 100.6 MHz, 300K).

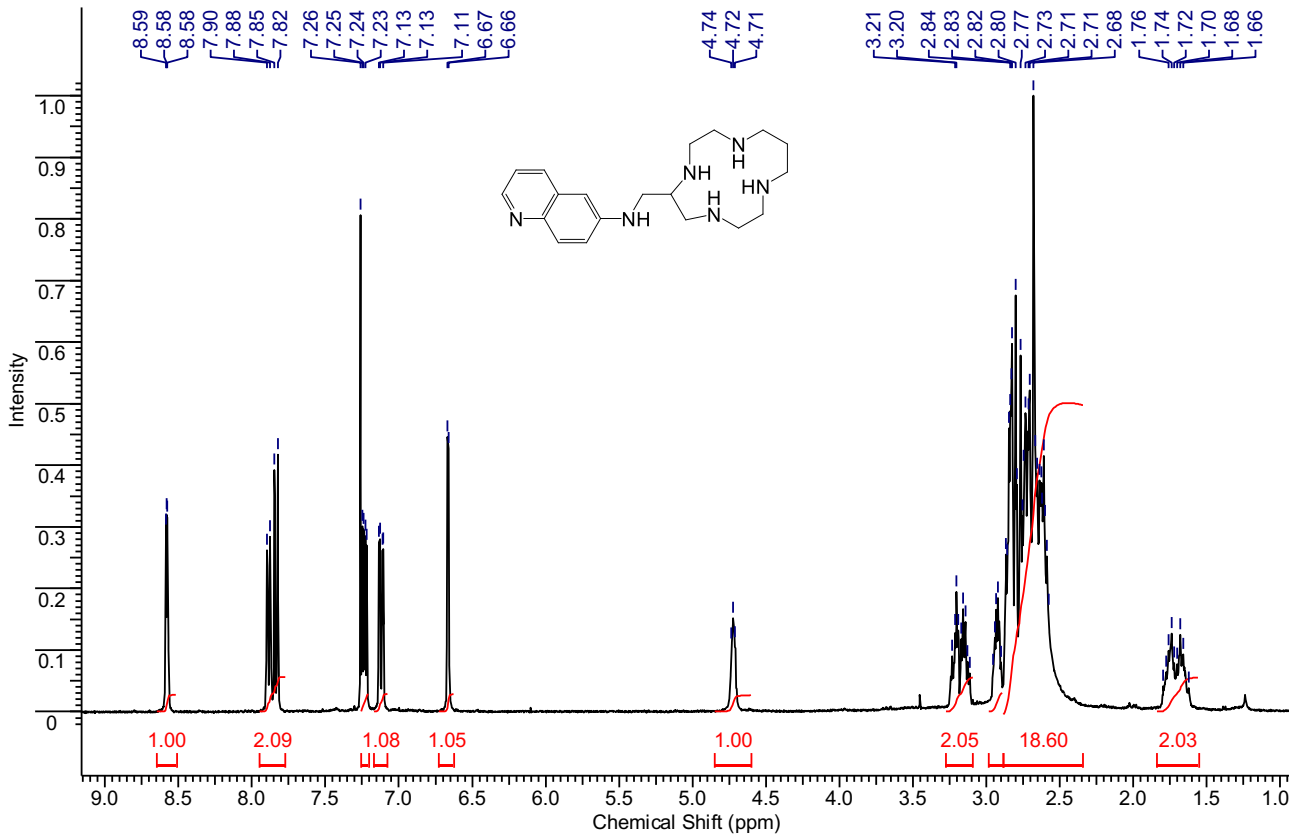

Figure S87. ^{1}H NMR spectrum of **9f** ($CDCl_3$, 400MHz, 300K).

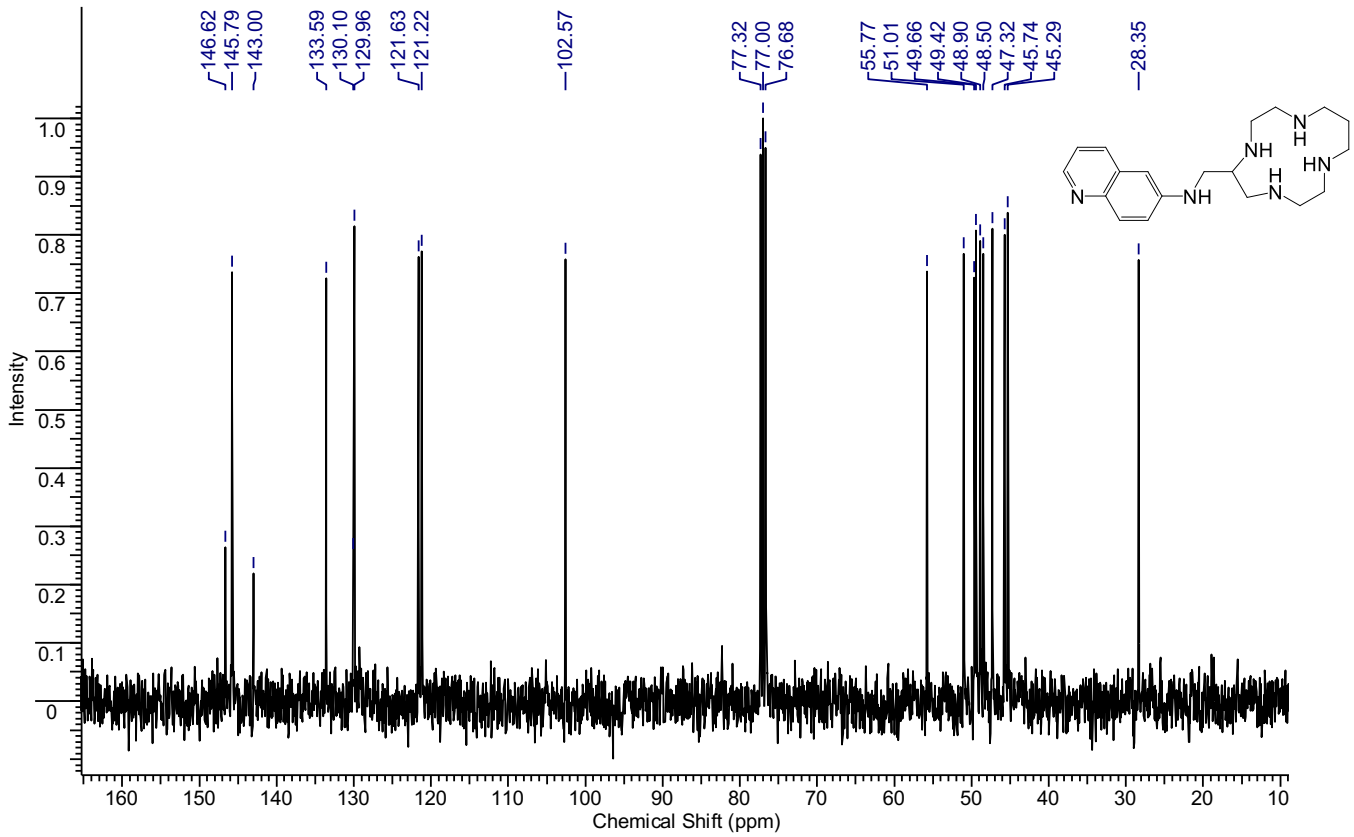

Figure S88. ^{13}C NMR spectrum of **9f** ($CDCl_3$, 100.6 MHz, 300K).

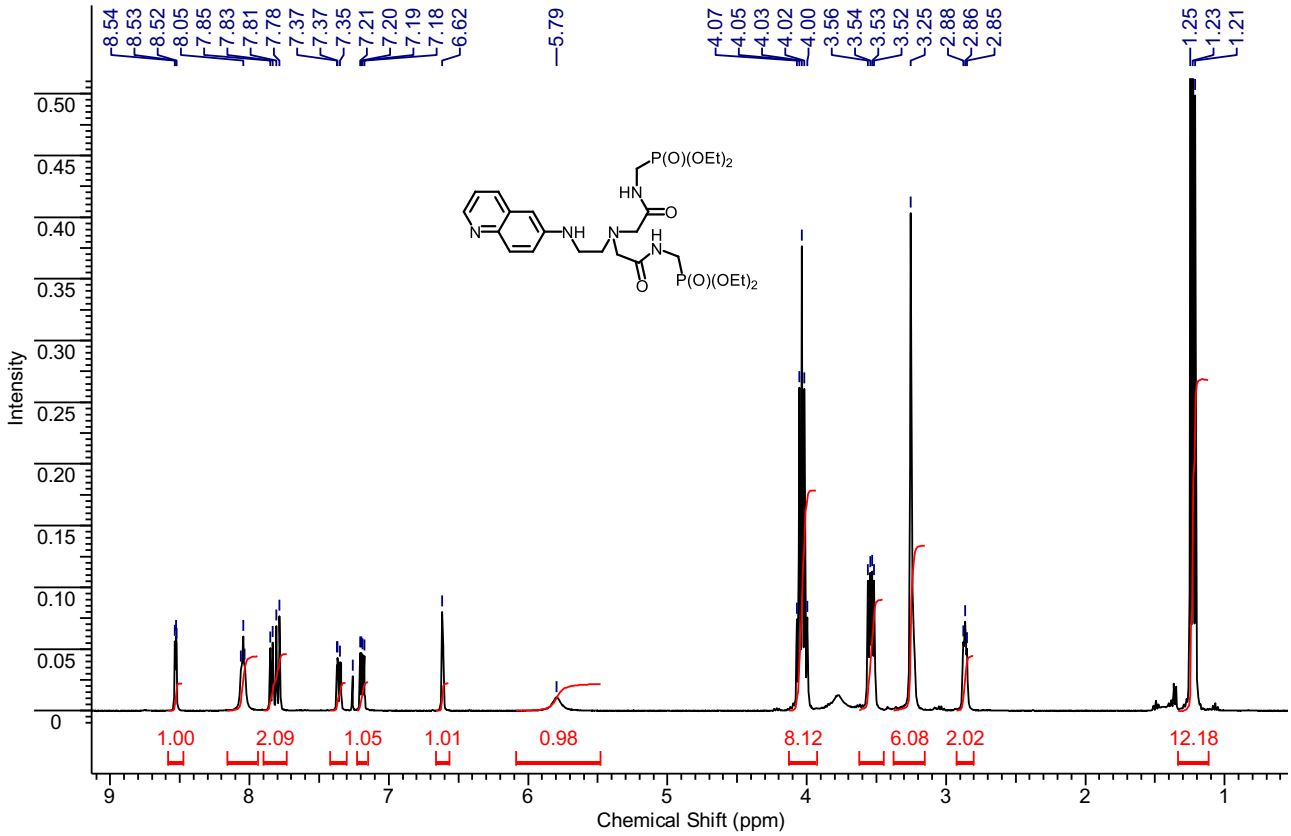

Figure S89. ^{1}H NMR spectrum of **5** ($CDCl_3$, 400MHz, 300K).

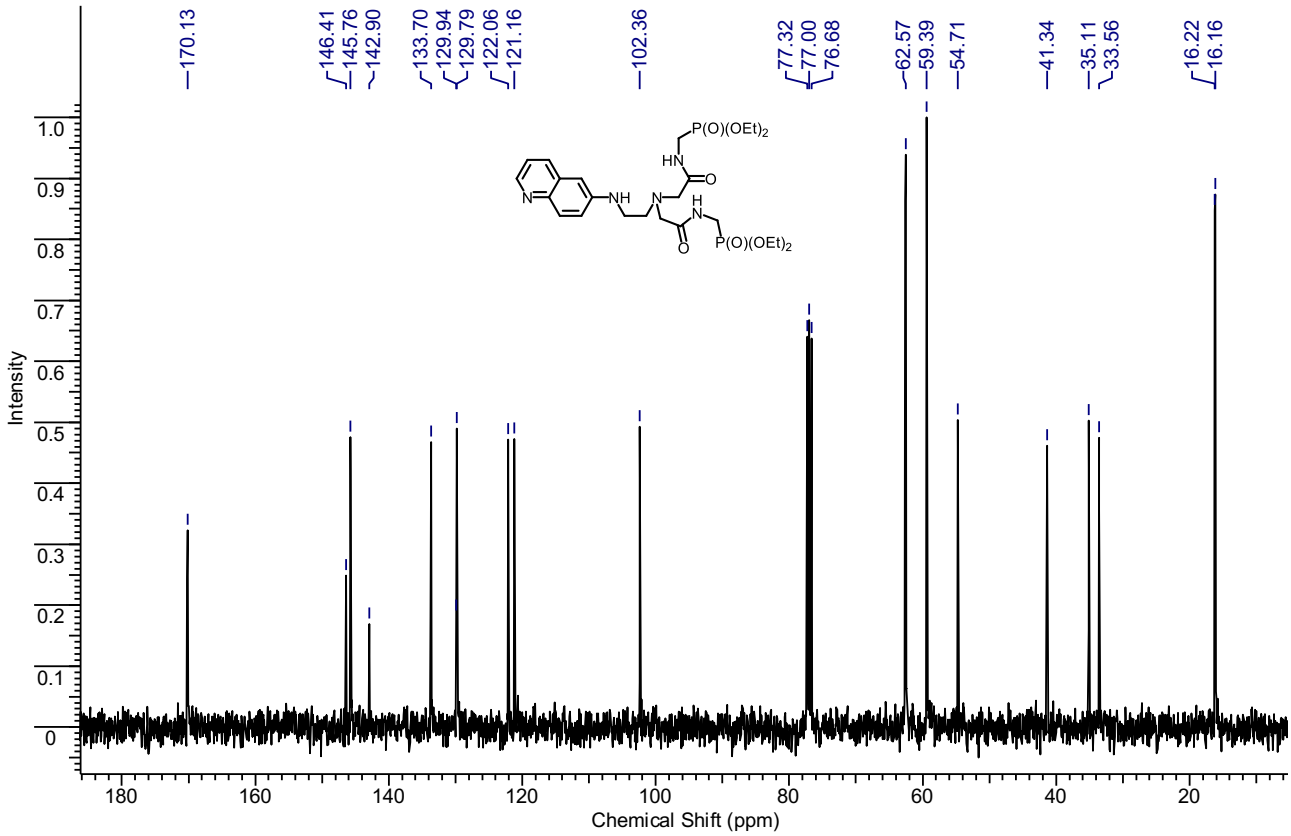

Figure S90. ^{13}C NMR spectrum of **5** ($CDCl_3$, 100.6 MHz, 300K).

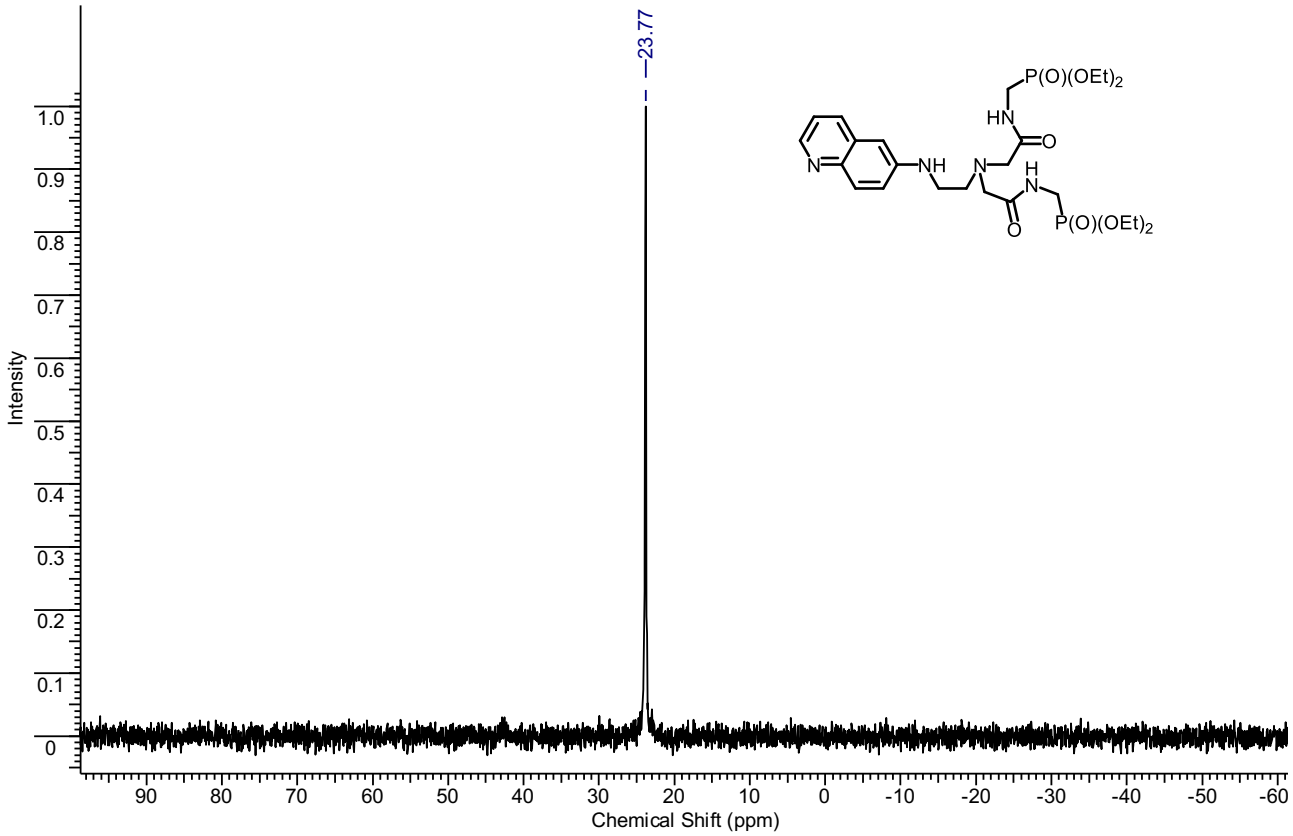

Figure S91. ^{31}P NMR spectrum of **5** ($CDCl_3$, 162.5 MHz, 300K).

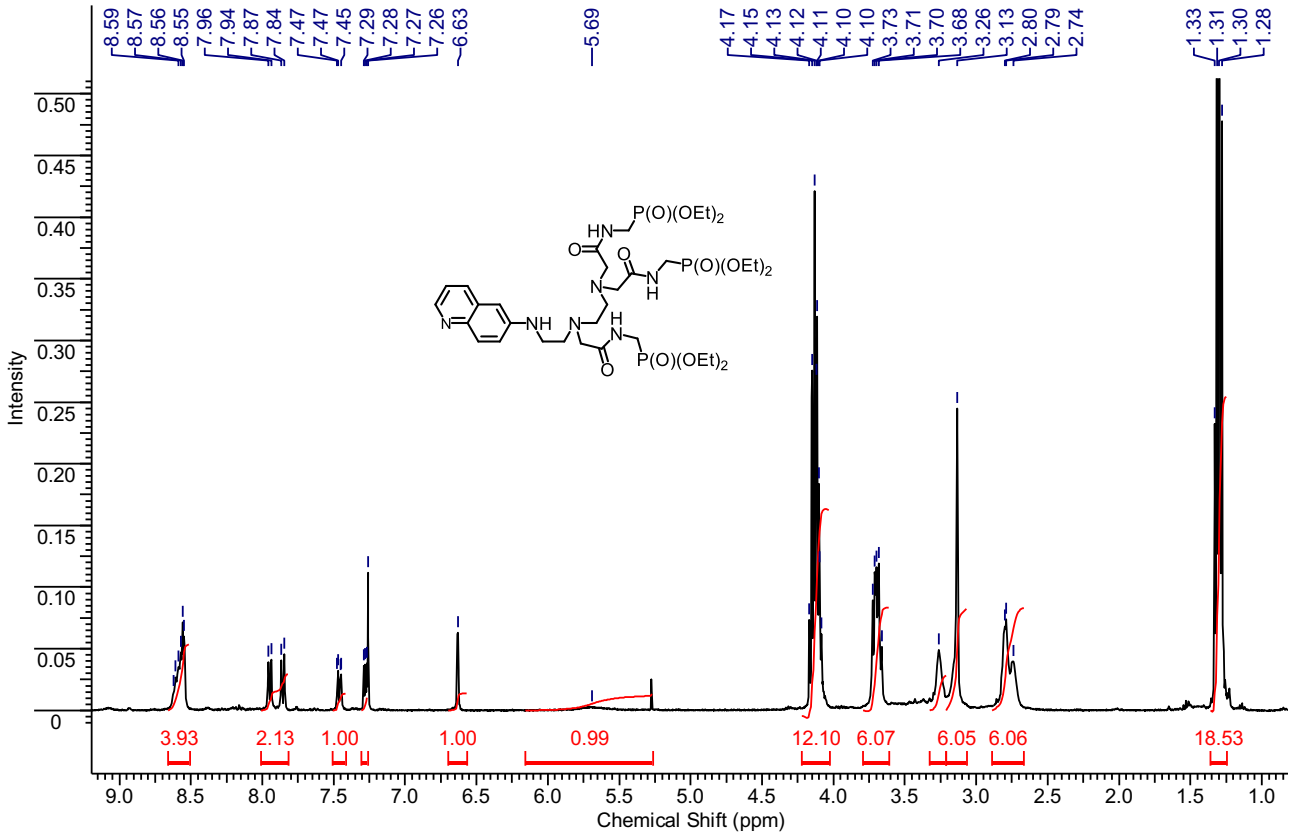

Figure S92. ^{1}H NMR spectrum of **6** (CDCl3, 400MHz, 300K).

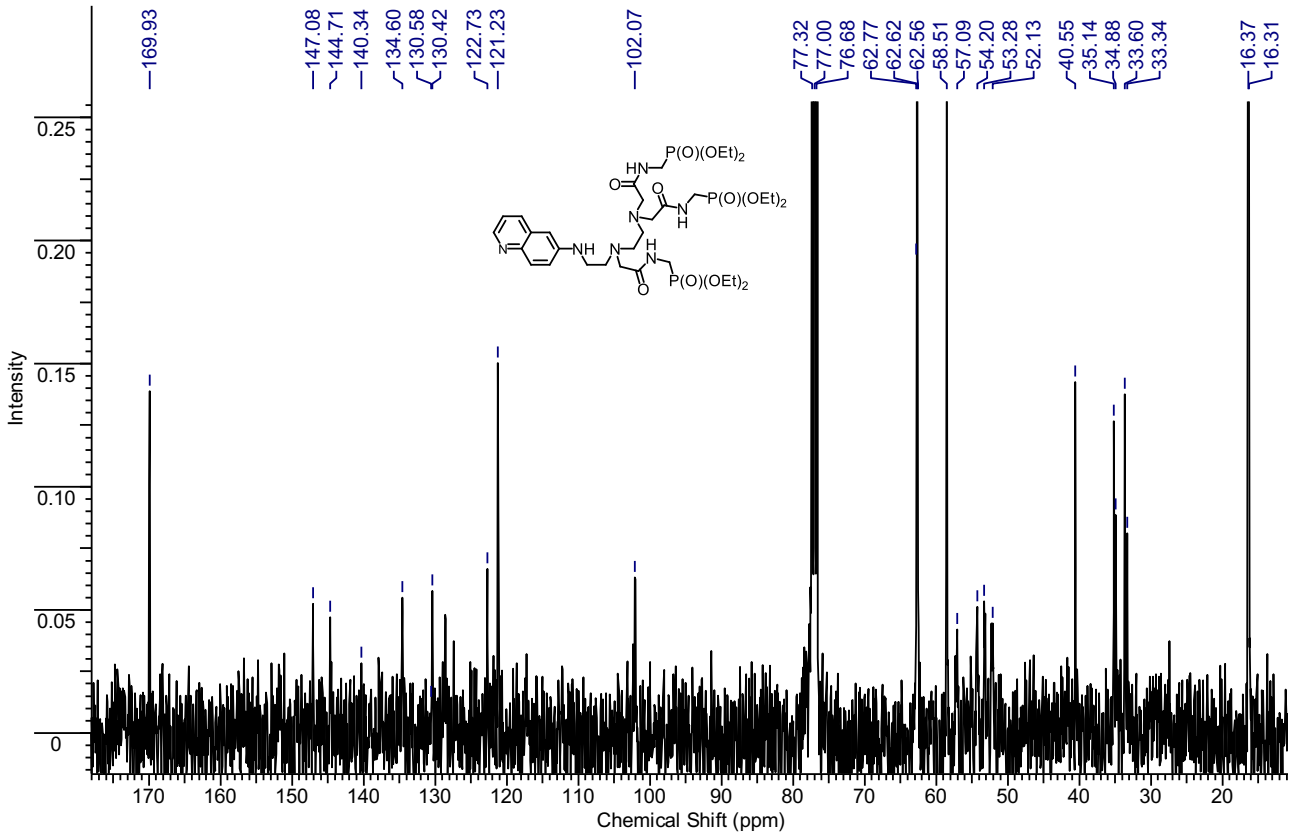

Figure S93. ^{13}C NMR spectrum of **6** ($CDCl_3$, 100.6 MHz, 300K).

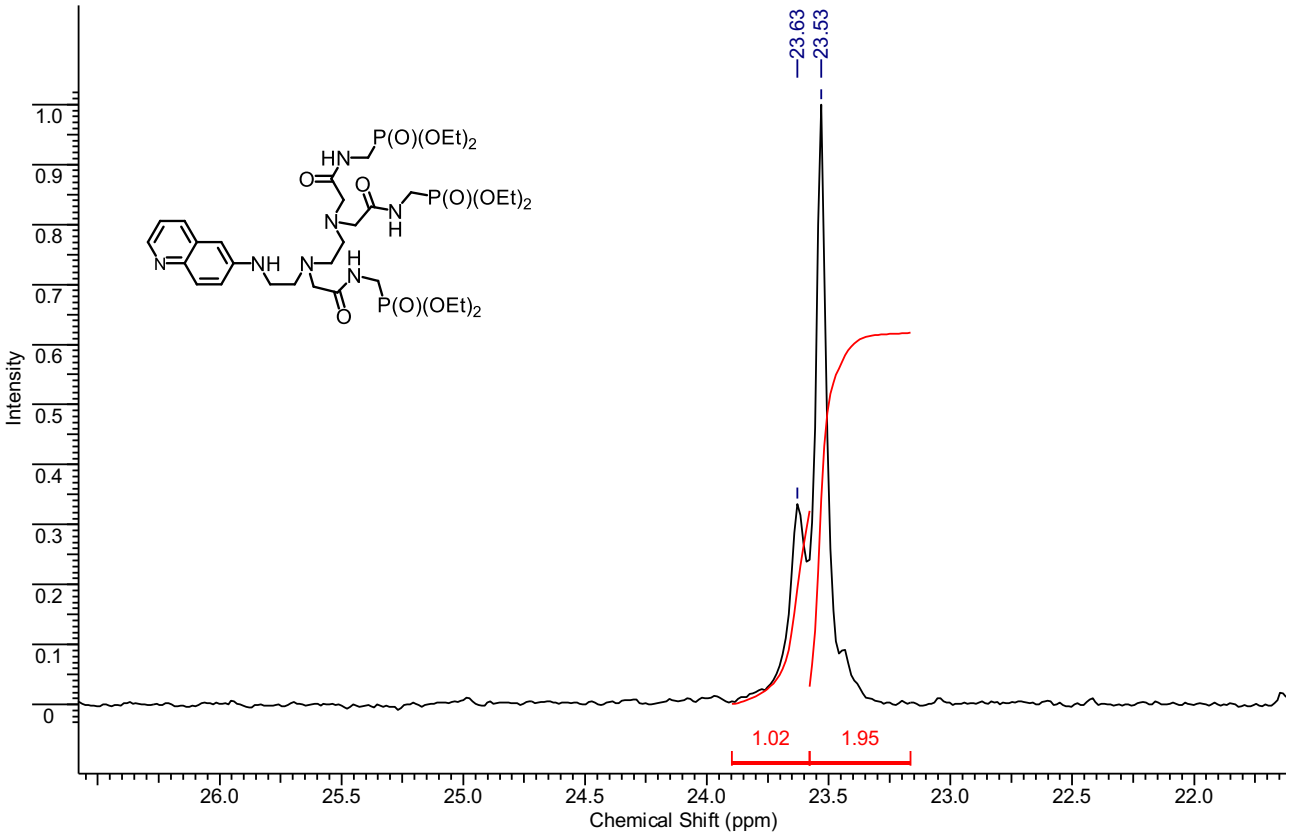

Figure S94. ^{31}P NMR spectrum of **6** ($CDCl_3$, 162.5 MHz, 300K).

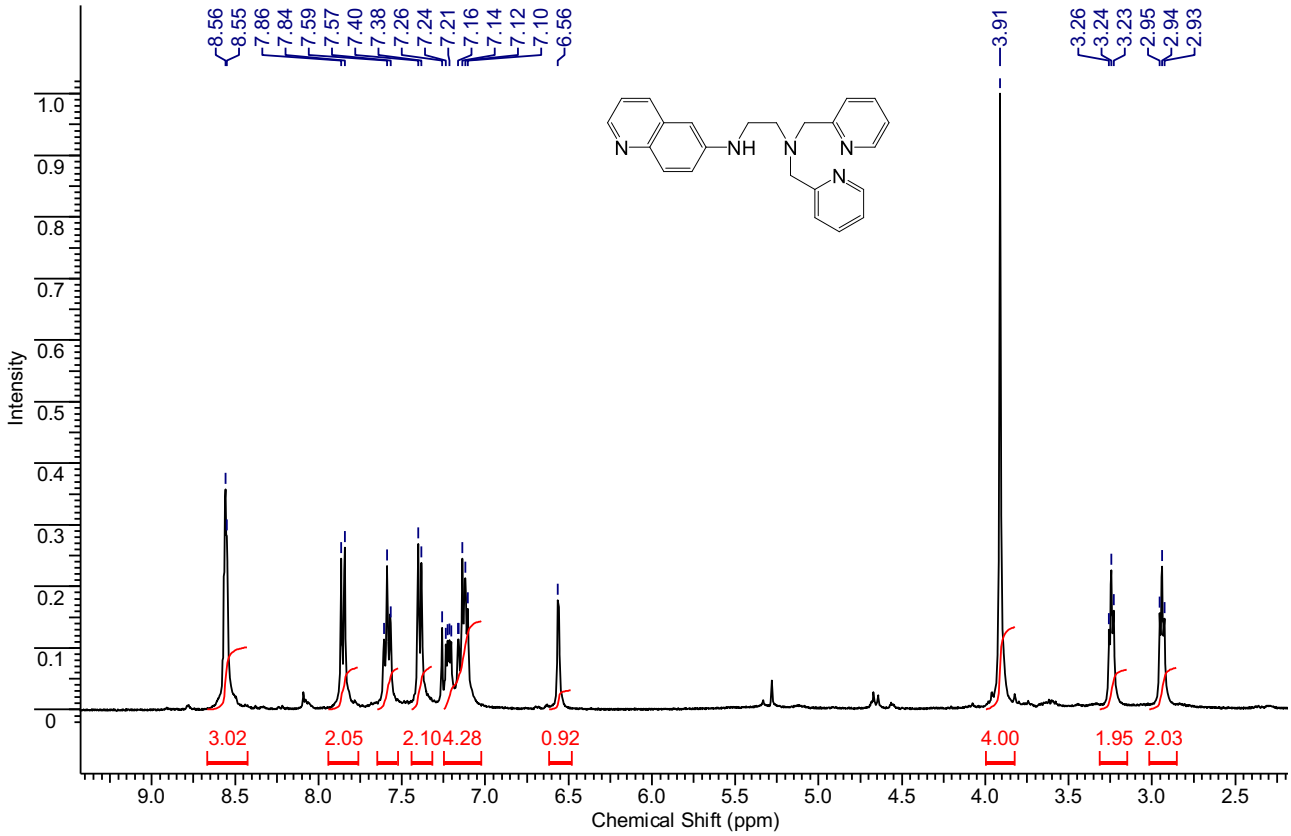

Figure S95. ^{1}H NMR spectrum of **10** ($CDCl_3$, 400MHz, 300K).

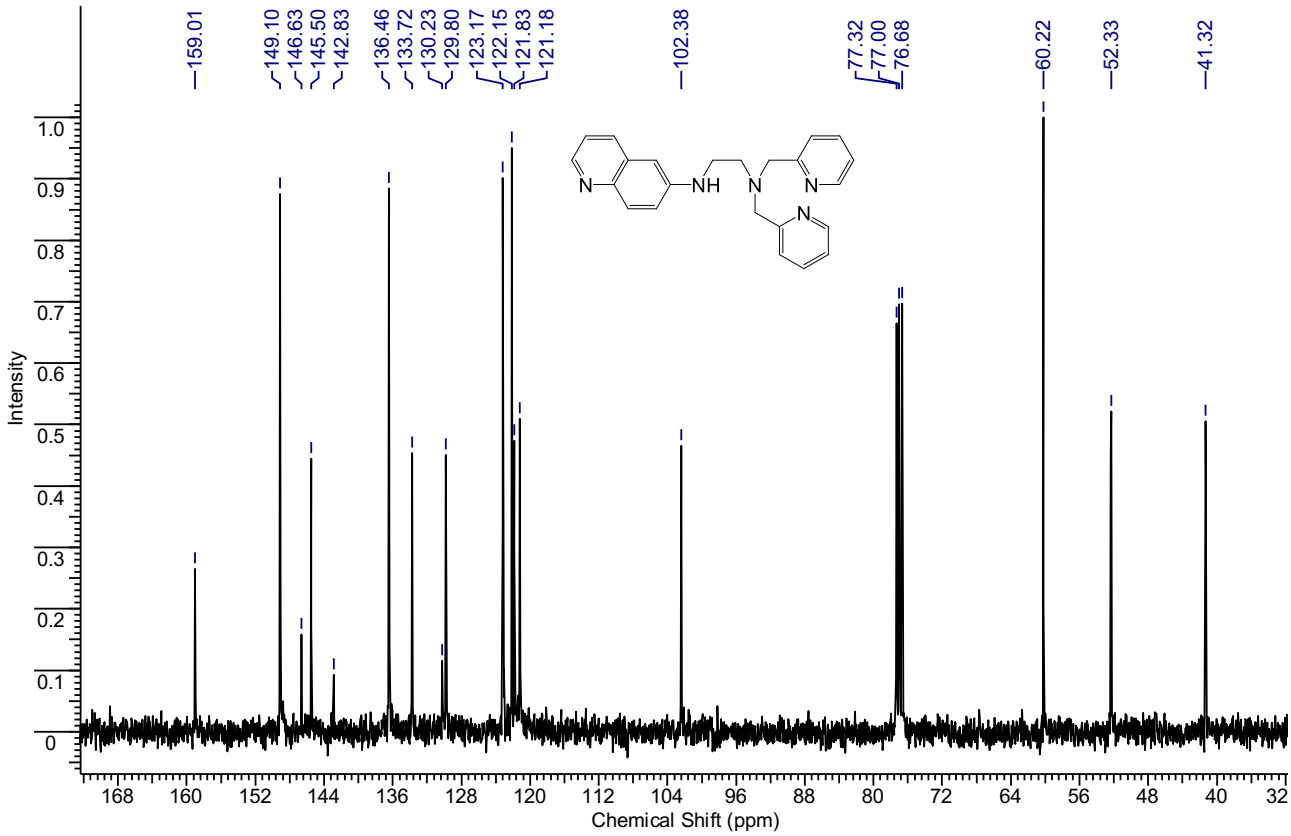

Figure S96. ^{13}C NMR spectrum of **10** ($CDCl_3$, 100.6 MHz, 300K).